TEMPORAL, SPATIAL AND TOXICOLOGICAL CHARACTERISTICS OF COARSE PARTICULATE MATTER IN AN URBAN AREA AND RELATION TO SOURCES AND REGULATIONS

by

Kalam Cheung

A Dissertation Presented to the
FACULTY OF THE USC GRADUATE SCHOOL
UNIVERSITY OF SOUTHERN CALIFORNIA
In Partial Fulfillment of the
Requirements for the Degree
DOCTOR OF PHILOSOPHY
(ENVIRONMENTAL ENGINEERING)

August 2012

Copyright 2012 Kalam Cheung

UMI Number: 3542209

All rights reserved

INFORMATION TO ALL USERS
The quality of this reproduction is dependent upon the quality of the copy submitted.

In the unlikely event that the author did not send a complete manuscript
and there are missing pages, these will be noted. Also, if material had to be removed,
a note will indicate the deletion.

UMI 3542209

Published by ProQuest LLC (2012). Copyright in the Dissertation held by the Author.

Microform Edition © ProQuest LLC.
All rights reserved. This work is protected against
unauthorized copying under Title 17, United States Code

ProQuest LLC.
789 East Eisenhower Parkway
P.O. Box 1346
Ann Arbor, MI 48106 - 1346

Dedication

To my grandparents

for their unconditional love and support.

Acknowledgements

This thesis arose, in part, out of the four years of research that has been conducted since I joined the aerosol lab at the University of Southern California (USC) in 2008. It is my great pleasure to convey my sincere thanks to all the people for their help along with my humble acknowledgement.

In the first place, I express deep sense of gratitude to my advisor Professor Constantinos Sioutas for his unflinching encouragement and guidance in my doctoral research work. His exceptional scientific intuition and passion in aerosol research has nourished my intellectual maturity and inspired my growth as a scientist. I would like to thank him for providing the extraordinary experiences throughout my graduate study.

I would also like to thank the members of my guidance committee, Professor Ronald C Henry, Professor Jiu-chiuan Chen and Professor Scott Fruin for their thoughtful suggestions on my research work. My sincere thanks are also due to Professor James J. Schauer, who always share insightful comments and contributed in various ways to the development of my dissertation.

Research in the aerosol lab is always a team effort. It has been a great pleasure to share my graduate studies and life with the former and current colleagues at USC: Dr. Katharine Moore, Dr. Andrea Polidori, Dr. Bangwoo Han, Dr. Maria Cruz Minguillon, Dr. Subhasis Biswas, Dr. Mohammad Arhami**,** Dr. Zhi Ning, Dr. Vishal Verma, Dr. Payam Pakbin, Neelakshi Hudda, Winnie Kam, Nancy Daher, James Liacos, Dongbin Wang and Sina Hasheminassab. Special thanks to Dr. Zhi Ning for his friendship and help in my graduate study. Without their support, involvement and compassions for work, this dissertation would not have been possible.

Lastly, I would like to thank my family for their persistent confidence and tolerance on me.

Table of Contents

List of Tables

List of Figures

Abstract

To advance our understanding on the relationship between the sources, chemical composition and toxicity of coarse particles, and help the regulatory community to design cost-effective control strategies, two comprehensive investigations were conducted in the Los Angeles Basin from 2008 to 2010 to characterize the physico-chemical and toxicological properties of ambient coarse particulate matter (CPM). The first study features of a year-long sampling campaign at 10 sampling sites throughout the basin in an attempt to study the spatial and seasonal characteristics of ambient coarse particles. An intensive study, focusing on the diurnal trends, was conducted at 3 sampling sites to examine how the change in meteorological conditions throughout a day may affect the source strength and formation mechanisms of coarse mode aerosols.

Overall, the group of crustal materials and other trace elements was the most dominant component of CPM, accounting for approximately half of the total reconstructed CPM mass. The contributions varied from 41% to 61% across the 10 samplings sites, with higher fractions in the inland areas. Organic materials, accounting for around 20% of the CPM mass, well correlated with crustal materials and the soil dust tracers of Ti and Fe, suggesting that humic substance is a major source of organic materials in coarse particles. This is confirmed by further investigation on individual organic compounds, which revealed that the predominant organic constituents in the coarse size fraction, including *n*-alkanoic acids and medium molecular weight (MW) *n*-alkanes (C25 to C35), were highly associated with crustal materials. Sea salt, on the other hand, accounted for an average of 9% of the reconstruct CPM mass, with higher levels in spring and summer when the onshore wind prevailed. Nitrate, the most dominant inorganic species in the

coarse size fraction, arose predominantly from the depletion of sea salt, and thereby mostly followed the temporal and spatial patterns of sea salt aerosols. Constituents with primary anthropogenic origins, such as elemental carbon, hopanes and steranes, experienced very low concentrations. On the other hand, natural sources such as mineral dust and the associated biota, and to a lesser extent fresh and aged sea salt, constituted to the majority of ambient CPM mass in the Los Angeles Basin.

In summer, ambient coarse particles were mostly re-suspended by wind, and their levels were generally higher in the midday and afternoon sampling periods, in parallel with the higher wind speeds. In winter, the levels of CPM were generally lower, with the exception of stagnation conditions, when particles accumulated in the atmosphere in episodes of low atmospheric dilution. During winter nighttime, the mixing height was lowest. Turbulences induced by vehicular movements became a dominant re-suspension mechanism of coarse mode aerosols, resulting in high levels of mineral and road dust at near-freeway sites. Overall, the contributions of inorganic species to CPM mass were generally higher overnight, suggesting that the lower temperature and higher relative humidity at nighttime favored the formation of these ions in the coarse mode.

To evaluate the toxic activity induced by CPM, a cellular assay was used to quantify the generation of reactive oxygen species (ROS). The ROS activity experienced a significant diurnal variation, with higher levels in summer than winter. During summertime, higher ROS activity was observed in the midday / afternoon periods, while the peak activity occurred overnight in winter. Using linear regression analysis, the ROS activity was highly associated with the water-soluble fraction of four elements (V, Pd, Cu and Rh), which have primary anthropogenic origins in the coarse size fraction. Based on the results of this investigation, coarse particles

generated by anthropogenic activities, although low in mass concentrations, are the key drivers of ROS formation, and therefore more targeted control strategies may be needed to better protect the public health from these toxic CPM sources.

Chapter 1 Introduction

1.1. Background

Particulate matter (PM) is defined as a suspension of liquid droplets or solid matter in a gas or liquid. PM is an extremely important component in the ambient atmosphere. It contributes to smog formation and visibility degradation in urban atmospheres, and influences the surface albedo by decreasing the amount of heat reaching the ground (Seinfeld and Pandis, 2006). Particles also play significant roles in biogeochemical cycles in the atmosphere, serving as reaction substrates and carriers for sorbed chemical and /or biological species (Dentener et al., 1996). More importantly, numerous epidemiological studies have shown associations between adverse health effects and ambient PM levels (Dockery et al., 1993; McConnell et al., 1999; Sram et al., 1999; Stayner et al., 1998). Therefore, understanding the physico-chemical and toxicological characteristics of PM is essential to evaluate its environmental and health consequences.

Atmospheric PM is a complex mixture of many classes of chemical constituents, with size ranging from a few nanometers (nm) to tens of micrometers (μm) in aerodynamic diameter. Sources of ambient PM can be both natural and anthropogenic. Natural sources include windborne dust, sea spray, forest fires, and volcanic emissions (Seinfeld and Pandis, 2006). Combustion activities such as burning of fossil fuels and biomasses are the major anthropogenic sources in an urban atmosphere. These particles are also known as primary pollutants since they are emitted directly into the atmosphere. On the other hand, particles can be formed by secondary processes, such as the photo-oxidation of SO_2 and NO_2 to form sulfate and nitrate particles, respectively. Once emitted to the atmosphere, aerosol properties, including size and chemical

composition, are subject to transportation and transformation by various chemical and physical processes (Hinds, 1999).

1.2. Characteristics of Particulate Matter

1.2.1. Particle size

Particle size is the most important parameter in describing particle characteristics including formation and removal mechanisms, atmospheric lifetime, as well as the site of deposition in human respiratory tract. There are three distinct size modes of particles based on an observed particle size distribution: (a) the coarse mode, particle with an aerodynamic diameter between 2.5 and 10 μm; (b) the accumulation mode, particle with an aerodynamic diameter between 0.1 and 2.5 μm; and (c) the ultrafine mode, particle with an aerodynamic diameter between 0.005 and 0.1 μm.

The three size modes differ in their means of formation and removal, chemical composition, deposition, and optical properties (Seinfeld and Pandis, 2006). Ultrafine particles primarily originate from combustion sources, as well as homogeneous or heterogeneous nucleation of atmospheric species. Ultrafine particles are removed from the mode predominantly through physical process of coagulation with larger particles. Accumulation mode particles compose a significant amount of PM mass and surface area. These particles are formed through coagulation of ultrafine mode particles, and growing of existing particles from condensation of gases. The accumulation mode particles have inefficient removal mechanisms since they are too small to be settled by gravity and too large to coagulate into larger particles, resulting in long residence times (Seinfeld and Pandis, 2006). Lastly, coarse mode aerosols are generated primarily by mechanical processes such as grinding, erosion, and wind re-suspension. These particles have relatively high

gravitational settling velocities, allowing them to settle out of the atmosphere in a relatively short amount of time. Coarse particles are also known to react with atmospheric gases. For example, formation of coarse particulate nitrate from reaction of nitric acid with mineral dust and sea salt particles was observed in many studies (Goodman et al., 2000; Usher et al., 2003; Zhuang et al., 1999). Unlike the formation of volatile compounds such as ammonium nitrate in the fine mode, the irreversible reactions between atmospheric gases and coarse particles, coupled with the lower residence time of coarse particles decrease the atmospheric lifetime and serve as an important removal pathway of gaseous pollutants.

1.2.2. Particle mass

Particle mass is an important parameter in terms of particle measurement. Particle mass concentration is used for regulatory purposes in the United States, and is dominated by the accumulation and coarse mode particles (Hinds, 1999). Ultrafine mode particles, on the other hand, comprise a relatively small percent of mass concentration in ambient atmospheres due to their small sizes.

1.2.3. Particle number

Particle number is another important characteristic that emerged in the field of PM measurement in the last decade. In contrast with particle mass, particle number concentration is dominated by ultrafine particles (UFPs). UFPs constitute to a majority of ambient particle number concentrations but only a small fraction of particle mass. Primary vehicular emissions and photochemical reactions are the major sources of particle number concentrations in an urban atmosphere (Fine et al., 2004b; Kulmala et al., 2004). Although not currently used for regulation in the United States, particle number emission limit was introduced in the Euro 5/6 standards in

recognition of the higher toxicity of ultrafine particles compared with particles in accumulation and coarse mode (Delfino et al., 2005; Li et al., 2003).

1.2.4. Health effects

The impact of ambient PM on human health is the most prominent motivation that drives aerosol researches. Numerous epidemiological studies linked elevated PM levels to various adverse health outcomes, including premature deaths (Hoek et al., 2002), respiratory and cardiovascular diseases (Gauderman et al., 2007; Pope and Dockery, 2006), and neurodegenerative disorders (Peters et al., 2006). A few other studies also presented negative impacts of PM exposure on liver functions (Folkmann et al., 2007) and reproductive systems (Sram et al., 1999). Both in-vitro and in-vivo studies demonstrated associations between particulate exposure to respiratory inflammation, mitochondrial damage, and lung cancer (Castranova et al., 2001; Costa and Dreher, 1997; Kleinman et al., 2007; Li et al., 2003). While some recent studies presented higher toxicity of ultrafine particles relative to the larger particles in the accumulation and coarse mode in urban atmospheres (Hu et al., 2008; Li et al., 2003), a few epidemiological studies have shown associations between coarse particles with adverse health outcomes in areas where higher fractions of coarse PM are found (Lipsett et al., 2006; Smith et al., 2000).

Particle size, governing the site of particle deposition along the respiratory tract, has an important role in health effects induced by PM exposure. Particles that are larger than 10 μm are usually not the point of interest in health studies due to their short atmospheric lifetimes. CPM ranging from 2.5 to 10 μm is generally referred as “inhalable coarse particles”, and primarily deposits on the upper respiratory tract including the nasal airway and pharyngeal/laryngeal

regions. A small fraction of coarse particles might also penetrate and deposit further in the respiratory tract. Particles in accumulation mode have low removal efficiency on the nasal airway, and generally penetrate deeper to the tracheobronchial tree and pulmonary regions. Ultrafine particles, on the other hand, have higher deposition efficiency in the nasal and alveolar regions. Some recent studies have also shown the presence of ultrafine particles in the brain and central nervous system (Oberdorster et al., 2004).

In spite of recent advancements in PM toxicity research, the relationships between aerosol properties (e.g., size, number, volatility, surface area, and composition) and specific health end points are not well understood and remain an area of active research. The production of reactive oxygen species (ROS) and the consequent generation of oxidative stress is proposed to play a direct role in PM-induced adverse health outcomes (Castro and Freeman, 2001; Tao et al., 2003). Oxidative stress refers to an imbalance within cells where more ROS is produced than eliminated, and high levels of oxidative stress can result in damage within a cell that can harm the cell's functions and lead to apoptosis (Pelicano et al., 2004). Both chemical and biological assays are available to quantitatively characterize the production of ROS, thereby allowing the examination of ROS activity with aerosols of various sizes and compositions.

1.3. Rationale of the Present Study

1.3.1. Motivation and objectives

Ambient PM is regulated under the Clean Air Act using size specific mass concentration standards. The National Ambient Air Quality Standards (NAAQS) for ambient PM were first established in 1971, when the standard of total suspended particle (TSP) was introduced. They have evolved over the years as a result of emerging epidemiological and toxicological studies that

linked elevated airborne PM mass concentration of different size fractions to a variety of adverse health outcomes as discussed in Section 1.2.4. In 1987, the PM_{10} (particles smaller than 10 μm in diameter) standard was used to replace the TSP (Total Suspended Particulate) standard. The $PM_{2.5}$ (particles smaller than 2.5 μm in diameter) standard was introduced in 1997 to specifically regulate fine particles. The 1997 standards also intended to regulate the "inhalable coarse particles" ranging from 2.5 to 10 μm (herein referred as CPM, PM_{CF}). However, most epidemiological studies reported only findings for PM_{10} and $PM_{2.5}$, and they were mostly conducted in urban areas where the levels of fine particles were higher than those of coarse particles (Abbey et al., 1995; Dockery and Pope, 1994; Dockery et al., 1993; Schwartz et al., 1994). Very limited studies provided clear quantitative evidence to link coarse particles to adverse health effects. Due to the abovementioned reasons, the Environmental Protection Agency (EPA) concluded at that time to continue to use PM_{10} standards to control thoracic coarse particles.

In the last few years, the difference between coarse and fine particle has become more explicitly understood and appreciated. There is a growing, but still limited, evidence of health effects induced by coarse particles. A number of epidemiological studies were conducted in areas of lower $PM_{2.5}$ / PM_{10} ratios such as Rena, NV and Phoenix, AZ (Chen et al., 2000; Lipsett et al., 2006; Smith et al., 2000), allowing a more relevant evaluation of health effects imposed by CPM. Some relatively inexpensive in-vivo and in-vitro tests developed in recent years also become readily available to stimulate PM-induced toxicological responses, which provide a scientific basis for understanding the pathological pathway of PM-induced health effects. Furthermore, since the $PM_{2.5}$ standard was in place in 1997, $PM_{2.5}$ levels have come down and thereby leading to more comparable levels of fine and coarse PM even in urban areas. As a result, there has been

a major consideration on establishing a new $PM_{10-2.5}$ standard to specifically regulate coarse particles. The potential change of PM standard has been controversial. There are concerns regarding the inconsistent CPM-induced adverse health outcomes demonstrated in health studies. The new standard may impact urban and rural areas differently because of the different sources and size distribution of PM in these areas. The implementation of a new $PM_{10-2.5}$ standard would also devalue the historical PM_{10} measurements and probably require additional monitoring stations and equipment.

Currently, CPM is regulated under the PM_{10} standards. PM_{10} consists of both fine and coarse particles, of which the sources, formation, and removal mechanisms are entirely different. Due to higher settling velocity and distinct origins, CPM is more affected by local sources, and is more heterogeneous compared with particles in the fine mode. Thus, the temporal and spatial variation of coarse particles, as well as the chemical composition could be different from place to place. Therefore, regulating CPM using PM_{10} standards might not be appropriate in controlling this thoracic coarse fraction of PM_{10}. Additionally, limited literature has studied coarse particles specifically, in contrast to the extensive monitoring network currently in place for PM_{10} and $PM_{2.5.}$ $PM_{10-2.5}$ measurements were often obtained using the difference between PM_{10} and $PM_{2.5}$, which introduced higher uncertainties, particularly in areas with high $PM_{2.5}$ / PM_{10} ratio. As a result, significantly less is known about the physico-chemical and toxicological characteristics of CPM. The distinct chemical composition in the fine and coarse fractions could also contribute to potentially different health outcomes. Since these parameters are important in distinguishing the characteristics and health effects of CPM from those of PM_{10} or $PM_{2.5}$, it is desirable to have comprehensive investigations on CPM based on independent ambient measurements.

In order to provide a scientific basis to develop cost-effective regulations to regulate CPM, two comprehensive investigations were conducted in Southern California to examine the physical, chemical and toxicological characteristics of coarse particles. The first project involved a year-long sampling campaign to collect ambient coarse particles in 10 sampling sites across the Los Angeles Basin, and the subsequent physical and chemical analyses of these samples. To better understand the toxicity of coarse particles, the production of reactive oxygen species (ROS) was used to characterize the oxidative potential of the collected CPM. In the second project, the diurnal variation of coarse particles was studied to improve the understanding of important atmospheric parameters that influence the ambient CPM concentration and composition, as well as public health impacts as a result of human exposure. The results of these two studies were integrated with published literature to provide a comprehensive investigation to establish the linkage between sources, composition, and the toxicity of coarse particles. The objectives of the present investigation work are:

1) To understand the cause of the temporal and spatial variation of CPM concentrations and chemical composition, and identify their sources in the atmosphere;
2) To identify the linkage between toxicity levels and source-specific chemical constituents in CPM with distinctive origins, and
3) To determine the most effective strategy to regulate CPM and provide valuable scientific information for environmental policy decision making.

The results of this investigation will ultimately help decide if a $PM_{10-2.5}$ standard is more beneficial than a PM_{10} standard to regulate coarse particles.

1.4. Thesis Overview

This thesis presents my doctoral research work under the supervision of Professor Costantinos Sioutas with the goal to provide a scientific basis for effective regulation of coarse particles. The thesis includes the following chapters:

Chapter 1 provides an overview of urban particulate matter, and the rationale of this investigation.

Chapter 2 presents the ambient CPM chemical composition at 10 distinct locations in the Los Angeles Basin. The sources and formation mechanisms of coarse particles are discussed. The contributions of different sources, as well as their temporal and spatial variations are also examined.

Chapter 3 focuses on the seasonal and spatial variations of CPM-bound individual organic compounds, and their relation to sources.

Chapter 4 describes the historical data (1986-2009) of CPM mass concentrations and chemical compositions in 3 different areas in the Los Angeles Basin, and discusses their relations to sources and air quality regulations.

Chapter 5 presents the diurnal chemical profile of CPM, which gives insights on the ambient conditions that affect the formation of coarse particles.

Chapter 6 explores the relationships between the chemical composition and the toxicological profiles of CPM. The results will help identify the sources that are responsible for driving the toxic activity of coarse particles.

Chapter 7 concludes the findings of the present investigation and outlines the possible strategies that would help establish cost-effective air quality standards to protect the public health

from CPM exposure. It also identifies limitations of the current investigation and provides suggestions for future research on this subject.

Chapter 2 Spatial and Temporal Variation of Chemical Composition and Mass Closure of Ambient Coarse Particulate Matter ($PM_{10-2.5}$) in the Los Angeles Area

2.1. Abstract.

To study the seasonal and spatial characteristics, as well as chemical composition of coarse particulate matter, 10 sampling sites were set up in different areas of the Los Angeles Basin. Ambient CPM was collected for a year-long in 24-hour periods once per week during weekdays, and was analyzed for elemental and organic carbon (EC-OC), water soluble inorganic ions, and total metals and elements. Five categories were used to reconstruct PM mass: 1) crustal materials and other trace elements 2) organic matter 3) elemental carbon 4) sea salt and 5) secondary ions. Overall, crustal materials and other trace elements were the most abundant category, accounting for an average of 47.5 ± 12% of the total reconstructed mass. Secondary ions (sulfate, nitrate and ammonium) and organic matter also contributed significantly at mass fractions of around 22.6 % and 19.7%, respectively. Elemental carbon was a less significant component, accounting for less than 2% of total mass across sites. Sea salt particles were more prevalent in spring and summer (12.7%) due to the strong prevailing onshore southwesterly wind in that period. Mass fractions of organic matter, as well as crustal materials and other trace elements were higher in fall and winter, indicating that their contributions were not affected by the lower wind speed and change in wind direction during that period. PM concentrations of sea salt particles decreased from coast to inland along the trajectory of LA Basin, while crustal materials and other trace elements became dominant at inland sites. On the other hand, organic carbon well-correlated with tracers of soil dust (R = 0.74 and 0.72 for Ti and Fe respectively), suggesting that humic substances might be the major constituent of organic matter in coarse mode aerosols in the Los Angeles Basin.

2.2. Introduction

Due to concerns of health effects of exposure to coarse particles, there has been considerable discussion about explicitly regulating CPM. Currently, coarse particles are regulated using PM_{10} standard. PM_{10} is a mixture of coarse and fine airborne particulate matter, both of which have diverse predominant sources and removal mechanisms; thereby, chemical composition is significantly different. Origins of $PM_{2.5}$ include fossil fuel combustion and photo oxidation of gas precursors, while CPM arises predominantly from mechanical disruption and attrition processes. Source apportionment studies showed that the composition of coarse particles varied widely depending on the study areas; major components include resuspended soil, road and street dust, fugitive dust, sea salts and biological materials (Hwang et al., 2008; Paode et al., 1999).

Unlike PM_{10} and $PM_{2.5}$, for which abundant data of continuous and time-integrated mass is generated by local and state agencies, a nationwide $PM_{10-2.5}$ monitoring network is not currently in place. Moreover, limited peer-reviewed studies have examined comprehensively the chemical composition of CPM in urban and rural areas of the U.S., thereby limiting the understanding of the link between their sources, their physico-chemical characteristics and their toxicological properties. In this study, 10 sampling sites were set up in different areas in the Los Angeles Basin to collect time-integrated ambient CPM for an entire year-long period. The characterization of the CPM physical properties, including the mass concentrations and its spatial and temporal variation, has been presented in our previous publications (Moore et al., 2010; Pakbin et al., 2010). This chapter focuses on the much-needed information on CPM chemical composition and their sources of formation, as well as their spatial and seasonal characteristics in urban and rural areas of the

Los Angeles Basin. This comprehensive dataset will be a key tool to policy makers in providing vital information for conducting epidemiological health studies, for setting up effective compliance monitoring in Southern California, and ultimately for designing effective CPM control strategies.

2.3. Methodology

2.3.1. Site description and sampling time

Ten sampling sites were selected and set up in the Los Angeles Basin to fully characterize the range of conditions encountered in Southern California. The location of each site is shown in Figure 2.1. Selection criteria and site characteristics were described in detail in a previous publication of this study (Pakbin et al., 2010). Sites were categorized according to their geographical locations. HUD is located in a residential and commercial neighborhood about 2 km inland of the Ports of Los Angeles and Long Beach. It is 100 m and 1.2 km away from the Terminal Island Freeway and I-710, respectively, representing a pollutant source region. LAN is situated in a desert-dominated rural region in the City of Lancaster in the north of the Los Angeles County. It is a typical desert site over 2 km west of freeway CA-14. The 8 remaining sites are mostly on the trajectory of Los Angeles Basin, which can be grouped into West LA (GRD and LDS), Central LA (CCL and USC), East LA (HMS and FRE) and Riverside (GRA and VBR) as moving from coast to inland. The 6 sites in the Los Angeles area (GRD, LDS, CCL, USC, HMS and FRE) are urban sites with most of them located near freeway (< 1 km) except for CCL and GRD. The two inland sites in Riverside County (GRA and VBR) are considered as semi-rural receptor sites.

The one-year sampling campaign was conducted from April 2008 to March 2009. A 24-hour time-integrated sample was collected at each site once per week from 12:00 AM Pacific Standard Time (PST) to 12:00 PM PST. All substrates were collected on weekdays and removed from samplers within 24 hours after collection. Data recovery was over 88% overall. A total of 470 daily samples were submitted for chemical analysis. Monthly concentrations were calculated as the arithmetic averages of daily concentrations for all the chemical species.

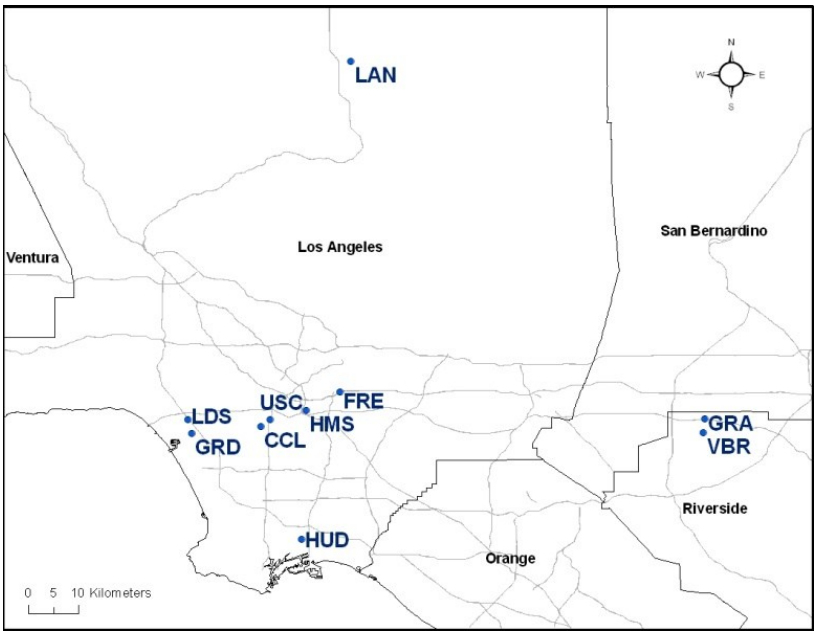

Figure 2-1: Map of the 10 sampling sites.

2.3.2. Sampling equipment and setup

At each site, dual Personal Cascade Impactor Samplers (PCIS) were employed with PM_{10} inlets (Pakbin et al., 2010) to collect size-segregated particles in the size range of 10-2.5 µm, 2.5-0.25 µm, and less than 0.25 µm at 9 liters per minute (LPM). 25mm Zefluor (3 µm pore, Pall Life Sciences, Ann Arbor MI) and quartz fiber (Whatman Inc., Florham Park, NJ) filters were used in the coarse stage of each PCIS. Zefluor filters were weighed before and after sampling for

determination of collected mass using a Mettler Microbalance (Mettler-Toledo, Columbus, OH; weight uncertainty ± 1 μg) after 24-hr equilibration under controlled temperature (21◦C ± 2◦C) and relative humidity (30% ± 5%).

A Coarse Particle Concentrator (Misra et al., 2001)—composed of a virtual impactor upstream of a filter holder—was set up in parallel to collect particles between 2.5-10 μm using the PM_{10} inlet as mentioned previously. The virtual impactor was operated at 50 LPM with a minor flow rate of 2 LPM. Particles were enriched by 25 times and collected on Teflon substrates (47mm, TefloTM, 2.0 μm pore size, Pall Cord, East Hills, NY). Substrates were also weighed before and after sampling to measure the collected mass. Comparisons between CPM mass concentrations measured by the PCIS (coarse fraction) and Coarse Particle Concentrator were described in Pakbin et al. (2010). In brief, they agree within 20% or less except in the site of Lancaster, which experienced particle bouncing at the PCIS (Pakbin et al., 2010).

2.3.3. Chemical analysis

Water extracts of the quartz filters collected from PCIS were analyzed for water soluble inorganic ions using ion chromatography (Lough et al., 2005). Elemental carbon and organic carbon were determined by the NIOSH Thermal Desorption / Optical Transmission method (Birch and Cary, 1996) using the same quartz filters. The PCIS Zefluor filters were analyzed by the Inductively Coupled Plasma-Mass Spectroscopy (ICP-MS) to determine the concentrations of the total metals and elements. Lough et al. (2005) described in detail the procedures for the process of analysis. In brief, filter membranes were extracted using a mixture of 1.5 mL of 16 N HNO_3, 0.2 mL of 28 N HF, and 0.5 mL of 12 N HCl, and subsequently digested in closed Teflon digestion vessels. Digestates were analyzed for total metals and elements using ICP-MS (PQ

Excell, ThermoElemental). Due to the issue of particle bouncing in the PCIS at the Lancaster site, substrates collected from the Coarse Particles Concentrator were used instead of those from the PCIS for the total ICP-MS analysis at this site. CPM samples collected using the Coarse Particle Concentrator contain a small fraction (4%) of fine PM that are inherently included in the minor flow of the virtual impactor. With the comparable levels of trace elements and metals in fine and coarse PM fractions previously reported in this basin (Krudysz et al., 2008; Sardar et al., 2005; Singh et al., 2002), it is unlikely that the concentrations of coarse-particulate metals and elements would be significantly affected by the inclusion of this small fraction of fine particles, so no corrections were made to account for this very small fraction of fine PM included in the coarse mode. A detailed description of the characteristics of individual metals and elements were presented in depth in a separate paper due to their importance in source apportionment and epidemiological studies, while this chapter focuses on the chemical composition, as well as the spatial and temporal properties of coarse particles. For all analytical measurements, the samples were analyzed along with field blanks, laboratory blanks, filter spikes and external check standards. On average, one blank filter was analyzed for every 10 samples. Sample spike recoveries were within the acceptance range of 85–115%. Uncertainties of the chemical measurements were propagated using the square root of the sum of squares method based on the analytical uncertainties and uncertainties from blank corrections.

2.4. Results and Discussion

2.4.1. Meteorology

Table 2.1 shows selected meteorological parameters for four seasons at sites clustered in five distinct geographical regions of the basin. Overall, mean temperature and relative humidity

exhibited little seasonality at urban Los Angeles sites, with more intense variability observed inland. With the exception of Lancaster, temperatures in fall were similar to those of summer, due to the extended warmer months of September and October, which is very typical in this region. Total precipitation was virtually insignificant in spring and summer while highest in winter. In Long Beach and along the coast, relative humidity levels were highest (61.6 - 76.8% and 58.3 – 81.0%, respectively) and peaked in summer. Further inland, at the Riverside and Lancaster sites, season-to-season fluctuations in temperature and relative humidity became more pronounced. Particularly, at the Lancaster site, the mean temperature spanned a broad range of 8.7 – 27.9°C over the seasons. Relative humidity was also lower than all other sites (26.9 - 55.9%) and dropped to as low as 26.9% in summer. These rather extreme oscillations highlight the "desert-like" conditions at this site.

Table 2-1: Selected meteorological parameters by location and season.

		Temperature (°C)	Relative humidity (%)	Precipitation (mm)	Wind (m/s)	
		Average	Average	Total	Speed (calm%)	Direction
Long Beach	Spring	16.3	65.2	12.0	1.6(4.1)	SW
	Summer	21.3	76.8	0.7	1.9(3.3)	SW
	Fall	19.9	67.8	54.8	1.2(5.6)	W
	Winter	13.8	61.6	168.9	0.7(2.9)	NW
West LA	Spring	15.0	69.0	10.9	1.7(9.8)	W
	Summer	19.4	81.0	1.5	0.7(26.2)	W
	Fall	19.0	65.3	98.0	0.2(50.2)	NE
	Winter	13.9	58.3	215.8	0.2(26.2)	NW
Central and East LA	Spring	17.2	59.0	9.7	2.1(0.6)	SW
	Summer	22.8	66.7	0.0	3.6(1.2)	SW
	Fall	20.9	55.5	184.9	1.6(4.6)	SW
	Winter	14.1	55.6	182.6	1.5(0.6)	NE
Riverside	Spring	17.4	63.4	1.8	2.6(5)	NW
	Summer	25.6	65.0	5.6	3.6(2.7)	W
	Fall	22.0	56.8	1.5	1.6(6.5)	NW
	Winter	13.8	61.8	78.5	1.3(3.9)	N
Lancaster	Spring	15.2	40.5	NA	4.1(13.5)	W
	Summer	27.9	26.9	NA	4.3(11.6)	W
	Fall	18.8	36.5	NA	1.5(30.5)	W
	Winter	8.7	55.9	NA	1.5(33.6)	W

Vector average wind speeds and directions are also shown in Table 2.1. As expected, wind direction across the sites was consistent with the prevailing air trajectory crossing the Los Angeles Basin from coast to inland (Eiguren-Fernandez et al., 2008). In the West LA, Central LA and East LA regions, winds originated from the southwest and west for most of the year, in accordance with the typical onshore flow patterns of the basin. As the air parcel proceeded inland to Riverside, the wind was deflected to northwesterly or westerly. However, this pattern was not as persistent in winter and / or fall as wind predominantly had a northerly component. In general, wind speeds were stronger away from the coast, and higher wind speeds were observed in spring and summer.

2.4.2. Data overview

Statistical summaries of annual mass concentrations of selected chemical species and gravimetric CPM are listed in Table 2.2, including the average concentrations and associated standard errors of gravimetric mass, prevalent inorganic ions, carbonaceous compounds, and the most significant elements and metals . Across the basin, CPM gravimetric concentrations were highest at HUD due to its proximity to industrial and vehicular CPM sources. In contrast, the CPM concentrations at the "desert-like" site LAN were the lowest because of its remote location from urban sources. Although not shown in the table, lower overall PM mass concentrations were observed in winter (6.93 ± 1.3 $\mu g/m^3$) compared to spring, summer and fall (12.3 ± 2.3 $\mu g/m^3$). This is consistent with the results of Sardar et al. (2005), which determined that wintertime conditions of low wind speeds and higher soil moisture lead to less re-suspension of road and soil dust, the main contributors to CPM.

Nitrate was the most predominant inorganic ion found at the 10 sampling sites, with concentrations of 1.60 ± 0.84 μg/m^3. These levels were relatively lower than those reported earlier in this basin (Sardar et al., 2005) averaging to 2.78 ± 1.7 μg/m^3. OC was overall a major CPM constituent across the basin, averaging 1.01 ± 0.56 μg/m^3, with more pronounced concentrations at the Riverside sites. Sardar et al. (2005) also reported relatively higher levels of coarse particulate OC (1.46 ± 0.62 μg/m^3) compared to this study. Among elements, those that are typical of crustal materials and soil, such as Fe, Ca, Al, Mg and Ti (Lough et al., 2005), were prevalent at all sites. Fe was the most dominant crustal element (395.5 ± 180 ng/m^3) across the basin with the exception of the Riverside and Lancaster sites, where concentrations of Fe and Al were similar. On the contrary to minerals, elements that are indicative of traffic origin in the form of re-suspended road dust, tire and brake wear, such as Ba, Zn and Cu (Lough et al., 2005), were less abundant. Their concentrations were generally lower than 50 ng/m^3, indicating the lower contribution of traffic-related emissions to coarse particles. EC was generally low across all sites (84.6 ± 94.3 ng/m^3), with the highest concentrations at HUD (190.4 ± 141 ng/m^3), consistent with its mixed residential/commercial nature and proximity to traffic.

Table 2-2: Statistical summary of annual concentrations (ng/m^3) of selected chemical species and gravimetric CPM mass concentrations.

	Long Beach	West Los Angeles		Central Los Angeles		East Los Angeles		Riverside		Lancaster
	HUD	GRD	LDS	CCL	PIU	HMS	FRE	VBR	GRA	LAN
NH_4^+	54.6±15.7	43.6±14.4	48.9±15.2	58.7±17.5	47.2±18.8	65±18.4	96.7±23.2	88.5±23.4	132±41.2	17±6.65
Cl^-	631±144	690±145	699±132	525±146	554±161	429±132	306±97.5	235±67.6	179±68	201±79.1
SO_4^{2-}	620±55.3	458±95.8	623±62.1	571±64.2	615±66.5	483±92.3	522±61.4	460±54.7	383±89.9	205±17.3
NO_3^-	1510±158	1430±172	1670±179	1860±202	1860±240	2010±257	1920±233	1720±239	1600±332	452±47.2
Mg	149±9.07	125±13.9	122±15.5	118±9.46	153±15.7	121±12.1	113±13.9	166±18.9	155±21.4	85.3±21.2
Al	357±39.6	160±20.1	248±39.8	192±23.4	293±30.2	234±17.4	237±42.2	433±43.8	366±46	335±83.6
Ca	340±33.2	173±24.1	183±15.2	243±39.8	328±29.4	250±16.3	246±37.2	432±42.5	389±48.6	213±51
Ti	28.9±3.14	16.5±2.48	20.9±3	23.5±2.95	28.7±3.08	23±1.32	27.9±3.3	34.6±3.33	32.6±4.1	30.1±7.16
Fe	462±61.2	286±50.3	367±46.4	397±63.3	487±58.4	373±26.1	410±38.8	461±42.1	425±49.4	307±62.9
Ba	21.3±3.1	16.9±3.24	21.2±3.07	28±4.93	28.9±3.78	22±1.78	25±2.04	15.2±1.55	16.1±1.6	8.7±1.49
Zn	14.1±2.13	5.88±1.24	5.62±0.99	8.3±1.4	8.95±1.19	8.01±0.8	11.2±2.86	5.96±0.58	9.62±2.22	5.17±0.73
Cu	12.8±1.85	18.8±2.59	20.9±2.34	24.1±3.02	22.9±2.39	15±1.47	21.6±2.58	10.5±1.33	10.9±1.41	21.5±8.82
OC	1190±214	767±121	809±125	1030±179	942±171	1070±121	1100±103	1380±214	1250±146	538±121
EC	190.4±43.6	63.2±19.2	54.7±20.3	87.1±27.2	81.4±27.7	88.8±32.2	80.9±21.9	84±23.2	84.2±20.6	34.9±10.1
Gravimetric CPM	13350±1059	9990±1101	9740±857.2	10080±964.9	11490±1447	10800±964.7	10010±1210	13180±1641	10550±1862	9373±1546

** Results reported as mean±standard error (ng/m^3).*

2.4.3. CPM mass reconstruction methodology

For the purpose of chemical mass reconstruction, chemical components were grouped into five categories: crustal materials and other trace elements (CM + TE), organic matter (OM), elemental carbon (EC), sea salt (SS), and secondary ions (SI). CM represents the sum of typical crustal materials, including Al, K, Fe, Ca, Mg, Ti and Si. Each of these species was multiplied by the appropriate factor to account for its common oxides based on the following equation (Chow et al., 1994; Hueglin et al., 2005; Marcazzan et al., 2001):

$$CM = 1.89Al + 1.21\ K + 1.43\ Fe + 1.4\ Ca + 1.66\ Mg + 1.7\ Ti + 2.14Si \qquad (1)$$

Elemental Si was estimated by multiplying Al using a factor of 3.41 (Hueglin et al., 2005) since it was not analyzed by the ICP-MS method used in this study. The Ca and Mg oxides were calculated using the non-sea salt (nss) portion of Ca and Mg. Since oxygen was not measured in the CPM samples, the mass of Ca and Mg oxides were estimated by multiplying Ca and Mg by 1.4 and 1.66, respectively, to account for the oxygen associated with these species. It should be noted that this approach would lead to an overestimation of the mass associated with Ca and Mg if they were ions associated with nitrate, sulfate or other directly measured ions, for which a multiplier is not needed, since these components of the Ca and Mg were measured directly. A sensitivity analysis was conducted to investigate the impact of this overestimation on the overall PM mass closure. The calculated maximum possible overestimation for Ca and Mg is 48.8 ± 7.6 ng/m^3 and 19.7 ± 2.1 ng/m^3 (mean ± standard error), respectively, which is < 1% of the overall reconstructed mass. Therefore, their impact on the overall mass closure is minimal. To test the effectiveness of summing metal oxides in estimating mineral content, Andrews et al. (2000) applied this approach to various measured soil compositions across the United States and found

that 50-90% of the measured PM sample mass could be accounted for, depending on the soil type. Other trace elements (TE) include elements such as nss-Na, Cu, Zn, and Ba. OM was obtained by multiplying the measured concentration of organic carbon (OC) by a factor of 1.8, which is based on an average of the recommended ratios of 1.6 ± 0.2 for urban aerosols and 2.1 ± 0.2 for aged or non-urban aerosols (Turpin and Lim, 2001). It should be noted that the average molecular weight per carbon weight ratio may vary with source characterization, site location, and between seasons. In our analysis, the same factor has been applied across the 10 sites and over four seasons, which may introduce some uncertainties in the overall estimations of OM to total mass. The SS contribution represents particles in the form of fresh sea salt. It is computed as the sum of measured chloride ion concentration plus the sea salt fraction of concentrations of Na^+, Mg^{2+}, K^+, Ca^{2+}, SO_4^{2-} based on the composition of seawater and ignoring atmospheric transformations (Seinfeld and Pandis, 2006):

$$SS = Cl^- + ssNa^+ + ssMg^{2+} + ssK^+ + ssCa^{2+} + ssSO_4^{2-} \quad (2)$$

where $ssNa^+ = 0.556\ Cl^-$, $ssMg^{2+} = 0.12\ ssNa^+$, $ssK^+ = 0.036\ ssNa^+$, $ssCa^{2+} = 0.038\ ssNa^+$, and $ssSO_4^{2-} = 0.252\ ssNa^+$ (Terzi et al., 2010). The EC contribution was reported as measured by thermal desorption. The SI contribution was calculated as the sum of nss-SO_4^{2-}, NH_4^+, and NO_3^-, where nss-SO_4^{2-} is total measured SO_4^{2-} minus the sea salt fraction of SO_4^{2-}.

Figure 2.2 shows a linear regression (least squares) of the daily reconstructed and gravimetric mass concentrations for all sites and all months. Thirteen out of 470 data points were omitted from this analysis, of which four data points were detected as outliers (standard deviation > 3) and nine data points were excluded due to incomplete chemical data. The gravimetric and reconstructed mass concentrations show a generally strong correlation, with a coefficient of

determination (R^2) of 0.69, indicating overall good agreement between the reconstructed mass and the gravimetric mass. Further analysis by season, as demonstrated in Figure 2.3 (a-d), reveals a seasonal trend in the correlation of the reconstructed and gravimetric mass concentrations. The season-based R^2 value ranges from 0.62 to 0.81. The overall ratio of reconstructed mass to gravimetric mass concentration is 0.89 ± 0.02 (mean ± standard error) with a seasonal variation of 0.95 ± 0.02, 0.75 ± 0.03, 0.84 ± 0.03, 1.02 ± 0.04 for spring, summer, fall and winter, respectively. These ratios are consistent with other published literature, with average ratios varying from 0.73 - 0.96 (Hueglin et al., 2005; Sillanpaa et al., 2006; Terzi et al., 2010). Higher fractions of unidentified mass were found in summer and early fall, which is consistent with other studies that showed more unidentified PM mass in summer than winter (Ho et al., 2005; Hueglin et al., 2005). The higher unidentified fraction could be attributed to the uncertainty in the OC multiplication factor used as discussed earlier coupled with some uncertainties in the conversion and estimation of elemental oxides. The discrepancy in the conversion factor used to estimate organic matter (OM) from organic carbon (OC) depends greatly on source characterization of organic component, which is generally not well known for coarse particles and may have considerable seasonal variation. For example, Zhao and Gao (2008b) demonstrated the presence of dicarboxylic acid, particularly oxalic acid, in coarse size fraction, and suggested that the formation of coarse particulate oxalate by possible photochemical reactions was favored at higher temperature. The conversion factor used in our study may also under-represent the contribution of organic matter from soils, which is likely to contain sugars and amino acids that have higher molecular weight per carbon weight ratio (Turpin and Lim, 2001).

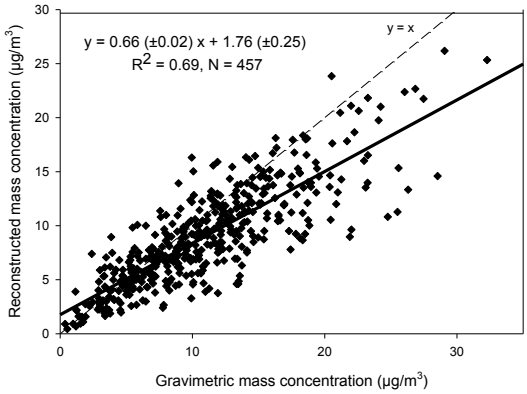

Figure 2-2: Linear regression of overall reconstructed vs. gravimetric mass concentrations. Values in parentheses represent standard errors of the slope and intercept.

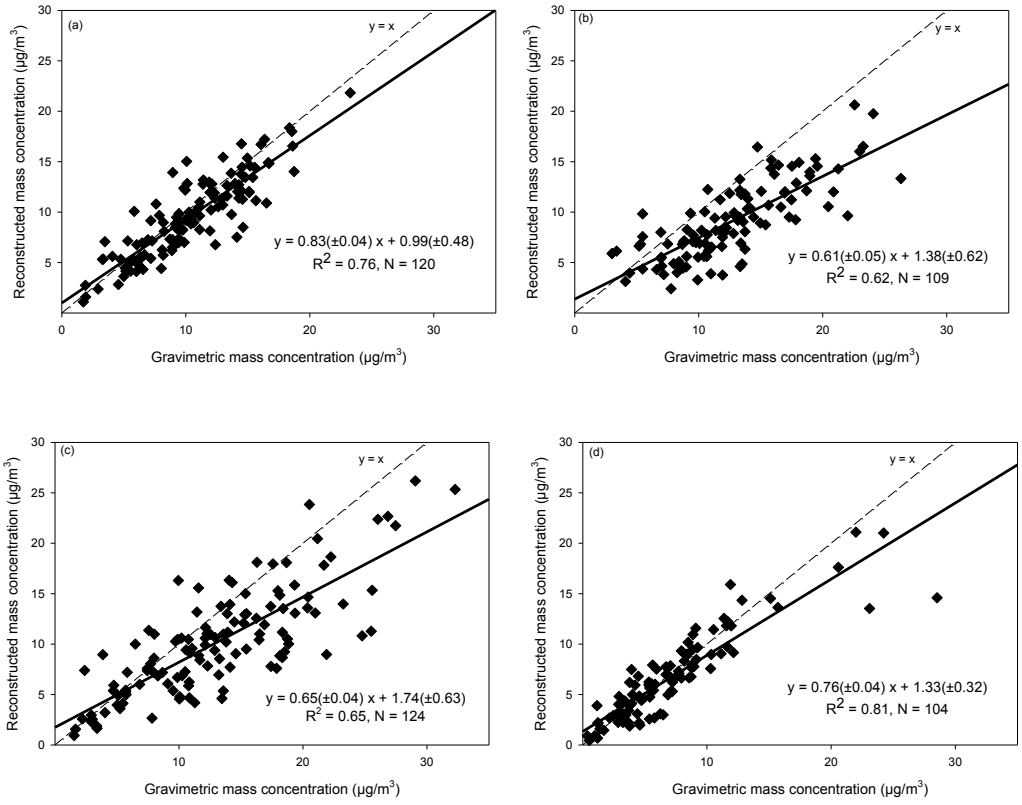

Figure 2-3: Linear regression of reconstructed vs. gravimetric mass concentrations in: (a) spring; (b) summer; (c) fall and (d) winter. Values in parentheses represent standard errors of the slope and intercept.

2.4.4. CPM mass chemical composition

Figure 2.4 (a-d) illustrates the chemical mass closure segregated by seasons (spring, summer, fall and winter) using the 5 main CPM categories, as mentioned previously. Sites were arranged according to their distance from coast (i.e. West LA, Central LA, East LA and Riverside) and their unique characteristics (i.e. the HUD site being dominated by traffic emissions, while LAN being a "desert" -like site). Annual mass ratios of the 5 categories against the total reconstructed mass, computed as the averages of all monthly mass concentrations, are shown in Table 2.3 to demonstrate the overall spatial variation in CPM mass composition.

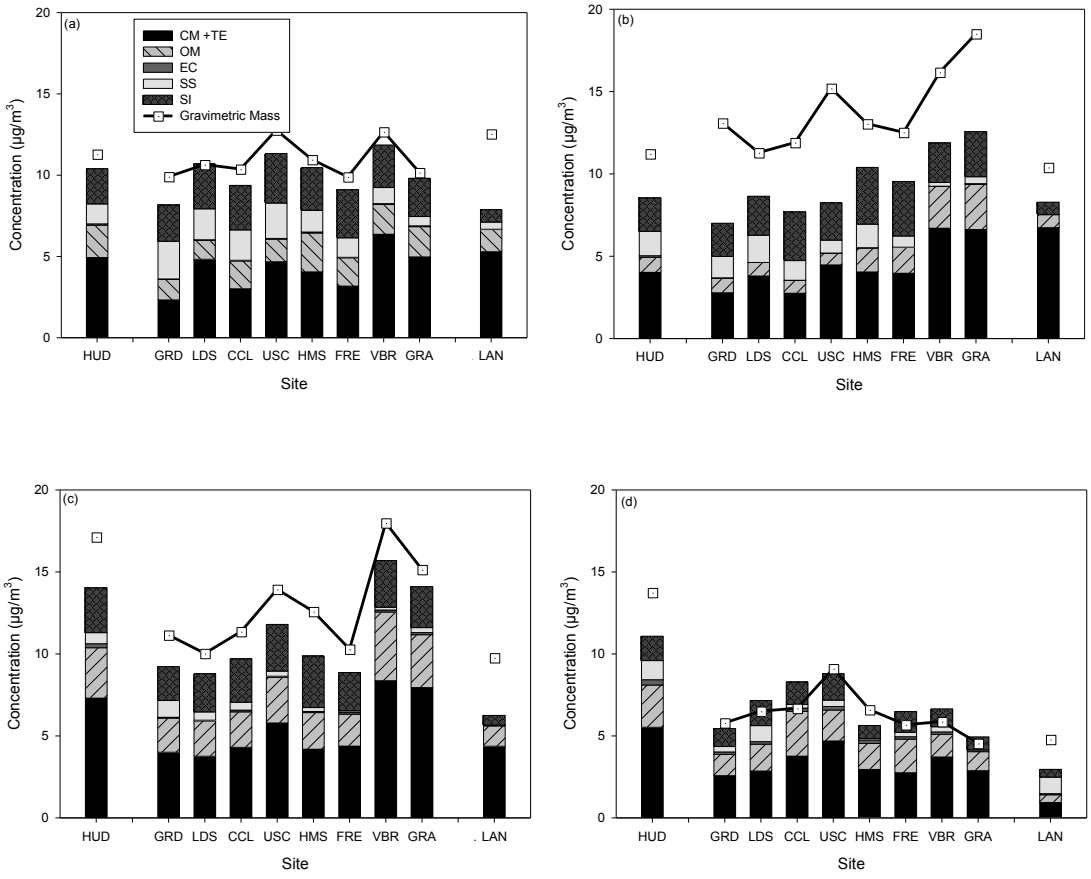

Figure 2-4: Chemical composition and gravimetric mass concentration by location in: (a) spring; (b) summer; (c) fall and (d) winter

Crustal materials and other trace elements. Crustal materials and other trace elements were the major contributors to CPM mass in all sites with an average percentage of 41.2, 44.0, 42.7, 54.7% of the total reconstructed mass in West LA, Central LA, East LA and Riverside, respectively, as shown in Table 2.3. In general, mass fractions of crustal materials and other trace elements at the two Riverside sites (VBR and GRA) and the Lancaster site (LAN) were higher than those in the urban Los Angeles sites for all seasons except winter. The elevated concentrations at the inland sites can be associated with the relatively higher wind speeds and lower relative humidity in these areas (particularly in spring and summer, as shown in Table 2.1), and their "rural" nature compared to the urban Los Angeles sites; therefore, windblown dust contributed more to the coarse particle mass concentration. The percentage of the Long Beach site (HUD), located near the I-710 freeway, was high at 49.4%. Increased levels at HUD may be attributed to its location in a pollutant "source" region of the basin and the enhancement of re-suspension of traffic emissions in the form of road dust. As discussed earlier, HUD is located near freeways with a large volume and high fraction of Heavy Duty Diesel Vehicles (HDDVs) due to its proximity to the Ports of Los Angeles and Long Beach (Pakbin et al., 2010). HDDVs are known to induce higher particle re-suspension (Charron and Harrison, 2005) with brake-wear emissions than light duty vehicles (Garg et al., 2000) thus contributing to higher roadway CPM emissions. The contribution of crustal materials and other trace elements was highest at 60.5% in Lancaster. Lancaster is a rural site with completely different chemical profile compared with other sites in the basin, and metals and elements were overall the most dominant components.

Table 2-3: Annual mass fractions (%) (mean ± standard deviation) of CPM components.

	Long Beach	West LA	Central LA	East LA	Riverside	Lancaster
CM+TE	49.4±6.7%	41.2±9.5%	44.0±10%	42.7±7.9%	54.7±8.0%	60.5±21.6%
OM	18.6±7.3%	18.0±8.3%	19.2±8.7%	22.1±7.0%	21.7±6.2%	16.0±11.2%
EC	1.75±1.3%	0.88±1.1%	0.94±1.0%	1.16±1.3%	0.99±0.9%	0.89±1.0%
SS	10.8±8.8%	15.1±8.6%	10.2±8.3%	6.94±6.6%	3.37±3.6%	10.2±17.3%
SI	19.4±5.3%	24.9±6.6%	25.6±9.1%	27.2±8.1%	19.2±7.7%	12.4±7.1%

With a few exceptions in spring and summer, when sea salt concentration was higher and inorganic aerosol formation was more prevalent, crustal materials and other trace elements were the most abundant species in coarse mode aerosols. In fall and winter, metals and elements were always the major contributors across all sites with the exception of the Lancaster site. In general, CPM mass concentrations were lower in cooler months due to stable atmospheric conditions, coupled with lower average wind speeds and higher average precipitation as shown in Table 2.1. Despite the lower CPM mass concentrations, the percentage contributions of crustal materials in winter (43.5 ± 9.8%) were similar to or higher than those of spring (38.3 ± 13%), summer (40.7 ± 16%) and fall (44.1 ± 11%), indicating the significant contribution of the soil dust materials to CPM in this basin.

In order to assess the relative contributions of anthropogenic vs. crustal sources of trace elements bound to CPM, crustal enrichment factors (CEFs) were calculated by dividing the selected element abundance in the PM sample by their average abundance in the upper continental crust (UCC) obtained from Taylor and McLennan (1985), after normalization to Al as the reference element. The CEFs of the 10 sampling sites are presented in Figure 2.5, with sites categorized geographically into Los Angeles (GRD, LDS, CCL, UCS, HMS and FRE), Long Beach (HUD), Riverside (VBR and GRA) and Lancaster (LAN). Typically, CEF > 10 are indicative of PM sources different from crustal material, notably anthropogenic sources. The

CEFs were generally higher at urban sites of Los Angeles and Long Beach, with lowest CEFs observed in Lancaster. Elements with the highest CEFs were Sb, Sn, Mo, S, Cu, Pb Zn, and Ba, which are indicative of traffic-related emissions (Lough et al., 2005). The higher CEFs observed at urban sites provide further evidence that the majority of these transition metals are released in the atmosphere through abrasive vehicular emissions, particularly the wear of brake and tire lining (Lin et al., 2005).

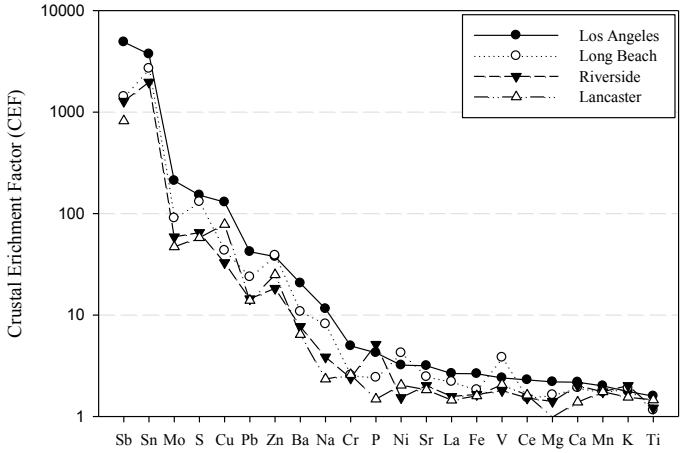

Figure 2-5: Crustal enrichment factors of individual elements at Los Angeles, Long Beach, Riverside and Lancaster. The reference element is Al.

In this study, Fe and Al were the two most abundant minerals, together with Si (which as we noted earlier was estimated from the Al concentrations), their sum accounted for an average of 62.0% of total measured crustal materials and other trace elements, and 29.5% of total reconstructed mass. This is consistent with other studies which show that crustal material is a major source of coarse mode aerosol in both urban and sub-urban environments (Hueglin et al., 2005; Sillanpaa et al., 2006). On the other hand, elements related to anthropogenic sources, such as Cu and Sb from brake wear (Lin et al., 2005), had concentrations that were low compared with

the mineral dust. Overall, natural crustal elements were the major component of this category, while anthropogenic sources contributed to a much lesser extent.

Carbonaceous compounds. Organic matter was a substantial constituent of CPM, with an average contribution of 19.7 ± 8.1% to the total reconstructed mass. EC concentrations were low in general, contributing to approximately 1.1% of total reconstructed mass, consistent with the literature that EC mostly exists in the fine PM mode (Huang and Yu, 2008). Seasonal average of OM fraction was generally higher in fall (23.0 ± 6.8%) and winter (24.5 ± 8.3%) compared with spring (16.5 ± 6.6%) and summer (14.6 ± 6.0%). Although PM mass concentrations were lower in winter, OM fraction increased in all sites. It suggested that OM in the coarse mode was not much affected by local meteorology and it probably had a stable source strength year-long. On the other hand, the concentrations of OM were generally lowest in summer in the basin with the exception of the two Riverside sites.

The two inland sites (VBR and GRA) had higher OM concentrations in summer and fall, when the corresponding gravimetric mass concentrations were also higher. Despite the lower OM concentrations in the source sites in summer, OM concentrations remained high in the two inland sites. With their proximity to the Chino dairy farm area which is located along the trajectories from coast to inland (Eiguren-Fernandez et al., 2008), it is possible that biological materials, including humic substances, have contributed to the high organic content. This is consistent with recent literature which showed that organic materials with biological origins, such as bacteria, viruses, fungus, spores, pollens, algae and plant debris, were a significant component of PM_{10} in urban atmospheres (Bauer et al., 2008; Winiwarter et al., 2009). The Lancaster site (LAN), on the other hand, was low in both mass fractions and concentrations of OM due to its “desert-like” site

characteristics. The Long Beach site (HUD) had the overall highest EC fraction (on average 1.75%) likely due to its location near freeways with higher number and proportion of HDDVs, which generally emit higher EC compared with gasoline vehicles (Biswas et al., 2009).

Table 2-4: Regression analysis of organic carbon (OC) vs. 4 main coarse PM categories and selected species in: (a) spring and summer and (b) fall and winter.

(a)	y=mx+c	R
OC-CM+TE	0.15x+194.9	0.56
OC-EC	-1.73x+914.9	-0.21
OC-SS	-0.07x+927.4	-0.15
OC-SI	0.09x+627.9	0.22
OC-Ti	31.26x+127.6	0.68
OC-Fe	2.27x+139.7	0.59
OC-Cu	-18.43x+1094	-0.27

(b)	y=mx+c	R
OC-CM+TE	0.2x+278.9	0.72
OC-EC	2.97x+755.7	0.43
OC-SS	-0.3x+12923	-0.19
OC-SI	0.29x+643.7	0.46
OC-Ti	39.16x+114.9	0.76
OC-Fe	2.39x+48.18	0.74
OC-Cu	11.86x+912.9	0.17

While OC particles in fine and ultrafine modes mostly originate from primary sources such as fossil fuel combustion (Arhami et al., 2010; Minguillon et al., 2008) and secondary sources by photochemical reactions in the atmosphere (Verma et al., 2009b), the sources of OC in CPM are not well understood. Previous studies have found good correlations between OC and EC in fine and ultrafine modes PM in the Los Angeles Basin, suggesting their shared common source from vehicle emissions (Geller et al., 2002; Sardar et al., 2005). However, the overall association between OC and EC is low (R = 0.36) in this study, indicating that the sources of OC in CPM might be different from- or in addition to those of EC. As previously mentioned, biological materials constitute a potential source of coarse mode OC. To investigate the sources of organics, linear regression analysis was performed against OC and other CPM categories and specific

tracers of some of these CPM groups. Table 2.4 (a-b) shows the regression equation and the corresponding correlation coefficient in different seasons. As mentioned above, low associations are found between EC and OC. Cu, a tracer of brake wear (Lin et al., 2005), also displayed low correlations with OC. On the contrary, OC is well-correlated with CM and TE, and soil dust tracers of Ti and Fe in all seasons (R = 0.56 – 0.76), consistent with results reported in other studies (Koulouri et al., 2008).

Table 2-5: Correlation coefficient (R) between organic carbon (OC) and soil dust tracers of Fe and Ti at the 10 sampling sites.

	HUD	GRD	LDS	CCL	USC	FRE	HMS	GRA	VBR	LAN
Fe	0.80	0.69	0.62	0.72	0.87	0.07	0.61	0.83	0.77	0.60
Ti	0.79	0.74	0.52	0.68	0.78	0.12	0.77	0.81	0.81	0.65

Site-specific correlations are shown in Table 2.5 to examine the spatial variability of these high associations between OC and soil dust tracers. With the exception of one site (FRE), which is located <50 m from freeway I-10, soil dust tracers are well-correlated with organic carbon (R = 0.52 - 0.87). These correlations indicate that OC and crustal materials either share common sources or that OC may be adsorbed or absorbed onto soil dust PM and collected simultaneously during sampling. Humic substances—a major organic component of soil, might be re-suspended with soil-derived dust particles, which could result in the observed high correlations. Overall, the low correlations between OC and traffic-related emissions, coupled with generally good correlations between OC and mineral dust tracers suggest that humic substances might be the major component in coarse particulate OC. Since the composition of OC in the coarse fraction might have important public health impacts, further investigation of coarse PM-bound OC composition is essential to evaluate its role in CPM-induced adverse health effects.

Sea salt. Chloride and sodium ions, and to a lesser extent magnesium and sulfate ions, comprise

the majority of sea salt components. Overall, sea salt particles contributed to an average of 9.1 ± 9% across all sites and months, indicating its significance in coarse mode particles in this basin. The percentage contributions during spring and summer (12.7 ± 9.7%) were higher than those in fall and winter (5.9 ± 7.7%). The higher standard deviations were driven mostly by spatial variations, but the overall trend of higher sea salt content in spring and summer was prevalent at every site with the exception of Lancaster. Concentrations of sea salt particles were generally higher in spring and summer due to the increased strength of southwesterly winds in the afternoon that transport air masses from the source areas along the coast to the inland receptor areas. Lower concentrations were observed in fall and winter because of the lower wind speed and the change of wind direction at certain sites (Table 2.1.)

Sea salt particles originate from the Pacific Ocean located in the west of the Basin. As a result, the mass fractions of sea salt decreased from west to east in all seasons, with an average fraction of 15.1, 10.2, 6.9, 3.4% in West LA, Central LA, East LA and Riverside respectively as shown in Table 2.3. GRD and HUD had highest concentrations due to their proximity to the ocean. The two inland sites in Riverside (about 80 km inland of downtown Los Angeles and about 100 km inland of the Pacific coast) on the contrary, had lower concentrations, of less than half of the concentrations of the coastal sites. Since the atmospheric lifetime of CPM typically varies from hours to days (Ruzer and Harley, 2004), depending on its aerodynamic diameter and wind speed, the loss of these species along the prevailing air parcel advection trajectory from the west to the east of the basin is consistent with expectations. Sea salt concentrations were higher in winter in the Lancaster site. The high concentrations might be attributed to specific local sources of chloride, the identification of which requires further investigation.

Secondary ions. Overall, secondary ions contributed on average 22.6 ± 8.7% of the total reconstructed mass, with nitrate being the major component. Sulfate particles of sea salt origins contributed to approximately 12.3% of total measured sulfate in this study, which is not included in this category. Mass fractions of secondary ions were higher in spring and summer (25.4 ± 8.7%) than in fall and winter (19.7 ± 7.9%). Spatially, sites that were further inland had lower mass fractions (19.2 ± 7.7% and 12.4 ± 7.1% for Riverside and Lancaster respectively) than sites in the West LA (24.9% ± 6.6%), Central LA (25.6 ± 9.1%) and East LA (27.2 ± 8.1%) regions as shown in Table 2.3.

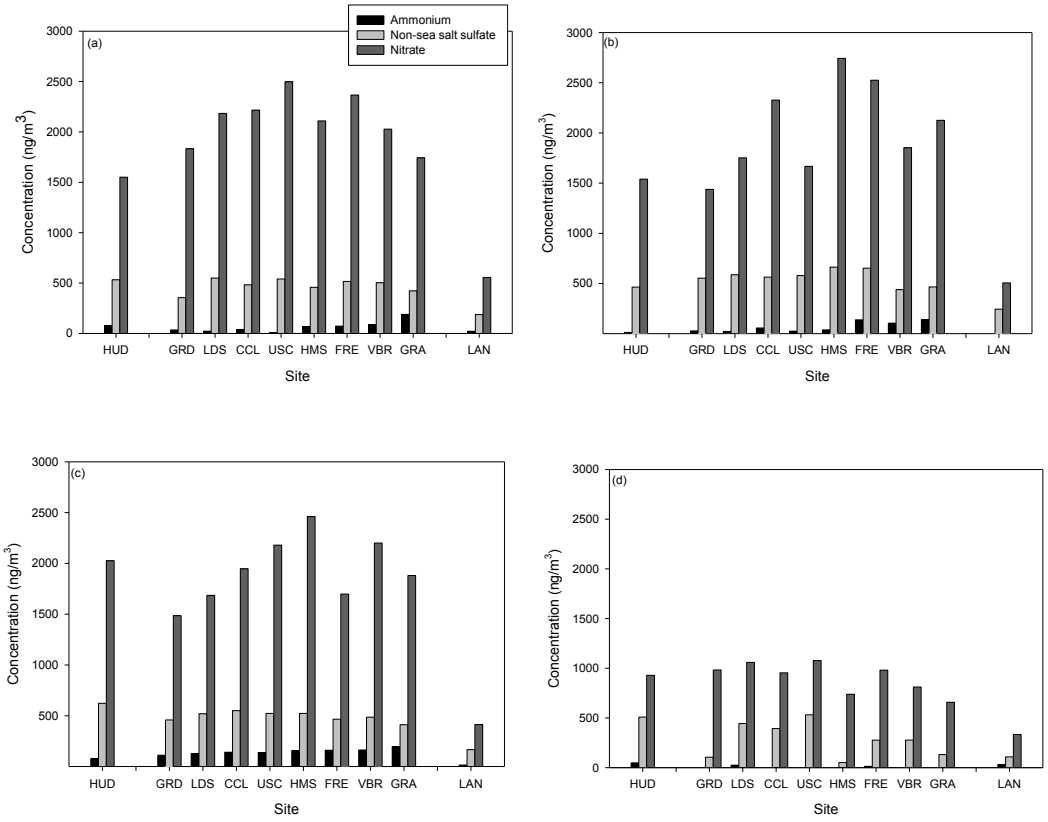

Figure 2-6: Ammonium, non-sea salt sulfate and nitrate concentrations by location in: (a) spring; (b) summer; (c) fall; and (d) winter.

Figure 2.6 (a-d) shows the seasonal concentrations of ammonium, nss-sulfate and nitrate ions. Nitrate was the most abundant inorganic ion of CPM, accounting for about 74% of the category of secondary ions. High levels of coarse particulate nitrate, formed by the reactions of nitric acid and its precursors with soil dust and sea salt aerosols, were observed in some other studies in urban areas (Noble and Prather, 1996; Zhuang et al., 1999). In fall and winter, mass fractions of nitrate were relatively lower (15.0 ± 6.2%) than those of spring and summer (19.7 ± 7.1%). Sulfate concentrations, on the other hand, were considerably lower than those of nitrate, probably because most of the measured sulfate in CPM reflects a "tail" of the upper size range of $(NH_4)_2SO_4$, which mostly exists in the fine PM mode (Lun et al., 2003; Seinfeld and Pandis, 2006). The presence of gypsum, which is slightly-to-moderately soluble in water, might also be a possible source of coarse particulate sulfate. The overall low concentration of sulfate ion, coupled with the relatively comparable sulfate concentration at the inland sites, suggests that the contribution of soluble gypsum to overall PM mass is not dominant in this basin. Little spatial variation was observed on sulfate across this basin (excluding Lancaster), with the exception of winter, when sulfate concentrations were generally lower, and significant spatial variation was observed. Ammonium concentrations were very low, contributing to an average of less than 1% to total reconstructed mass, consistent with many studies that showed ammonium particles mostly exist in the fine mode (Karageorgos and Rapsomanikis, 2007; Sillanpaa et al., 2006). NH_4NO_3 and $(NH_4)_2SO_4$ are formed by the reactions of ammonia with acidic gases and are the two major forms of PM ammonium in the urban atmosphere; both ammonium salts exist predominately in the fine mode, with a minor fraction extended to the size range of coarse particles (Lun et al., 2003; Yoshizumi and Hoshi, 1985). Thus, the low ammonium concentrations observed here might

reflect the tail of the upper size range of $PM_{2.5}$-bound ammonium salts. Ammonium concentrations were particularly low in winter, probably because acidic gases—forming primarily from photochemically initiated reactions—were less abundant in that time period. Higher ammonium concentrations were generally observed in the Riverside sites (VBR and GRA) possibly due to the higher ammonia concentrations in that area, generated by the nearby dairy farm (Geller et al., 2004; Hughes et al., 1999).

2.4.5. Coefficients of divergence (COD) calculations for chemical species concentrations

To study the intra-urban variability of different chemical species, seasonal CODs were calculated across all sites (with the exception of LAN) for the monthly concentrations. COD value is a measure of the heterogeneity between sites with a range from 0 to 1. A low COD value (< 0.2) indicates a high level of homogeneity in concentrations between sites, while CODs larger than 0.2 are considered heterogeneous (Wilson et al. 2005). It is important to note that the analytical uncertainty might also increase the COD values, particularly for the species with lower concentrations.

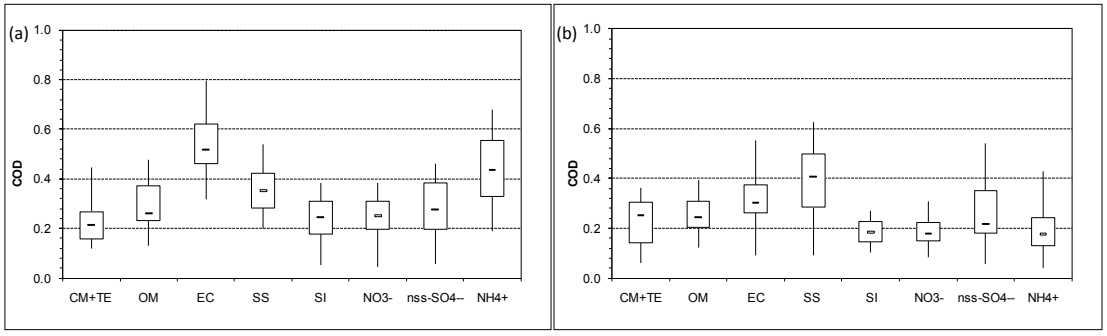

Figure 2-7: Coefficients of divergence (COD) for all sites (excluding Lancaster) in: (a) spring and summer and (b) fall and winter.

Figure 2.7 (a-b) shows the COD for the 5 main categories and the ionic species in spring and summer, and fall and winter. Box plots were used to show the minimum, lower quartile (Q1), median, upper quartile (Q3) and maximum values observed. Overall, the median CODs range from 0.21 to 0.52 in spring and summer, and 0.18 to 0.41 in fall and winter. In spring and summer, nss-sulfate and nitrate ions, as well as the categories of CM + TE and OM experienced modest heterogeneity, as shown by the relatively lower median COD values. On the other hand, the highest median COD value was found for EC, probably because its concentrations varied depending on proximity to freeways or heavy-duty vehicles. Given the low EC concentrations, analytical measurement uncertainty might have also contributed to its high COD value. In fall and winter, median COD value was lowest for secondary ions. In particular, nitrate ion has both a low median COD value and a small inter-quartile range, consistent with the results in spring and summer, highlighting its low spatial and temporal variation in this basin. On the other hand, sea salt particles experienced higher heterogeneity and had a large inter-quartile COD range, consistent with their high spatial variation as discussed previously. The concentrations of nss-sulfate also varied significantly across sites in winter, as shown in Figure 2.6d. The variations are illustrated in the higher range of COD of nss-sulfate. Overall, the categories of EC and SS had relatively higher COD values than the rest of the measured species or groups of CPM because their concentrations depend heavily on the proximity to their sources. In contrast, CM + TE, OM and nitrate had relatively lower COD values, consistent with our discussion in previous sections indicating that these species are dominant components at every site and have relatively stable source strengths year-long.

2.5. Summary and Conclusions

Crustal materials and other trace elements comprise overall the major fraction of CPM mass. The annual mass fractions vary from 41.2% - 60.5% across the 10 sampling sites, with higher fractions inland. Secondary ions (nitrate, nss-sulfate and ammonium) also contributed significantly to the CPM mass, with an average ratio of 22.6 %. In particular, particulate nitrate accounted for about 17.2% of the total reconstructed mass. Carbonaceous compounds comprised a substantial portion of coarse particles. Organic matter contributed to an average of 19.7%, while elemental carbon was a much less significant component at 1.1%. Sea salt particles accounted for an average mass fraction of 9.14%, with generally higher fractions in spring and summer, due to the strong prevailing onshore winds in that period. The origin of organic carbon was investigated using linear regression analysis. Organic carbon was found to be well correlated with crustal materials and other trace elements. Higher correlation coefficients were found with soil dust tracers ($R = 0.74$ and 0.72 for Ti and Fe, respectively), suggesting that OC and mineral dust either share common origins or that OC may be adsorbed or absorbed onto soil dust particles and collected simultaneously during PM sampling.

2.6. Acknowledgements

The work presented in this paper was funded by the Science to Achieve Results program of the United States Environmental Protection Agency (EPA-G2006-STAR-Q1). The authors would like to thank the staff at the Wisconsin State Laboratory of Hygiene and Mike Olson of University of Wisconsin, Madison for the assistance with chemical analyses.

Chapter 3 Seasonal and Spatial Variations of Individual Organic Compounds of Coarse Particulate Matter in the Los Angeles Basin

3.1. Abstract

To study the organic composition of ambient coarse particulate matter (CPM; 2.5-10 μm), CPM were collected one day a week from April 2008 to March 2009 at 10 sampling sites in the Los Angeles Basin. Samples were compiled into summer (June to September 2008) and winter (November 2008 to February 2009) composites, and were analyzed for individual organic constituents using gas chromatography-mass spectrometry. *n*-alkanoic acids and medium molecular weight (MW) *n*-alkanes (C25 to C35)– the major constituents in the coarse size fraction– showed good associations with crustal materials. Polycyclic aromatic hydrocarbons (PAHs) and hopanes (both in low concentrations), as well as high MW *n*-alkanes (C37 and C38), were associated with traffic-related emissions. In the summer, when prevailing onshore winds were strong, the downwind/rural sites had higher concentrations of PAHs, *n*-alkanes and *n*-alkanoic acids. An opposite trend was observed at the urban sites, where the levels of PAHs, *n*-alkanes and *n*-alkanoic acids were higher in the winter, when the wind speeds were low. In general, the contribution of organic compounds to CPM was higher in the winter, due to a reduction in the fraction of other CPM components and/or the increase in source strengths of organic compounds. The latter is consistent with the traffic-induced re-suspension of mineral and road dust, as previously observed in this basin. Overall, our results suggest that emissions from natural sources (soil and associated biota) constitute the majority of the organic content in coarse particles, with a more pronounced influence in the semi-rural/rural areas in Riverside/Lancaster compared with urban Los Angeles in the summer.

3.2. Introduction

Evidence has linked exposure to coarse particulate matter (CPM) to adverse health outcomes, including hospital admissions and mortality (Brunekreef and Forsberg, 2005; Qiu et al., 2012). Investigators suggest that these associations may be driven by specific chemical components (Castillejos et al., 2000). Mineral dust, sea salt, secondary ions and organic matter are the dominant components of CPM. Organic matter (OM) contributed to ~10-20% of the CPM gravimetric mass in most studied areas (Cheung et al., 2011b; Ho et al., 2005). Despite its significant contribution, the organic composition of coarse particles has remained largely uncharacterized. Organic content in the fine PM mode mostly originates from primary emissions, such as fossil fuel combustion (Fine et al., 2004a), and secondary formation by photochemical reactions (Docherty et al., 2008). Good correlations between organic carbon (OC) and elemental carbon (EC) were observed in studies conducted in the Los Angeles Basin measuring fine and ultrafine PM (Geller et al., 2002; Sardar et al., 2005), suggesting vehicular emission as a major source of OC. Yet, particles originating from combustion and secondary formation mostly reside in the fine mode, with only a minor fraction intercalating into the coarse size fraction (Gertler et al., 2000), thereby making their contribution to the OC measured in CPM rather unlikely. On the other hand, biological material, such as bacteria, viruses, spores, pollens, and plant debris, was shown to be a significant component of PM_{10} in urban atmospheres (Bauer et al., 2008; Samy et al., 2011). Using scanning electron microscopy, Falkovich et al. (2004) also demonstrated the adsorption of organics species onto mineral dust particles. Nonetheless, our understanding on the sources and formation mechanisms of CPM-bound organic species is still quite limited.

To study the physico-chemical properties of CPM, a comprehensive study was conducted at 10 sampling sites in the Los Angeles Basin from April 2008 to March 2009. The chemical mass closure was reported in a previous publication of this study (Cheung et al., 2011b), and an overall low association between OC and EC was reported (R=0.36), suggesting that the sources of OC in the coarse mode might be different from-or in addition to those of EC. This paper focuses on characterizing individual organic compounds in CPM. The examination of the spatial and seasonal variations of these constituents further elucidates their sources and formation mechanism. This information is vital in understanding the role of organic compounds in CPM-induced toxicity, and may help the regulatory community to design more effective strategies to control the emissions and ambient levels of these particles.

3.3. Methodology

Details of the sampling location, equipment and methods are described in the previous chapter (Chapter 2).

3.3.1. Chemical analysis

The quartz substrates were analyzed for organic carbon (OC), elemental carbon (EC), and water-soluble inorganic ions, while the Zefluor substrates were used for the analysis of total elements. The quantification of these species allowed the chemical mass reconstruction of the sampled coarse particles, the results of which were reported and discussed in detail in a previous publication of this study (Cheung et al., 2011b). The quantification of particulate organic compounds – including *n*-alkanes, organic acids, hopanes, steranes and PAHs– constitutes the core of this article. These organic molecular markers were selected because they have been traditionally used for source characterization. To measure the level of individual organic species,

quartz substrates were composited for two seasons: (1) summer, from June to September 2008 and (2) winter, from November 2008 to February 2009. The overall average CPM mass concentrations were 13 (±4.6) and 7.6 (±5.0) μg/m^3 for the summer and winter, respectively. Samples were extracted in a 50/50 dichloromethane/acetone solution using Soxhlets, followed by rotary evaporation and volume reduction under high-purity nitrogen, until the final volume of 100 μl was reached for each sample. The samples, along with field blanks, laboratory blanks, filter spikes, and check standards, were subsequently analyzed for organic composition using gas chromatography-mass spectrometry (GCMS) (Sheesley et al., 2004). Total uncertainties were propagated using the square root of the sum of squares method based on the analytical uncertainties and uncertainties from field blanks, which account for the uncertainties arising from field handling, storage, shipping and analytical instruments. Detection limit is defined as two times the total uncertainty in this study. Concentrations were reported after field blank subtraction to account for the background levels of the measured species.

3.4. Results and Discussion

3.4.1. Overview

The meteorological conditions during the sampling campaign are presented in Chapter 2. In brief, the subtropical Mediterranean climate of the Los Angeles Basin was highlighted by a warmer summer (avg. temperature=23±3.1^{o}C) and a cooler winter (avg. temperature=14±2.3^{o}C). The diurnal variation of temperature could also be substantial in this basin, and the difference between the highest and lowest temperature in a day exceeded 10^{o}C in the summer and winter. Westerly onshore winds were prevalent in the summer (ca. 0.75-3.8 m/s), resulting in the long-range transport of atmospheric pollutants from coast to inland. Wind speeds were lower in

the winter (ca. 0.17-1.4 m/s), with a more diverse wind direction. Seasonal fluctuations of meteorological parameters at the inland sites (Riverside and Lancaster) were more pronounced, as highlighted by the more extreme oscillations of temperature.

Table 3.1 shows the concentrations (ng/m^3) of organic compound class at the 10 sampling sites in the summer and winter. PAHs are segregated into 4 categories according to their molecular weights: MW=202 g/mole [fluoranthene, acephenanthrylene, pyrene], MW=228 g/mole [benz(a)anthracene, chrysene], MW=252 g/mole [Benzo(b)fluoranthene, benzo(k)-fluoranthene, benzo(j)fluoranthene, benzo(e)pyrene and benzo(a)pyrene, perylene] and MW≥276 g/mole [Indeno(1,2,3-cd)pyrene, benzo(ghi)perylene, dibenz(ah)anthracene, picene, coronene, and dibenzo(ae)pyrene]. The overall concentrations of PAHs were low, with mostly undetectable levels. Hopanes and steranes, both tracers of vehicular emissions, were also present in low concentrations (<1 ng/m^3). The group of *n*-alkanes was calculated as the sum of *n*-alkanes analyzed in this study, ranging from C11 to C38. The levels of C11 to C19 were below detection limits for all sites/seasons, likely due to the semi-volatile nature of these light alkanes (Schnelle-Kreis et al., 2005).Total *n*-alkanes levels were significant at all samplings sites (~3.5-15 ng/m^3). The group of *n*-alkanoic acids (sum of C15 to C30) is the most prominent compound class in this study, with concentrations ranging from 9.3-64.2 ng/m^3. Levels under the detection limit were treated as zero in these sums. The level of detection (LOD) of the sum of a group of compounds was calculated as 2 times the square root of the sum of squares of the uncertainties for each species in the limit as the concentration of the species approaches zero. The spatial and seasonal variations of these compound classes are discussed in detail in the following sections.

Table 3-1: Summary table of organic component concentration (ng/m^3) at the 10 sampling sites in: (a) summer and (b) winter. BDL denotes below detection limit.

(a)	HUD	GRD	LDS	CCL	USC	HMS	FRE	VBR	GRA	LAN
[1]∑ PAHs, MW=202	*BDL*	*BDL*	*BDL*	*BDL*	*BDL*	*BDL*	*BDL*	*BDL*	*BDL*	*BDL*
[2]∑ PAHs, MW=228	0.081	*BDL*	*BDL*	*BDL*	*BDL*	*BDL*	0.11	0.083	*BDL*	*BDL*
[3]∑ PAHs, MW=252	0.095	*BDL*	*BDL*	*BDL*	*BDL*	*BDL*	0.20	0.10	0.084	*BDL*
[4]∑ PAHs, MW≥276	*BDL*	*BDL*	*BDL*	*BDL*	*BDL*	*BDL*	*BDL*	*BDL*	*BDL*	*BDL*
[5]∑ Hopanes	0.10	*BDL*	0.041	0.11	0.18	0.12	0.067	0.065	0.12	0.22
[6]∑ Steranes	*BDL*	*BDL*	*BDL*	*BDL*	*BDL*	*BDL*	*BDL*	*BDL*	*BDL*	0.054
∑ n-Alkanes	3.5	4.8	5.3	4.0	8.1	4.9	7.9	10.8	10.9	8.7
∑ n-Alkanoic acids	26.9	20.3	20.4	19.1	35.0	24.9	26.1	64.2	53.3	26.6

(b)	HUD	GRD	LDS	CCL	USC	HMS	FRE	VBR	GRA	LAN
[1]∑ PAHs, MW=202	0.092	*BDL*	*BDL*	*BDL*	*BDL*	*BDL*	*BDL*	*BDL*	*BDL*	*BDL*
[2]∑ PAHs, MW=228	0.12	*BDL*	*BDL*	*BDL*	*BDL*	*BDL*	0.086	0.041	*BDL*	*BDL*
[3]∑ PAHs, MW=252	0.16	*BDL*	*BDL*	0.14	*BDL*	*BDL*	0.11	*BDL*	*BDL*	*BDL*
[4]∑ PAHs, MW≥276	0.069	*BDL*	*BDL*	*BDL*	*BDL*	*BDL*	*BDL*	*BDL*	*BDL*	*BDL*
[5]∑ Hopanes	0.81	0.17	0.18	0.28	0.28	0.24	0.087	0.18	0.18	0.088
[6]∑ Steranes	0.28	*BDL*	*BDL*	0.045	*BDL*	0.043	*BDL*	*BDL*	*BDL*	*BDL*
∑ n-Alkanes	14.6	9.8	8.0	8.8	7.4	10.3	7.0	10.0	6.9	4.6
∑ n-Alkanoic acids	31.1	21.2	26.4	53.4	32.8	26.3	24.3	40.4	23.3	9.3

1. The level of detection for ∑ PAHs, MW=202 is 0.055 ng/m^3
2. The level of detection for ∑ PAHs, MW=228 is 0.038 ng/m^3
3. The level of detection for ∑ PAHs, MW=252 is 0.051 ng/m^3
4. The level of detection for ∑ PAHs, MW≥276 is 0.061 ng/m^3
5. The level of detection for ∑ Hopanes is 0.031 ng/m^3
6. The level of detection for ∑ Steranes is 0.023 ng/m^3

3.4.2. PAHs

Mounting evidence has documented adverse health effects caused by PAHs (Schwarze et al., 2007; Sram et al., 1999). Particulate phase PAHs are mostly sub-micron particles originating from combustion emissions and gas-to-particle partitioning (Miguel et al., 2004). In the coarse size fraction, PAHs are likely to originate either from the debris of tire abrasion (Rogge et al., 1993a), and/or the condensation of semi-volatile species on CPM surfaces. Figure 3.1 shows the levels of PAHs, as well as the LOD, among the 10 sampling sites, segregated by MW. In the summer, chrysene, which could be found in both industrial and vehicular emissions (Khalili et al., 1995), contributed to the sum of PAH with MW=228 g/mole, with the highest concentrations at FRE (0.11 ng/m^3), where it is ~50 m north of Freeway I-10. In Riverside (a receptor area particularly during the summer when onshore winds were strong), PAHs with MW=228 g/mole and MW=252

g/mole had generally higher levels in the summer than in the winter, a finding consistent with an earlier study conducted in Claremont, CA, a downwind receptor location, where elevated levels of PAHs were observed in the coarse mode in the spring and summer (Miguel et al., 2004). In the winter, fluoranthene and pyrene (both of which are semi-volatile PAHs that partition between gas and particle phase) contributed to the sum of low MW PAHs (MW=202 g/mole) in the Long Beach site (HUD). Among the 10 sampling sites, HUD and FRE, both in close proximity to traffic (within 100 m from nearby highway/freeway), had the highest overall PAH levels.

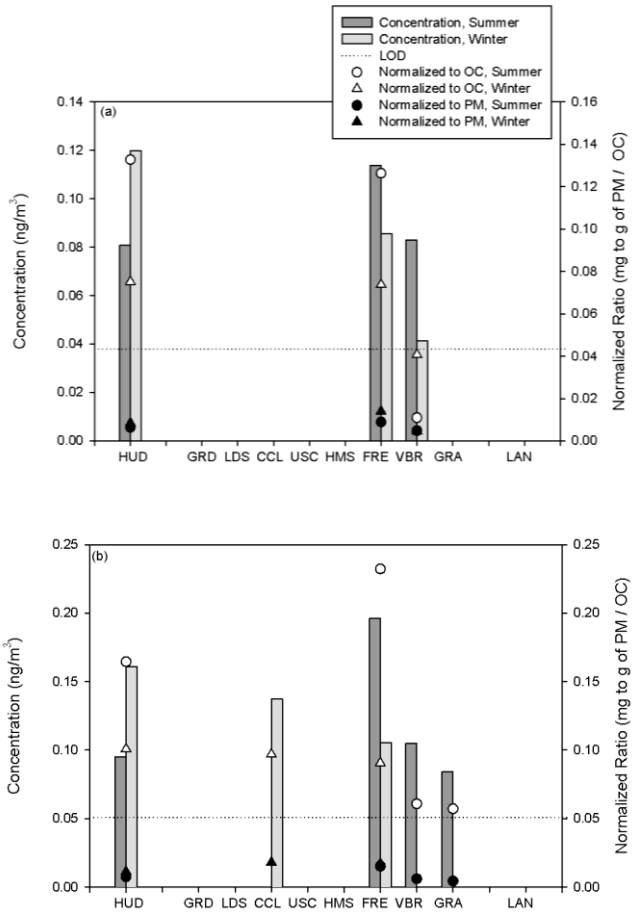

Figure 3-1: Concentration (ng/m^3) of PAHs with (a) MW = 228 g/mole and (b) MW = 252 g/mole. The level of detection (LOD) of the compound class is shown as a reference line.

3.4.3. Hopanes and steranes

Hopanes and steranes are indicators of fossil fuel combustion (Simoneit, 1999). In particular, they are known to be emitted from gasoline and diesel vehicles primarily through the use of engine lubricating oil, and are widely used as the organic markers of vehicular emissions in urban environments (Fine et al., 2004a). Wang et al. (2009) showed that the majority of hopanes resided in the fine PM mode, and lower hopane levels were observed in the coarse size range. Thus, the low hopane level (avg.=0.18 ±0.17 ng/m^3) observed in this study is consistent with the published literature.

In the summer, the average hopane concentration was 0.10±0.052 ng/m^3 across the 10 sampling sites. The highest hopane level was found in Lancaster (Figure 3.2), which was unexpected due to its remote location. It is possible that road dust is enriched by anthropogenic particles over time in that area, particularly in the summer when atmospheric transport is strong. In the winter, hopane levels were higher, with an average of 0.25±0.21 ng/m^3. The high standard deviation was driven by the peak at the Long Beach site (HUD), which coincides with the high level of EC in the same period. This site is located ~2 km from the Port of Los Angeles and the Port of Long Beach, and is influenced by port-related emissions. Therefore, the high EC and hopane levels in the winter may be attributable to emissions from heavy-duty diesel vehicles and, to a lesser extent, marine vessels. These emissions could accumulate around the harbor area when atmospheric dilution was low. Furthermore, with the exception of Lancaster, the levels of hopanes were all elevated in the winter. The normalized ratios (to PM) were also much higher in the winter (ca. 3 times), suggesting stronger source strengths of vehicular emissions during that period. Considering the relative consistency of traffic volume and composition in the Los Angeles

Basin throughout the year, the elevated hopane levels are likely due to the lower atmospheric mixing and / or the increased re-suspension by traffic during cooler periods (Cheung et al., 2012).

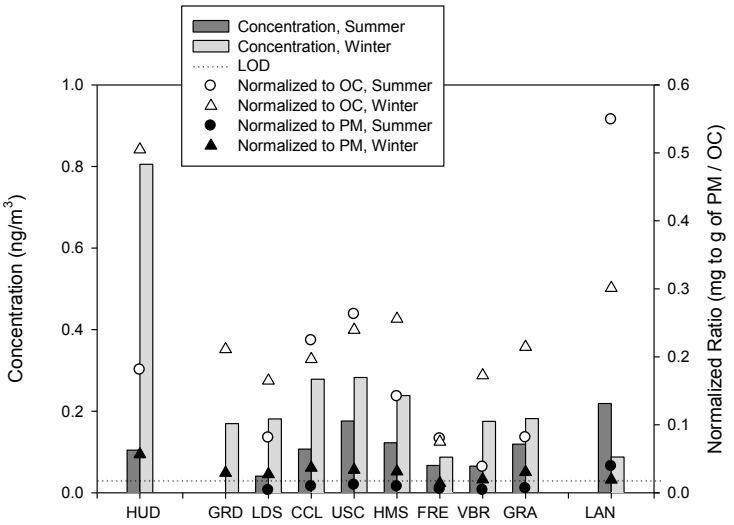

Figure 3-2: Concentration (ng/m^3) of sum of hopanes. The level of detection (LOD) of the compound class is shown as a reference line.

Table 3.2 shows the correlation coefficients among individual organic component, compound class, OC, EC, selected elements and meteorological parameters. The method of quantification of OC, EC and total elements, as well as their results were described in two previous publications produced from this study (Cheung et al., 2011b; Pakbin et al., 2011), and they are not discussed in detail here. Overall, the high correlation ($R=0.91$, $p<0.001$) between hopanes and EC, a tracer of vehicular emission, confirms traffic as the dominant source of hopanes in CPM. Although the levels of steranes were much lower, with most of the data points below detectable levels (Table 3.1), their results were consistent with those observed for hopanes, with more detectable concentrations and a significant peak at the HUD site in the winter.

Table 3-2: Correlation coefficients (R) among individual organic component, compound class, organic carbon (OC), elemental carbon (EC), selected elements and meteorological parameters. Species with less than half data points with detected levels are excluded in this analysis.

	∑Alkanes	∑Alkanoic Acid, C15-C30	Tricosane, C23	Nonacosane, C29	Heptatriacotane, C37	Octadecanoic acid, C18	Triacontanoic acid, C30	Pinonic acid	Levoglucosan	OC	EC	Al	Ti	Cu	Zn	Ba	Relative humidity	Temperature	Wind Speed
∑Hopanes	0.66	0.16	0.42	0.38	0.58	-0.07	-0.14	-0.13	0.30	0.45	0.91	0.30	0.40	0.24	0.73	0.52	-0.29	-0.30	-0.25
∑Alkanes		0.54	0.71	0.84	0.67	0.42	0.45	0.47	0.30	0.73	0.63	0.59	0.72	0.14	0.40	0.48	-0.35	-0.04	-0.07
∑Alkanoic Acid, C15-C30			0.38	0.78	0.22	0.89	0.75	0.71	0.48	0.74	0.11	0.68	0.71	-0.11	0.19	0.32	-0.05	0.38	0.35
Tricosane, C23				0.64	0.45	0.39	0.31	0.47	0.25	0.64	0.41	0.43	0.56	0.23	0.45	0.47	-0.36	-0.01	0.03
Nonacosane, C29					0.30	0.75	0.78	0.80	0.23	0.78	0.33	0.83	0.89	0.01	0.25	0.27	-0.38	0.28	0.23
Heptatriacotane, C37						0.00	0.00	-0.03	0.57	0.56	0.65	-0.06	0.13	0.18	0.38	0.68	-0.13	-0.54	-0.36
Octadecanoic acid, C18							0.89	0.81	0.12	0.59	-0.15	0.73	0.66	-0.37	-0.11	-0.10	0.03	0.52	0.46
Triacontanoic acid, C30								0.87	-0.03	0.59	-0.12	0.69	0.62	-0.44	-0.13	-0.14	0.03	0.41	0.36
Pinonic acid									-0.08	0.56	-0.18	0.73	0.77	-0.11	-0.14	0.04	-0.26	0.53	0.49
Levoglucosan										0.56	0.42	-0.18	0.01	0.38	0.31	0.67	-0.19	-0.49	-0.39
OC											0.55	0.47	0.62	-0.03	0.48	0.63	-0.07	-0.03	-0.04
EC												0.11	0.24	0.15	0.74	0.60	-0.16	-0.53	-0.51
Al													0.92	-0.09	0.17	-0.06	-0.26	0.59	0.45
Ti														0.16	0.27	0.26	-0.45	0.48	0.43
Cu															0.10	0.54	-0.66	-0.09	-0.09
Zn																0.50	-0.07	-0.18	-0.18
Ba																	-0.27	-0.32	-0.25
Relative humidity																		0.06	-0.17
Temperature																			0.82

3.4.4. *n*-Alkanes

The group of total *n*-alkanes is a predominant compound class in CPM, with an average of 6.9±2.8 ng/m^3 and 8.7±2.7 ng/m^3 in the summer and winter, respectively. At the three inland sites (VBR, GRA and LAN), total *n*-alkanes concentrations were higher in the summer (Figure 3.3). This is probably due to the "receptor" location of these areas, where pollutants are transported from the upwind locations. These inland sites are also more rural, with more vegetation and open fields that could be biogenic sources of these species. In contrast, higher *n*-alkane concentrations were observed in the winter in the urban areas, namely Long Beach (HUD), West L.A. (GRD and LDS), and to a lesser extent Central and East L.A. (CCL and HMS). These elevated levels could be due to the lower atmospheric transport in the winter that limited the dilution of total *n*-alkanes, and/or the increase in the source strengths of these species in the winter. The carbon preference index (CPI), calculated using the wide range of n-alkanes (∑C13-C35/∑C12-C34), was used to estimate the sources of these *n*-alkanes in coarse mode aerosols. Emissions from fossil fuel exhibit a CPI near unity, whereas a CPI greater than 2 indicates a dominance of biogenic sources

(Daher et al., 2011). The average CPI in this study was 2.1±0.75, suggesting an overall prevalence of biogenic origins for these *n*-alkanes.

To further investigate the origins of *n*-alkanes, the relative mass concentration (percent of sum of *n*-alkanes) is calculated for C19-C38 analyzed in this study, as presented in Figure 3.4. In general, peaks were observed for C29 and C31, to a lesser extent C23, C37 and C38 in both summer and winter. These distributions are compared to the source profiles of PM garden soil, road dust, brake wear, leaf abrasion products and total suspended tire wear, developed by Rogge et al. in the 1990s (Rogge et al., 1993a, b). The most dominant peaks of C29 and C31 in CPM are similar to the profile of soil, leaf abrasion (both dead and green) and road dust, suggesting that these peaks originate mainly from mineral and road dust. This is confirmed by the high correlation between C29 and Al, a soil dust tracer ($R=0.83$, $p<0.001$). Furthermore, the two Riverside sites (VBR and GRA) experienced higher levels of C31 than C29, which is a signature of soil and leaf abrasion (as opposed to road dust, which has a higher peak at C29 than C31), highlighting the suburban nature of the Riverside area. On the other hand, peaks in C37 and C38 are consistent with the profile of tire wear, which dominates the higher molecular weight *n*-alkanes. Although vegetative detritus is also a source of heavy alkanes (Zygadlo et al., 1994), the moderate correlations of C37 with EC ($R=0.65$, $p=0.004$) and Ba ($R=0.68$, $p=0.002$) and its insignificant associations with Al ($R=-0.06$, $p=0.81$) and Ti ($R=0.13$, $p=0.60$) further confirm tire wear and road dust as the dominant sources of C37 and C38.

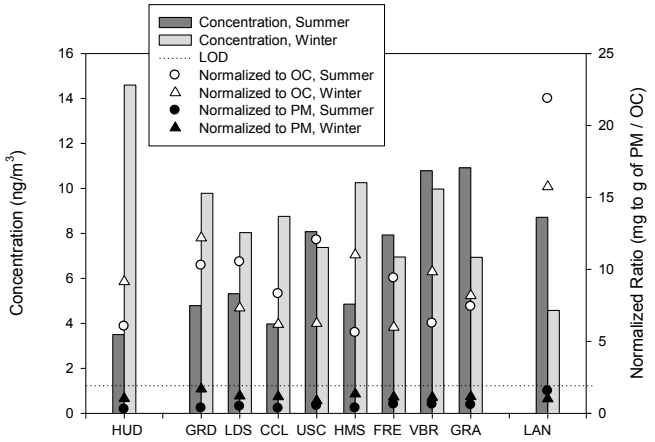

Figure 3-3: Concentration (ng/m^3) of sum of *n*-alkanes. The level of detection (LOD) of the compound class is shown as a reference line.

The spatial and seasonal patterns of C37 and C38 were different from those of *n*-alkanes (Figure 3.3), C29 and C31. In contrast to the significant spatial and seasonal patterns among the 10 sampling sites for *n*-alkanes, C29 and C31 (higher concentrations at the inland sites in the summer and higher concentrations at the urban sites in the winter), most sampling sites displayed less variation for C37 and C38, as highlighted by the low standard deviations (<15%) of both species across the 10 sampling sites in both seasons. This suggests that source strengths of these two species were relatively stable throughout the basin and during different seasons, consistent with the relatively low variability of traffic volume and composition– the source of tire wear emissions in this basin. Both C37 and C38 experienced slightly elevated levels in the winter (avg.=0.78±0.059 ng/m^3 and 0.91±0.058 ng/m^3 respectively) compared to summer (avg.=0.65±0.082 ng/m^3 and 0.77±0.098 ng/m^3 respectively). As discussed earlier, traffic-induced re-suspension of coarse particles is more dominant in the winter, which might explain the higher levels of these tire wear particles in the cooler period. Note the significant levels of C23, and to a lesser extent C22 and C21, in our study that do not fit the source profiles of exhaust emission,

cooking, tire and brake wear, road dust, garden soil or leaf abrasion (Rogge et al., 1993a, b, 1998; Rogge et al., 1991), which are mostly developed using fine particles, with the exception of tire wear from total suspended particles. C23, tricosane, could be a component of OC that is more dominant in CPM than in fine particles. Its moderate correlations with Al, Ti, Zn and Ba (R range from 0.43-0.56) suggest that it has both natural and anthropogenic origins.

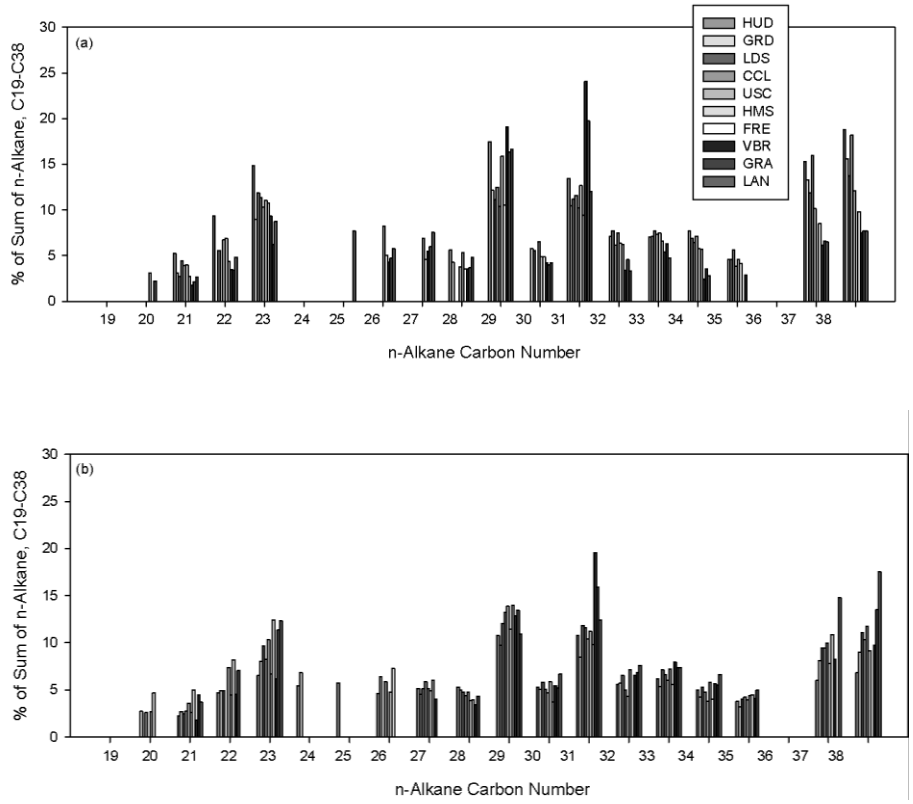

Figure 3-4: Concentration distribution (per sum of *n*-alkanes, C19-C38) of coarse particulate matter for *n*-alkanes in: (a) summer and (b) winter.

3.4.5. *n*-Alkanoic acids

The *n*-alkanoic acids group is the most abundant organic compound class identified in CPM at all sampling sites, with average levels of 32±16 ng/m^3 and 29±12 ng/m^3 in the summer and winter, respectively. In the more downwind/rural locations (Riverside and Lancaster), levels of

n-alkanoic acids were higher in the summer (Figure 3.5). Their normalized ratios (to PM) are also generally higher than other sites, suggesting the source strengths of *n*-alkanoic acids were stronger in the downwind areas in summertime. In the winter, when long-range transport is limited due to lower wind speeds, *n*-alkanoic acid levels were either similar to or higher than their summer levels at the urban sites. When normalized to OC (shown as open symbols in Figure 3.5), the ratios in the winter are either similar to or lower than those in the summer. It indicates that the relative contribution of *n*-alkanoic acids to OC concentration was generally lower in the winter. The CPI of *n*-alkanoic acids, calculated as the ∑C24-C30/∑C23-C29, was higher in the summer (avg.=2.3±1.1) than winter (avg.=2.0±0.58), particularly at the two Riverside sites in the summer, where the CPI was 4.7 and 3.8 at VBR and GRA, respectively.

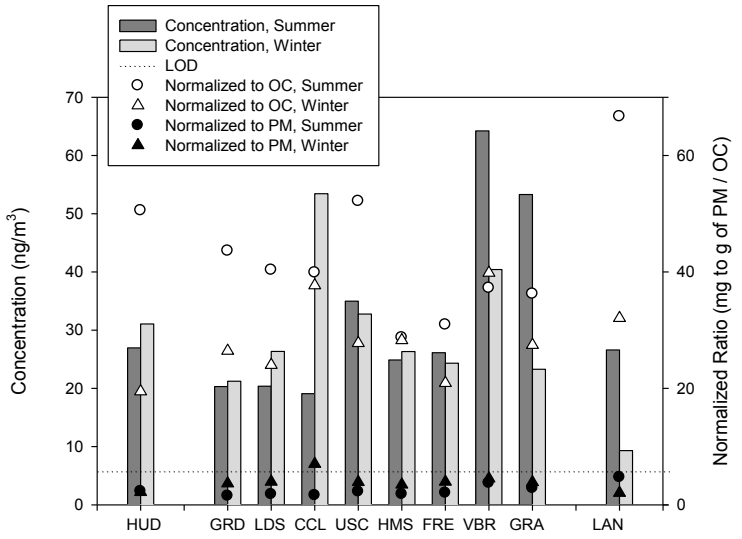

Figure 3-5: Concentration (ng/m^3) of *n*-alkanoic acids, as a sum of C15-C30. The level of detection (LOD) of the compound class is shown as a reference line.

Figure 3.6 shows the distribution of relative mass concentrations (percent of sum of *n*-alkanoic acids, C15 to C30). The dominant peaks in hexadecanoic acid and octadecanoic acid (C16 and C18) are consistent with the source profiles of tire wear, PM road dust and green leaf

debris (Rogge et al., 1993a, b). Note that C16 and C18 are the most common fatty acids present in biological matter (Simoneit, 1986), and they may also arise from many other sources such as fireplace use (Dutton et al., 2010), food cooking (Schauer et al., 2002) and fossil fuel combustion (Cheung et al., 2010). The high association between C18 and Al ($R=0.73$, $p<0.001$) coupled with the insignificant associations with Ba ($R=-0.10$, $p=0.69$), EC ($R=-0.15$, $p=0.53$) and levoglucosan (to be discussed later, $R=0.12$, $p=0.64$) suggest its dominant origin as soil dust as opposed to traffic-related emissions and biomass burning. The source profiles of soil and dead leaf abrasion showed dominance within the higher MW *n*-alkanoic acid range (≥C22) (Rogge et al., 1993b). Using our data, C30, a heavier alkanoic acid that is predominant in the wax filaments of plants (Yue and Fraser, 2004), also demonstrated good associations with Al and Ti ($R=0.69$, $p<0.001$ and $R=0.62$, $p=0.004$ respectively). This finding is consistent with some studies that demonstrate the presence of biological materials in the urban/suburban aerosols of PM_{10} (Jia et al., 2010). In particular, Cahill et al. (2010) showed that sugars (including glucose, sucrose and fructose) dominated the coarse size fraction of PM in particles collected in California's Central Valley, and attributed its sources to biological materials of plant detritus, spores, etc.

On the other hand, wind speed may affect the levels of some CPM constituents, such as mineral dust tracers of Al and Ti ($R=0.45$ and 0.43 respectively; $p=0.045$ and 0.057 respectively), and to a lesser extent *n*-alkanoic acids ($R=0.35$, $p=0.13$). Similar degrees of associations are observed when the analysis is done using the data from the summer only. The moderately low associations are likely due to the suppressed effects of meteorology in 24-hour samples, as well as their differential contributions to urban and rural areas (Cheung et al., 2011). In particular, wind speed could be an important parameter of CPM levels in rural areas, where local emissions and

re-suspension of dust by anthropogenic activities are minor, as evident by the stronger associations between wind speed and Al (R=0.86; p=0.026) when the correlation analysis is restricted to the three inland sites (GRA, VBR and LAN). The higher wind speed in the summer increased both local re-suspension and possibly long-range transport of upwind air pollutants to these sites, contributing to the elevated concentrations of these constituents in the summer. Overall, the good associations between *n*-alkanoic acids and soil dust tracers (R=0.68, p=0.001 for Al; R=0.71, p<0.001 for Ti) suggest that re-suspended dust contains a mixture of crustal materials and vegetative debris, and that mineral dust is enriched with biological matter in coarse particles sampled in Southern California.

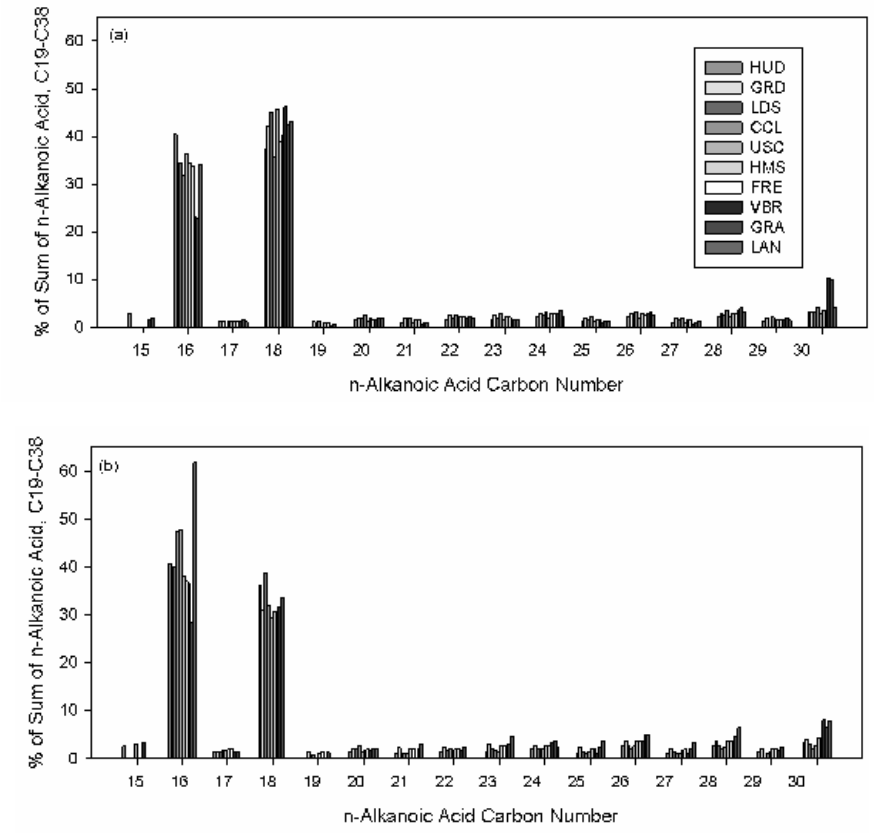

Figure 3-6: Concentration distribution (per sum of *n*-alkanoic acids, C15-C30) of coarse particulate matter for *n*-alkanoic acid in: (a) summer and (b) winter.

3.4.6. Other carboxylic acids

Figure 3.7 (a-c) shows the levels of pinonic acid, palmitoleic acid and oleic acid respectively. Pinonic acid, formed primarily from the oxidation of pinenes, is considered a biogenic secondary organic aerosol (Cheng et al., 2011). Pinonic acid had slightly higher concentrations in the summer (avg.= 0.68±0.35 ng/m^3) than in the winter (avg.=0.56±0.12 ng/m^3), consistent with a recent study conducted in Europe, which showed higher levels of pinonic acid in coarse mode aerosols during spring and summer than autumn and winter (Zhang et al., 2010). In particular, high concentrations of pinonic acid were found in the receptor and rural sites in the summer, when temperatures are higher and the formation of secondary aerosol is more dominant in inland areas (Sardar et al., 2005). The high associations between pinonic acid and crustal material tracers of Al and Ti (R=0.73 and 0.77, respectively; $p<0.001$ for both) suggest that although pinonic acid arises from a different formation mechanism with crustal materials, it might be adsorbed onto or absorbed into soil dust and collected simultaneously during sampling.

Palmitoleic acid, on the other hand, could be found in marine aerosols (Simoneit et al., 2004) and food cooking (Rogge et al., 1991), and it displayed a distinct seasonal variation. The higher summer concentrations (avg.=0.60±0.14 ng/m^3), which parallel the strong onshore winds that transport sea salt particles from the coast to inland, suggest that marine aerosols are the primary source of palmitoleic acid in CPM in this basin. Oleic acid experienced higher levels in the winter than in the summer and a peak level at CCL in the winter. This observation is consistent with an earlier study conducted in the basin, which revealed winter maxima and extended summer minima of oleic acid, and the investigators attributed the discrepancy to the enhanced photo-oxidation of this species during summer months (Rogge et al., 1993c). High level of oleic

acid (~1100 µg per g of sample) was previously reported in the total suspended debris of tire wear (Rogge et al. 1993a). The same group of investigators also found significant levels of oleic acid in road dust, vegetative detritus, and emissions from wood burning (Rogge et al., 1993a, b, 1998). Therefore, these could be the potential sources of oleic acid in coarse mode aerosols.

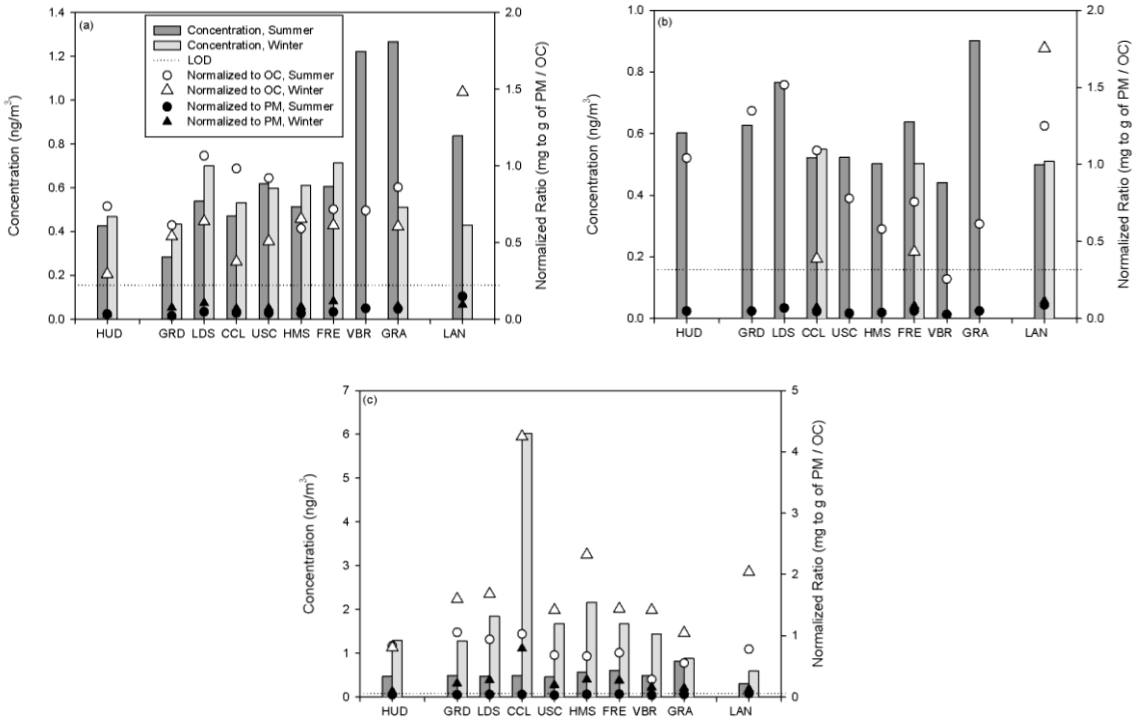

Figure 3-7: Concentration (ng/m^3) of: (a) pinonic acid, (b) palmitoleic acid and (c) oleic acid. The level of detection (LOD) of each organic compound is shown as a reference line.

3.4.7. Levoglucosan

Levoglucosan, a pyrolysis product of cellulose, is widely used as a major marker of biomass burning (Simoneit, 1999). It could be emitted from various wood combustion (Hays et al., 2011), cigarette smoke (Kleeman et al., 2008), as well as wildfires (Yue and Fraser, 2004) or management burns (Zhang et al., 2008a). Fine et al. (2004a) showed higher levels of

levoglucosan in the accumulation mode particles at the USC sampling site in the winter (~47 ng/m^3) than in the summer (~4.2 ng/m^3), and attributed the difference to the increased residential wood combustion activity during wintertime. In this study, the overall concentration of levoglucosan was low (avg.=3.3 ng/m^3), consistent with its combustion origins, which yield only a minor fraction of particles in the coarse mode (Herckes et al., 2006).

Figure 3.8 shows the concentrations of levoglucosan across the 10 sampling sites in the two seasons. Levoglucosan concentration was significantly higher in the winter (4.9±3.0 ng/m^3) than the summer (1.8±0.41 ng/m^3), paralleled with the seasonal variation of water-soluble potassium – another tracer of wood smoke (Chow et al., 2007) – in this study, and is consistent with the higher wood burning activity in the cooler period. The higher normalized ratios in the winter at most sites indicate that the higher contribution of levoglucosan to both OC/PM in cooler months. The moderate correlations between levoglucosan and CPM of anthropogenic origins including tracers of tire and brake wear (R=0.67 and 0.38 for Ba and Cu respectively), as well as vehicular emissions (R=0.42 for EC) are unexpected due to their distinct origins and formation mechanisms. Note that high correlations between species do not imply common origins due to possible confounding and CPM re-suspension of a common primary mechanism. The high association between levoglucosan and EC could be also driven by their seasonal pattern (higher levels in the winter than the summer). The higher levels of coarse particulate levoglucosan in the winter, driven by increased wood burning activities, might accumulate in the mineral and road dust, and be re-suspended together with Ba, Cu or EC by vehicular-induced turbulence in the cooler period.

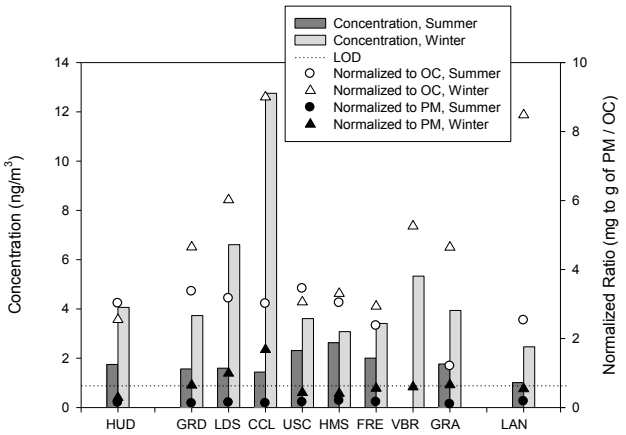

Figure 3-8: Concentration (ng/m^3) of levoglucosan. The level of detection (LOD) of levoglucosan is shown as a reference line.

3.5. Summary and Conclusions

In summary, *n*-alkanoic acids, to a lesser extent *n*-alkanes, are the predominant classes of organic compounds in CPM. Constituents of vehicular emissions, including PAHs, hopanes and steranes experienced low concentrations in the coarse mode. The profiles of *n*-alkanoic acids are similar to those from leaf abrasion, garden soil, tire wear and road dust. Coupled with the high correlations with Al and Ti, our results suggest that *n*-alkanoic acids in CPM are mostly derived from mineral and road dust. On the other hand, *n*-alkanes in the coarse size fraction originate from both biogenic and anthropogenic sources. Medium MW *n*-alkanes (C29, C31) highly correlated with Al and Ti, while high MW *n*-alkanes (C37, C38) moderately correlated with Cu and Ba. Previous studies conducted in the Los Angeles Basin showed that vehicular emissions and secondary photo-oxidation are the major sources of organic compounds in the fine and ultrafine modes (Fine et al., 2004a). Based on the analysis conducted using only samples of ambient coarse particles, soil and the associated biota represent the predominant source of organic constituents in CPM. In general, the mass fraction of organic compounds to CPM was higher during wintertime,

due to lower concentrations of other components (sea salt, secondary ions, etc.) and/or the increase in source strengths of organic compounds, the latter of which is supported by traffic-induced re-suspension of mineral and road dust in cooler months. The distinct organic composition of fine and coarse PM might have important implications on the chemical mass reconstruction of PM. Higher fractions of unidentified mass fraction are usually observed for coarse particles compared with fine and ultrafine PM in ambient environments (Ho et al., 2005). Organic matter from soil and the associated biota, which could contain sugars and amino acids that have a higher molecular weight per carbon weight ratio, might be underestimated by the typical conversion factor (ranging from 1.4 to 2.1) used to estimate the average molecular weight per carbon weight for the organic aerosol (Turpin and Lim, 2001). The dominance of biological materials in CPM suggests that a biogenic-specific conversion factor needs to be developed for coarse particles to improve closure between gravimetric and chemical measurements of coarse particles.

3.6. Acknowledgements

The work presented here is funded by the United States Environmental Protection Agency through the Science to Achieve Results program (EPA-G2006-STAR-Q1). We would like to thank the staff at the Wisconsin State Laboratory of Hygiene and Mike Olson of University of Wisconsin, Madison for the assistance with chemical analyses. Although the research described in this article has been funded wholly or in part by the United States Environmental Protection Agency, it has not been subjected to the Agency's required peer and policy review and therefore does not necessarily reflect the views of the Agency and no official endorsement should be inferred.

Chapter 4 Historical Trends in the Mass and Chemical Species Concentrations of Coarse Particulate Matter (PM) in the Los Angeles Basin and Relation to Sources and Air Quality Regulations

4.1. Abstract

To assess the impact of past, current and proposed air quality regulations on coarse particulate matter (CPM), the concentrations of CPM mass and its chemical constituents were examined in the Los Angeles Basin from 1986 to 2009 using PM data acquired from peer-reviewed journals and regulatory agency database. PM_{10} mass levels decreased by approximately half from 1988 to 2009 at the three sampling sites examined- located in downtown Los Angeles, Long Beach and Riverside. Annual CPM mass concentrations were calculated from the difference between daily PM_{10} and $PM_{2.5}$ from 1999 to 2009. High CPM episodes driven by high wind speed / stagnant condition caused year-to-year fluctuations in the 99^{th} / 98^{th} percentile CPM levels. The reductions of average CPM levels were lower than those of $PM_{2.5}$ in the same period, despite their comparable concentrations; therefore the decrease of PM_{10} level was mainly driven by reductions in the emission levels of $PM_{2.5}$ (or fine) particles. This is further confirmed by the significant decrease of Ni, Cr, V, and EC in the coarse fraction after 1995. On the other hand, the levels of several inorganic ions (sulfate, chloride and to a lesser extent nitrate) remained comparable. From 1995 to 2008, levels of Cu, a tracer of brake wear, either remained similar or decreased at a smaller rate compared with elements of combustion origins. This differential reduction of CPM components suggests that past and current regulations may have been more effective in reducing fugitive dust (Al, Fe and Si) and combustion emissions (Ni, Cr, V, and EC) rather than CPM from vehicular abrasion (Cu) and inorganic ions (NO_3^-, SO_4^{2-} and Cl^-) in urban areas.

4.2. Introduction

In the last decade, a significant body of new research has documented substantive differences of fine and coarse particles, and there is a growing evidence of health effects induced by CPM (Chen et al., 2005; Yeatts et al., 2007). As a result, the need for a new $PM_{10-2.5}$ standard was proposed in a recent review (2006) of NAAQS (U.S.EPA, 2006). The proposed $PM_{10-2.5}$ standard was suggested to be 65-85 $\mu g/m^3$, in the form of a 98^{th} percentile, and it was intended to be generally equivalent to the 1987 24-hour PM_{10} standard (150 $\mu g/m^3$, with a 99^{th} percentile form). Due to the different sources and size distribution of PM in urban and rural areas, the proposed CPM standard would impact these areas differently. Nonetheless, the effects of the proposed standard on industrial and agricultural communities, as well as local regulatory agencies, are largely unknown.

The study described here examines the trend of CPM mass concentration and chemical composition in the Los Angeles Basin over the past two decades, as well as the implications of the proposed $PM_{10-2.5}$ standard given the nature and sources of PM components in the basin. The Los Angeles Basin is located in Southern California, and is the second most populous metropolitan area in the United States. The basin is served by the nation's largest port complex, a large freight and passenger rail infrastructure, numerous airports and an extensive network of freeways and highways. Due to its local topography and meteorological conditions, heavy reliance on vehicles and traffic activity from the ports, Los Angeles is ranked among the worst cities for ozone and particulate pollution (Association, Available at: http://www.stateoftheair.org. Accessed November 30, 2011.), and has been an area of active air quality research. Studies examining characteristics of ambient aerosols across the basin have been conducted since the

1940s (Neiburger and Wurtele, 1949), and a large body of historical PM data is available from regulatory agencies and academic institutes. Additionally, the contribution of coarse particle to PM_{10} is relatively high (on average 33-58%) in Los Angeles (Gauderman et al., 2000; Pakbin et al., 2010) compared to several other large US metropolitan areas (U.S.EPA, 2004), thereby making it feasible to study coarse particle trends / composition with lower uncertainty. All of these provide a unique opportunity to examine the historical trends of coarse particle in this basin, which will allow us to assess how the CPM fraction has been impacted by past and current air quality regulations, as well as implications of the proposed $PM_{10-2.5}$ standards.

4.3. Methodology

To study the CPM trend in the Los Angeles Basin, three representative areas (downtown Los Angeles, Long Beach and Riverside) were selected based on the availability of historical datasets. Figure 4.1 shows a map of the sampling sites in the three regions. Downtown Los Angeles (sites DLA and USC) is a typical urban area with high commercial and traffic activity. The downtown area is characterized by dense freeway networks and a high volume of both heavy and light-duty vehicles. DLA is a monitoring site maintained by the South Coast Air Quality Management District (SCAQMD) and is located within 900 m of freeways I-5 and I-110. The other site in Los Angeles (USC) is located about 150 m east of I-110. Long Beach (sites HUD, NLB, LBCC and S3) is a mixed residential and commercial neighborhood. The sampling sites in Long Beach are in close vicinity to the Port of Los Angeles and Port of Long Beach, and are highly influenced by heavy-duty diesel vehicle traffic related to harbor activity. NLB and HUD are maintained by the SCAQMD. NLB is located approximately 600 m north of I-405 and 1.2 km east of I-710. HUD is about 100 m east of Terminal Island Freeway and 1.2 km west of I-710. LBCC is located at the

campus of Long Beach City College approximately 2.5 km north of I-405. The S3 site was one of the sampling sites in a study that examined size-segregated PM in communities of the Los Angeles Harbor (Arhami et al., 2009), and it is about 900 m south of the HUD site. Riverside (sites VBR, RUB, UCR, and RIV) is a sub-urban area located 80 km inland and downwind of Los Angeles, and is generally considered to be a receptor site for pollutants generated in urban Los Angeles and advected to the area within a few hours after their emissions. VBR and RUB are SCAQMD monitoring sites located about 2.5 km and 800 m south of CA-60 respectively. The UCR site is situated at the Citrus Research Center and Agricultural Experiment Station of the University of California, Riverside, and it is upwind of surrounding freeways. RIV is located at a retirement home which is 15 km southeast of downtown Riverside.

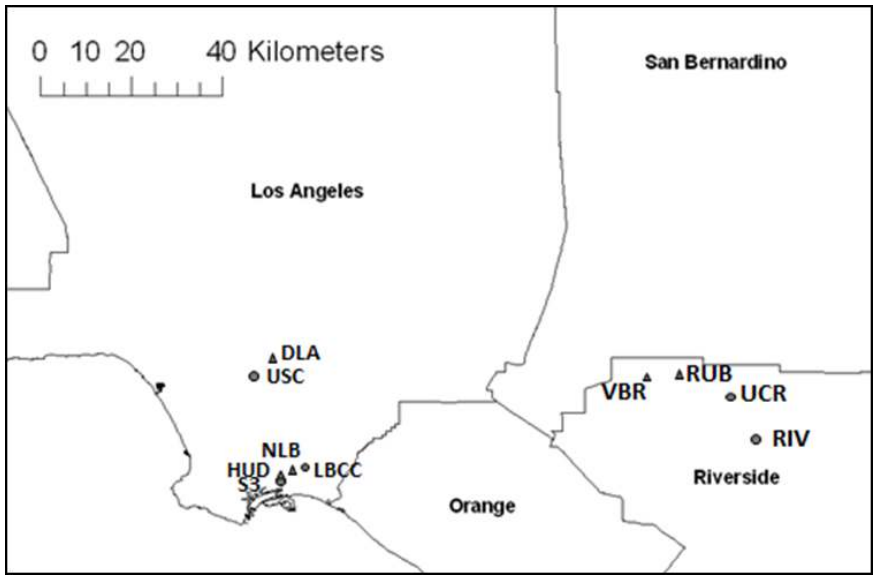

Figure 4-1: Map of the samplings sites in downtown Los Angeles (DLA and USC), Long Beach (NLB, HUD, LBCC and S3) and Riverside (RUB, VBR, UCR and RIV). Sites operated and maintained by the SCAQMD are represented in triangles.

The CPM mass concentration data presented in Figures 4.2-4.4 were calculated as the difference between PM_{10} and $PM_{2.5}$ levels (the subtraction method). Daily PM_{10} and $PM_{2.5}$ measurements were obtained from the online database of California Air Resources Board (CARB). The three sampling sites (DLA, NLB and RUB) used in this analysis were maintained by the SCAQMD, and the details of the sampling methods are described under Title 40 Part 58 of Code of Federal Regulations. In brief, daily $PM_{2.5}$ measurements were quantified gravimetrically using sequential samplers operating at 16.7 L/min (Andersen Model Reference Ambient Air Sampler 2.5-300), loaded with a 2-μm Teflon substrate. PM_{10} measurements were determined gravimetrically using high-volume samplers (General Metal Works Model 1200) loaded with a quartz micro-fiber filter. Daily PM_{10} concentrations from 1988 to 2009 were analyzed. $PM_{2.5}$ measurements were only available after 1999, and daily CPM mass concentrations were calculated from 1999 to 2009 using the "subtraction method" when both measurements were available for the same day. Note that the reported mass concentrations were collected using samplers with no denuders. The distinct flow rates used in the PM_{10} and $PM_{2.5}$ samplers might contribute to the differential loss of semi-volatile compounds, in additional to other sampling artifacts that could be different in the two samplers. Since the majority of semi-volatile compounds resides in the fine PM fraction (Miguel et al., 2004; Yoshizumi and Hoshi, 1985), the estimation of CPM using the subtraction method (calculated based on reported concentrations from the low-volume-$PM_{2.5}$ sampler and the high-volume-PM_{10} sampler) might have underestimated the mass concentrations of coarse particles. Nonetheless, the sampling artifacts of semi-volatile organics are likely to be reduced by the long sampling time (24 hours) and higher mass loadings (Mader et al., 2003; Sardar et al., 2005). On the other hand, due to the stronger

removal process of CPM compared to fine PM, coarse particles could be more spatially heterogeneous (Pakbin et al., 2010), and the extrapolation of this analysis to other air basins needs to be proceeded with cautions. Daily PM_{10} levels were generally measured once every six days, with an average yearly count of 59 ± 3.5, 85 ± 27 and 57.8 ± 3.4 from 1988 to 2009 in downtown Los Angeles, Riverside and Long Beach respectively. The higher number count in Riverside was driven by the more frequent measurements (once every three days) from 2000 to 2009. $PM_{2.5}$ was measured more frequently, with an average annual measurement count of 305 ± 58, 308 ± 56 and 303 ± 60 from 1999 to 2009 in DLA, RUB and NLB respectively. The higher standard deviation was driven by the lower count in year 1999 when the measurements first started.

Table 4-1: Sampling location, sampling time and frequency, sampling instrument and method, analytical method and other background information of the seven studies analyzed.

	1986, CARB	Chow et al., 1994	Kim et al., 2000	Sardar et al., 2005	Polidori et al., 2009	Arhami et al., 2009	Cheung et al., 2011
Location	AQMD Los Angeles (DLA)	AQMD Los Angeles (DLA)	AQMD Los Angeles (DLA)	USC in Los Angeles	Riverside retirement home (RIV)	S3 in Long Beach	USC in Los Angeles
	AQMD Rubidoux (RUB)	AQMD Rubidoux (RUB)	AQMD Rubidoux (RUB)	UCR in Riverside			AQMD Van Buren (VBR)
	AQMD Long Beach (NLB)	Long Beach City College (LBCC)					AQMD Long Beach (HUD)
Sampling Period	Jan-Dec 1986	11 days in Jun-Sep, 6 days in Nov-Dec in 1987	Jan 1995-Feb 1996	USC: Oct 2002-Sep 2003; UCR: Mar-Jun 2001	Aug-Oct 2006, Jan-Feb 2007	Mar-May 2007	Apr 2008-Mar 2009
Sampling Time	Once every 6th day, daily samples	Sequential samples for each episode (5 in summer, 3 in winter)	Once every 3rd or 6th day, daily samples	Once every week, daily samples	7 weekly samples	6 weekly samples	Once every week, daily samples on Wednesday
Filter Type	PTFE and quartz	Teflon and quartz	Teflon and quartz	Teflon and aluminum	Zefluor	Zefluor and quartz	Zefluor and quartz
Sampling Method	PM_{10}: 16.7 lpm through a PM_{10} inlet, 5.6 lpm through each filter	PM_{10}: 110 lpm through a PM_{10} inlet, 30 lpm through each filter	PM_{10}: 97 lpm through a PM_{10} inlet, 10 lpm through each filter	Micro-Orifice Uniform Deposition Impactor (MOUDI) operated at 30 lpm; Partisol sampler with PM_{10} and $PM_{2.5}$ inlets operated at 16.7 lpm	Personal Cascade Impactor Sampler (PCIS) operated at 9 lpm with a PM_{10} inlet	PCIS operated at 9 lpm with a PM_{10} inlet	USC Virtual Impactor (VI) operated at a total flow of 50 lpm and a minor flow of 2 lpm with a PM_{10} inlet; PCIS operated at 9 lpm with a PM_{10} inlet
	$PM_{2.2}$: 24.8 lpm to a cyclone separator with a cut point of 2.2 μm; 3-4.6 lpm through each filter	$PM_{2.5}$: 110 lpm to a cyclone separator with a cut point of 2.5 μm; 35 lpm through each filter	$PM_{2.5}$: 112 lpm to a cyclone separator with a cut point of 2.5 μm; 20 lpm through each filter				
Analytical Method	X-ray fluorescence	X-ray fluorescence	X-ray fluorescence	X-ray fluorescence	ICP-MS	ICP-MS	ICP-MS
(For elements, ions, and carboneous contents)	Ion chromatography.	Ion chromatography. Automated colorimetry, atomic absorption	Ion chromatography	Ion chromatography	NA	Ion chromatography	Ion chromatography
	Thermal desorption/ optical transmission	Thermal manganese oxidation	Optical thermal carbon analyzer	Thermal desorption/ optical transmission	Thermal desorption/ optical transmission	NA	Thermal desorption/ optical transmission
CPM Calculation	Indirect, difference between PM_{10} and $PM_{2.5}$	Indirect, difference between PM_{10} and $PM_{2.5}$	Indirect, difference between PM_{10} and $PM_{2.5}$	Direct	Direct	Direct	Direct
Statistics	Average	Average	Average	Average	Average	NA, composites	Average

Concentrations of CPM mass and chemical constituents presented in Figures 4.5-4.7 were obtained from studies fully or in part published in the peer-reviewed literature before 2010.

Although a number of studies have examined the chemical composition of ambient PM in Los Angeles, very few of them report data for coarse particles (or allow the calculation of such). Seven studies, providing chemical speciation of elemental species, were included in our analyses. The earliest study that performed chemical speciation on both PM_{10} and $PM_{2.5}$ in the Los Angeles Basin was conducted in 1986. The year-long dataset was available at CARB (Solomon et al., 1988) and part of the PM data were published in peer-review literature (Eldering et al., 1991; Solomon et al., 1989; Solomon et al., 1992). Shortly after, Chow et al. conducted an intensive study in 1987 to capture photochemical episodes in warmer periods (June to September) and stagnation episodes in cooler periods (November to December) (Chow et al., 1994). A more comprehensive project was carried out by the SCAQMD from January 1995 to February 1996 to investigate the chemical composition of ambient PM_{10} and $PM_{2.5}$ in an effort to better characterize emission inventories and improve performance of modeling tools (Kim et al., 2000a, b). From 2000 to 2009, a few additional studies were conducted in Los Angeles, Long Beach and Riverside to examine the chemical composition of size-fractionated airborne PM to advance the understanding of the sources, atmospheric processing of ambient particles and their human health impacts (Arhami et al., 2009; Polidori et al., 2009; Sardar et al., 2005). In 2008, a comprehensive investigation on ambient CPM was conducted to study the chemical mass closure, as well as the spatial and temporal variation of CPM in the Los Angeles Basin (Cheung et al., 2011b; Cheung et al., 2011c; Moore et al., 2010; Pakbin et al., 2010; Pakbin et al., 2011). Table 4.1 summarizes the sampling location, sampling time and frequency, sampling instrument and method, analytical method, and other background information of each study. CPM concentrations were obtained using the difference between reported PM_{10} and $PM_{2.5}$ levels in the three earlier studies (Chow et

al., 1994; Kim et al., 2000a; Solomon et al., 1988). The more recent studies employed samplers segregating particles by size, and CPM concentrations and chemical composition were obtained directly as measured in the coarse fraction (Arhami et al., 2009; Cheung et al., 2011b; Polidori et al., 2009; Sardar et al., 2005).

4.4. Results and Discussion

4.4.1. Trends in CPM mass concentrations

Selected meteorological parameters at the downtown Los Angeles (DLA), Long Beach (NLB) and Riverside (RUB) sampling sites, respectively were acquired from the online database of CARB; only data after 1994 were available at the three sampling sites. The annual averages of temperature and relative humidity were calculated based on hourly data. Overall, annual mean temperatures were consistent (Avg. = 17.9 ^{o}C, standard deviation = 0.81 ^{o}C) from 1994 to 2009, while higher year-to-year fluctuations (Avg. = 59.3%, standard deviation = 11%) were observed for the relative humidity (RH). In general, the annual mean temperature and relative humidity was similar in Los Angeles and Long Beach. Riverside's inland location was highlighted by the higher mean temperature and standard deviation, coupled with the lower relative humidity. Wind originating from the west dominated most of the year, in accordance with the typical onshore flow patterns in the LA basin. The prevailing westerly onshore wind from the Pacific Ocean started in late morning and remained strong until evening. At night, wind direction reversed and the northerly / northeasterly wind prevailed. The wind speed was generally lower overnight. Overall, large-scale meteorological conditions were relatively consistent in this basin, and did not appear to influence the observed PM trends, as discussed and presented below.

Table 4-2: Linear regression analysis of PM data (PM_{10} from 1988 to 2009, $PM_{10-2.5}$ and $PM_{2.5}$ from 1999 to 2009) in: (a) downtown Los Angeles, (b) Long Beach and (c) Riverside. Values in parentheses represent standard errors of the slope and intercept.

a) Downtown Los Angeles

		Linear regression	R^2	p
PM_{10}	99th percentile	y = -3.71(±0.39) x + 136(±5.2)	0.82	<0.001
	98th percentile	y = -3.21(±0.36) x + 124(±4.8)	0.80	<0.001
	50th percentile	y = -1.19(±0.12) x + 54.0(±1.6)	0.83	<0.001
	Average	y = -1.33(±0.12) x + 57.4(±1.6)	0.86	<0.001
$PM_{10-2.5}$	99th percentile	y = -0.02(±1.1) x + 37.5(±7.1)	0.00	0.98
	98th percentile	y = -0.42(±0.82) x + 36.4(±5.6)	0.03	0.62
	50th percentile	y = -0.54(±0.23) x + 19.5(±1.6)	0.37	0.05
	Average	y = -0.39(±0.23) x + 18.9(±1.5)	0.25	0.11
$PM_{2.5}$	Average	y = -0.92(±0.09) x + 24.6(±0.64)	0.91	<0.001

b) Long Beach

		Linear regression	R^2	p
PM_{10}	99th percentile	y = -2.60(±0.64) x + 110(±8.1)	0.46	<0.001
	98th percentile	y = -2.46(±0.60) x + 103(±7.5)	0.47	<0.001
	50th percentile	y = -0.62(±0.11) x + 40.5(±1.3)	0.64	<0.001
	Average	y = -0.76(±0.11) x + 44.8(±1.4)	0.72	<0.001
$PM_{10-2.5}$	99th percentile	y = -0.50(±0.69) x + 41.0(±4.7)	0.06	0.48
	98th percentile	y = -0.59(±0.30) x + 34.9(±2.0)	0.31	0.08
	50th percentile	y = -0.37(±0.14) x + 17.1(±0.96)	0.43	0.03
	Average	y = -0.22(±0.11) x + 17.0(±0.74)	0.31	0.07
$PM_{2.5}$	Average	y = -0.87(±0.09) x + 22.4(±0.61)	0.91	<0.001

c) Riverside

		Linear regression	R^2	p
PM_{10}	99th percentile	y = -5.38(±0.85) x + 207(±11),	0.67	<0.001
	98th percentile	y = -4.72(±0.77) x + 189(±10),	0.65	<0.001
	50th percentile	y = -1.59(±0.21) x + 82.2(±2.8),	0.74	<0.001
	Average	y = -1.76(±0.23) x + 84.6(±3.0),	0.75	<0.001
$PM_{10-2.5}$	99th percentile	y = -2.36(±1.1) x + 93.8(±7.7),	0.32	0.07
	98th percentile	y = -1.77(±0.98) x + 84.2(±6.7),	0.27	0.11
	50th percentile	y = -0.56(±0.37) x + 35.2(±2.5),	0.21	0.16
	Average	y = -0.57(±0.29) x + 35.7(±2.0),	0.30	0.08
$PM_{2.5}$	Average	y = -1.69(±0.12) x + 33.5(±0.84),	0.96	<0.001

In downtown Los Angeles, the 99th percentile for PM_{10} (Figure 4.2a) and CPM (Figure 4.2b) ranges from 56.7 – 88.6 μg/m^3 and 22.7 – 60.4 μg/m^3 respectively from 1999 to 2009. The spike in the 99th and 98th percentile in 2007 was driven by two days of high CPM concentrations (69 and 51 μg/m^3 in April and October, respectively). The PM_{10} level was in attainment of the federal 24-hour standard (150 μg/m^3) while in violation of the California standard (50 μg/m^3) throughout the entire study period. Since the current PM_{10} standard is expressed in the 99th percentile form and the proposed CPM standard is set in the 98th percentile form, their comparability is examined. The difference between the 99th and 98th percentile is more apparent in the early 90s, with insignificant difference after 1998. The average and median PM_{10} concentrations agree fairly well. The slope of the 99th percentile concentration is -3.71 with a R^2 of 0.82 (Table 4.2a), indicating an average annual decrease of 3.71 μg/m^3 of the 99th percentile PM_{10} mass concentration from 1988 to 2009. The corresponding reduction is 1.33 μg/m^3 for the average PM_{10} concentration. CPM levels did not exhibit the typically consistent decreasing trend observed in the PM_{10} data. The slope of the average CPM concentration is -0.39 μg/m^3 ($p = 0.11$) from 1999 to 2009 (corresponding slope is -1.33 μg/m^3 and -0.92 μg/m^3 for PM_{10} and $PM_{2.5}$ respectively, both with a p-value < 0.001), indicating that the reduction of PM_{10} is mostly driven by the decrease of $PM_{2.5}$ given the comparable levels of fine and coarse PM (average annual fine-to-coarse ratio = 1.18 ± 0.21 from 1999 to 2009). To investigate the degree of equivalency between the current PM_{10} and the proposed $PM_{10-2.5}$ standard, the number of exceedances was examined using the 99th percentile of PM_{10} level and the 98th percentile of the CPM level from 1999 to 2009. In both cases, zero violations were observed. For further comparisons of the two standards, the ratio of the annual PM level to the corresponding standards (i.e., calculated as the annual 99th percentile PM_{10} to 150

$\mu g/m^3$ for the PM_{10} standard and the annual 98th percentile CPM to 70 $\mu g/m^3$ for the CPM standard) was examined. Using the data from 1999 to 2009, the ratios for the PM_{10} and proposed $PM_{10-2.5}$ standard were 0.48 ± 0.12 and 0.48 ± 0.07 respectively, suggesting that the two standards are comparable in downtown Los Angeles.

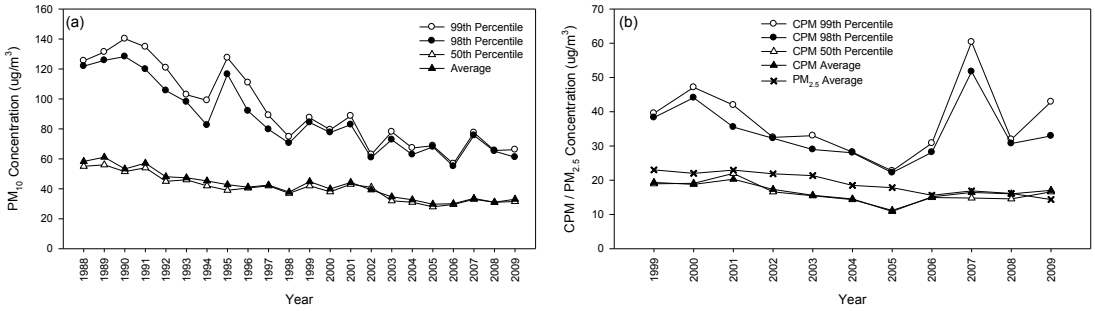

Figure 4-2: Annual concentrations of: (a) PM_{10} from 1988 to 2009, and (b) CPM / PM2.5 from 1999-2009 in downtown Los Angeles.

In Long Beach, the 99th percentile PM_{10} level experienced a fluctuating decreasing trend with a R^2 of 0.46 (Figure 4.3a). The spike in 1995 was driven by an episode of high PM_{10} level from mid-November to early December. The wind speed during that period was low with more than 70% of the time with "calm" conditions (wind speed < 0.5 m/s). It is possible that the high PM_{10} levels were due to the low dispersion of the emissions generated from the nearby harbor activity. The 99th percentile PM_{10} level ranges from 52.5 to 143.1 $\mu g/m^3$ from 1988 to 2009, attaining the EPA standard but violating the California standard. The decreasing trend of the average PM_{10} levels exhibits a high R^2 of 0.72 from 1988 to 2009 (Figure 4.3a and Table 4.2b). However, the average PM_{10} reduction rate is lower in the last 5 years, as evident by the lower slope of -0.14 $\mu g/m^3$ (standard error = 0.25 $\mu g/m^3$) from 2005 to 2009. Similarly, the average

CPM concentration was not significantly reduced from 1999 to 2009, as demonstrated by the close to zero slope (m = -0.22 $\mu g/m^3$, p = 0.07) in Table 4.2b, in contrast to the significant reduction in $PM_{2.5}$ levels (m = -0.87 $\mu g/m^3$, p < 0.001). The Long Beach site is heavily impacted by the Port's traffic activity. In addition to particle re-suspension by wind, CPM is re-entrained into the atmosphere by traffic-induced turbulence (Pakbin et al., 2010). Heavy-duty vehicles generally induce higher roadway re-suspension than light-duty vehicles (Charron and Harrison, 2005). Therefore, it is likely that the effort of PM reduction has been counterbalanced by the increase in the number of heavy-duty vehicles resulted by the expansion and increasing activity of the LA Ports, as the container volume grew from 1 million in 1985 to 7.8 million in 2010 at the Port of LA. In Long Beach, none of the recorded PM_{10} and calculated CPM levels violated the current federal PM_{10} and proposed CPM standards. The ratio of the 99th percentile PM_{10} and 98th percentile CPM to the current PM_{10} and proposed $PM_{10-2.5}$ standard was 0.46 ± 0.08 and 0.45 ± 0.05 respectively, again demonstrating that the two standards are comparable in Long Beach.

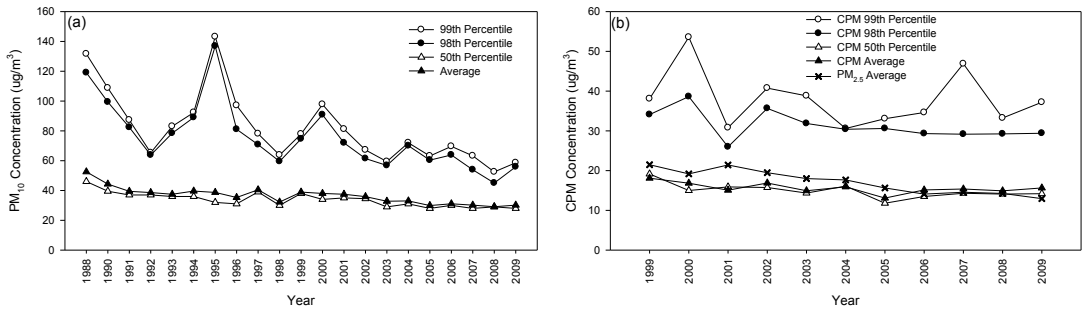

Figure 4-3: Annual concentrations of: (a) PM_{10} from 1988 to 2009, and (b) CPM / $PM_{2.5}$ from 1999-2009 in Long Beach.

Due to its downwind receptor location and sub-urban nature, PM_{10} / CPM mass concentrations in Riverside were higher than those observed in Los Angeles. The 99th percentile PM_{10} concentration (Figure 4.4a) was higher than the federal 24-hour standard of 150 μg/m^3 in 1988-91, 1993-95, and 2003, and experienced a moderately fluctuating downward trend from 1988 to 2009 ($R^2 = 0.67$). This is probably due to the sub-urban nature of the area, where high level of PM_{10} is mostly driven by particle re-suspension in episodes of high wind speed (Cheung et al., 2011b; Pakbin et al., 2010). As shown in Table 4.2c, the average PM_{10} level experienced a more consistent reduction with a R^2 of 0.75. From 1999 to 2009, the reduction of average PM_{10} was largely driven by the decrease in fine PM concentrations ($m = -1.69$ μg/m^3, $p < 0.001$), with a minor contribution from CPM ($m = -0.57$ μg/m^3, $p = 0.08$). The slope of the 99th percentile and average PM_{10} concentration is -5.38 and -1.76 μg/m^3 respectively from 1988 to 2009. The reduction of CPM mass concentration is significantly lower than that observed in the PM_{10}, and the trend is more variable, although, overall, a decreasing trend is seen as evident by the negative slopes of -2.36 and -0.57 for the 99th percentile and average CPM levels respectively. The relatively low coefficient of determination in the 99th percentile ($R^2 = 0.32$) is driven by the spike in 2003, due to a week of high CPM levels in October (91.0, 96.3 and 111 μg/m^3 on Oct 21, 24 and 27 respectively). In Riverside, where the contribution of coarse particles to PM_{10} is generally higher than in Los Angeles and Long Beach due to the high levels of crustal materials in the sub-urban area (Cheung et al., 2011b), the proposed $PM_{10-2.5}$ standard was not equivalent with the current PM_{10} standard. Using the data from 1999 to 2009, the annual 99th percentile PM_{10} level was higher than the current PM_{10} standard of 150 μg/m^3 only in 2003. However, the annual 98th percentile CPM level was higher than the proposed CPM standard of 70 μg/m^3 five times

(1999-2001, 2003 and 2006) from 1999 to 2009, suggesting that the proposed standard is more stringent than the existing standard in areas dominated by coarse particles, and that Riverside could be in frequent violations with the proposed $PM_{10-2.5}$ standard.

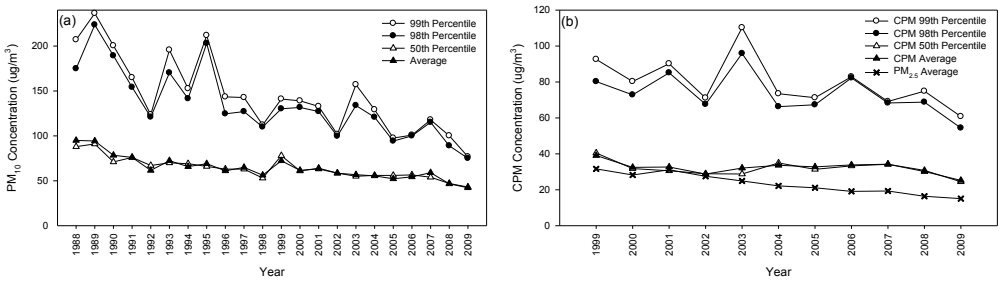

Figure 4-4: Annual concentrations of: (a) PM_{10} from 1988 to 2009, and (b) CPM / $PM_{2.5}$ from 1999-2009 in Riverside.

4.4.2. Trends in chemical CPM components

While CPM mass concentrations provide a metric of the overall mass reduction of coarse particles, the examination of CPM chemical composition provides insights on changes in the contribution of different sources to coarse particles, and may thus assist regulatory agencies in the design and implementation of more effective air quality strategies to protect public health. Figures 4.5-4.7 present concentrations of CPM chemical constituents, including organic and elemental carbon, elements and inorganic ions in downtown Los Angeles, Long Beach and Riverside, respectively. Note that the analyses described below focused on the study conducted in 1986 (Solomon et al., 1988), 1995-1996 (Kim et al., 2000b) and 2008-2009 (Cheung et al., 2011b), all of which compiled comprehensive CPM datasets of one year or more, and their results are presented as bar charts in Figures 4.5-4.7. Although sampling of the three year-long studies was conducted not daily, but rather once every 3rd, 6th or 7th day, the long sampling period was likely to diminish the impact of temporal variation, and could therefore provide a more

representative characterization of CPM. Other studies that were conducted in shorter time frames / smaller spatial scales were shown as line plots, and their results were likely to be influenced by seasonal variations of ambient CPM. Studies conducted before and after 1995 are represented by black and open symbols, respectively.

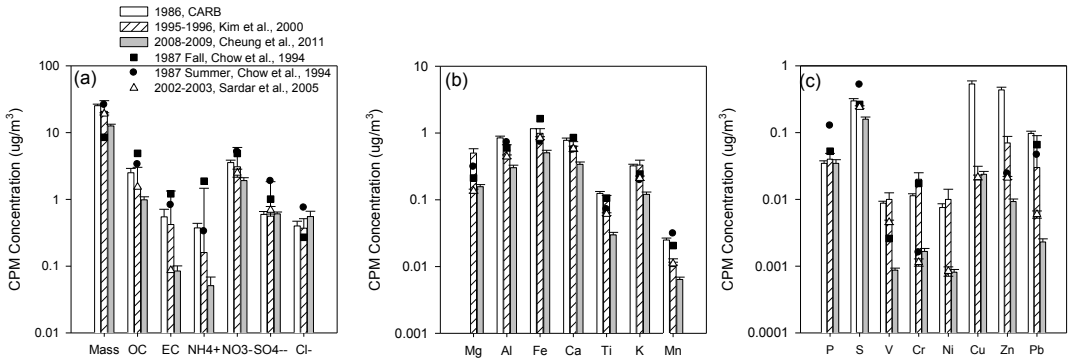

Figure 4-5: CPM concentrations of: (a) mass, organic and elemental carbon and inorganic ions, (b) elements of crustal origins, and (c) elements of anthropogenic origins in downtown Los Angeles. Error bars show standard errors of the average when available.

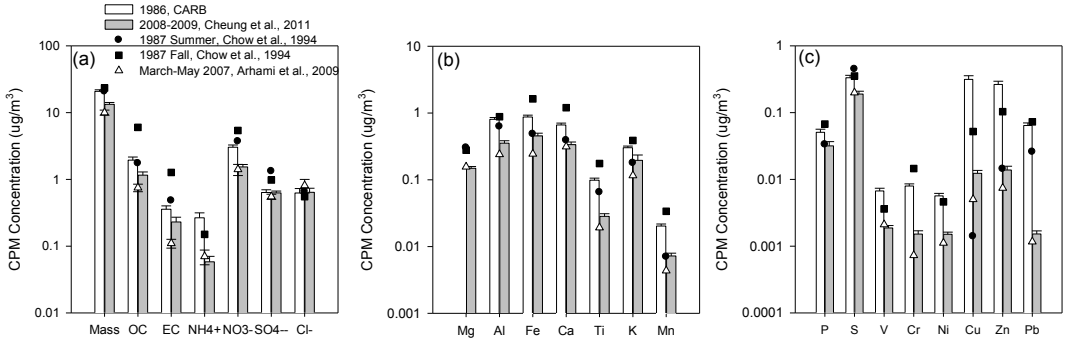

Figure 4-6: CPM concentrations of: (a) mass, organic and elemental carbon and inorganic ions, (b) elements of crustal origins, and (c) elements of anthropogenic origins in Long Beach. Error bars show standard errors of the average when available.

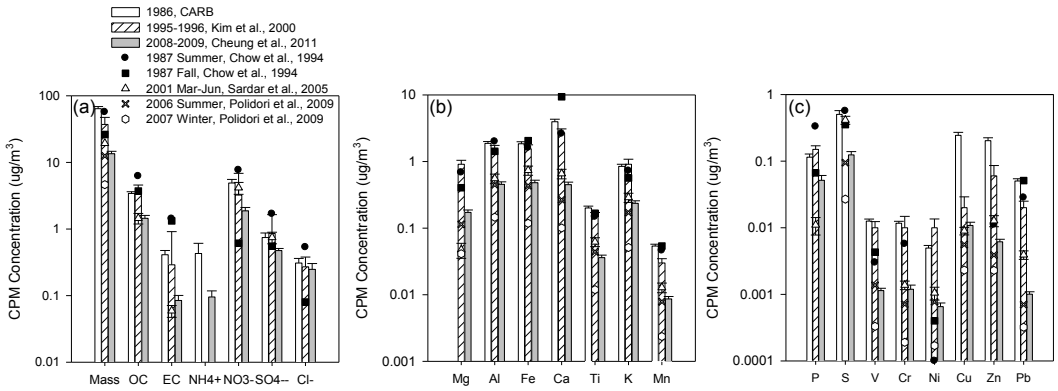

Figure 4-7: CPM concentrations of: (a) mass, organic and elemental carbon and inorganic ions, (b) elements of crustal origins, and (c) elements of anthropogenic origins in Riverside. Error bars show standard errors of the average when available.

Mineral dust. Many studies have shown that mineral and road dust are major components of CPM, contributing to 22-65% of CPM mass concentrations in studies conducted in Los Angeles, Athens, Helsinki, Amsterdam, and Eastern Mediterranean (Cheung et al., 2011b; Koulouri et al., 2008; Sillanpaa et al., 2006). Mineral dust comprises largely of eroded soil particles that have been mobilized and re-suspended into the atmosphere by wind and anthropogenic activities. Industrial activities, such as construction and cement plant operations, may contribute to the emission and re-suspension of dust. Si, Al and Fe are the three most abundant major elements in the upper continental crust (Usher et al., 2003) and thereby may serve as tracers of mineral dust (Lough et al., 2005; Pakbin et al., 2011). Note that although Fe in the coarse fraction arises predominantly from crustal materials, it could be enriched from anthropogenic sources such as brake wear in urban areas (Garg et al., 2000). Other crustal-dominated elements include Na, Ca, Ti, K, Mn and Mg, and their abundances vary depending on location and rock type. The decreasing trends of crustal materials were very consistent in the last two decades. From 1986 to 1995, levels of coarse particulate Al, Fe and Ti decreased by 34, 15 and 20% respectively in downtown Los Angeles.

Further reductions were observed from 1995 to 2008, when Al, Fe and Ti concentrations were reduced by 46, 49 and 70% respectively. Such reduction trends were reinforced by the data from Sardar et al., where sampling was conducted from 2002 to 2003 (Sardar et al., 2005) and the average concentrations of Al, Fe and Ti stayed between those from Kim et al. (2000a) and Cheung et al. (2011b). The contribution of crustal materials and trace elements to CPM mass were higher in Riverside (54.7%) compared with Los Angeles (42.6%) (Cheung et al., 2011b). In Riverside, CPM Al and Ti concentrations were reduced by 19 and 25%, respectively, from 1986 to 1995, where the corresponding reductions were 70 and 76% from 1995 to 2008. In 1986, the SCAQMD implemented Rule 1112.1 to limit PM emissions from cement kilns. Rule 1186 was adopted in 1997 to reduce the re-entrainment of fugitive dust of PM_{10} emissions from paved and unpaved roads as well as livestock operations. This rule requires owners and operators of paved public roads to remove visible roadway accumulations within 72 hours of notifications. It also requires the paving or stabilization of heavily used unpaved public roads or the reduction of vehicular speed on such roads. In 2005, Rule 1157 was introduced to control PM_{10} emissions from aggregate and related operations by reducing various dust sources from loading, unloading and transferring activities, process equipment, paved and unpaved roads inside the facilities, etc. The use of dust suppressants or other control methods is required during transfer and loading activities. The observed high reductions of mineral dust could be due to the effectiveness of these regulations in reducing the sources and levels of re-suspension of dust particles.

Combustion emissions from vehicles, industries and ships. Although particles from combustion sources mostly reside in the fine mode, the "upper tail" of that source function can extend to the lower range of the CPM fraction. For example, Huang and Yu (2008) demonstrated that elemental

carbon (EC), a tracer of vehicular emissions, experienced a bimodal pattern in both ambient and tunnel environments, with a major fine mode and a minor coarse mode. Studies conducted in the Los Angeles Basin in the 20th century also demonstrated that, while dominant in the fine PM fraction, metals emitted by combustion sources could also contribute to a minor fraction of CPM (Krudysz et al., 2008; Singh et al., 2002).

The tailpipe emissions of CPM is often associated with high emitting and poorly controlled vehicles (Kleeman et al., 1999). In downtown Los Angeles, CPM elemental carbon was reduced from an annual average level of 0.55 μg/m^3 to 0.42 μg/m^3 from 1986 to 1995 (23% reduction), and further to 0.08 μg/m^3 (80% reduction) from 1995 to 2008 (Figure 4.5a). The sampling sites in Riverside were located in residential areas adjacent to major roadways, and again, a similar reduction trend was observed (29% reduction from 1986 to 1995 and 71% reduction from 1995 to 2008) (Figure 4.7a). The U.S. EPA requires automobiles of 1975 model year and after to be equipped with catalytic converters to control tailpipe emissions. In 1984, the Smog Check Program was implemented in California. In addition to various emission standards adopted for light-duty vehicles, heavy-duty diesel trucks and bus engines in the 1990s, a number of programs were developed to remove the older and more polluting cars from the road. For example, California's Carl Moyer Program has provided funding to encourage the retrofit and replacement of diesel engines in an effort to reduce emissions from diesel-powered vehicles and equipment. In the last decade, the SCAQMD also adopted / amended a few rules to promote cleaner on-road vehicles used by the public sector. The high reductions of EC, particularly after the 1990s, highlight the effectiveness of various controls implemented by the regulatory agencies to control tailpipe emissions.

In addition to tailpipe emissions, industrial activities also serve as potential sources of CPM in this basin. Metal processing facilities could emit high levels of heavy metals including Fe, Cu, Zn, As, Cd and Pb (Newhook et al., 2003). In particular, smelters could release metals in the coarse size range either as stack or fugitive emissions (Chan et al., 1983; Harrison and Williams, 1983), and could contribute to the high levels of Cu, Zn and Pb in 1986 as shown in Figures 4.5-4.7. In 1992, the SCAQMD adopted Rule 1420 to reduce emissions of lead– one of the six criteria pollutants identified by the U.S. EPA. This regulation requires all emission points of a lead-processing facility (including facilities that produce lead-oxide, brass and bronze) to be vented to an emission collection system. Furthermore, facilities are required to conduct air quality monitoring at their property lines, in addition to the source-oriented monitors placed by the SCAQMD at or beyond the facilities' fence lines. The high reductions of Cu, Zn and Pb from 1986 to 1995 (96, 84 and 69% respectively in downtown Los Angeles) could largely result from the effective control of emissions from metal processing facilities.

Oil refinery is also a major source of industrial emissions. Various coarse elements including Pb, Ce, La, Zn, V, Cu, Co, and to a lesser extent Cr , Ni and Mo could be emitted from refinery fluid catalytic cracking stacks (Campa et al., 2011). Using principal component analyses, Pakbin et al. (2011) showed that CPM-bound Ni and Cr are markers of industrial emissions, with V originating from ship emissions in the Los Angeles / Long Beach Harbor based on coarse particles sampled from 2008 to 2009. In general, the lower concentrations of these elements in the coarse mode support that they originate from combustion sources in this basin. In downtown Los Angeles, the reductions of V, Cr and Ni were higher from 1995 to 2008 (> 90% reduction calculated using 1995 and 2008 data), compared with those from 1986 to 1995 (Figure 4.5c). In

Riverside, the corresponding reductions of Ni, Cr and V were 93, 88 and 89%, respectively, from 1995 to 2008, consistent with the observations in downtown LA. The significant reductions after 1995 could be resulting from series of regulations targeted to control emissions from stationary sources, as evident by the reductions in PM_{10} emissions from industrial processes, manufacturing and industrial sources from 1995 to 2010 according to the emission inventory of the South Coast Air Basin acquired from CARB. For example, Rule 1105.1, aiming to reduce PM_{10} and ammonia emissions from fluid catalytic cracking units used in petroleum refineries, was adopted in 2003. Additionally, the Los Angeles / Long Beach ports approved an incentive program that promotes the use of cleaner-burning fuel in cargo ships transiting within 40 miles of the Bay and at berth in 2008. Note that the efforts to control ship emissions began in the early 20^{th} century, consistent with the historical trend of vanadium, which experienced similar annual averages in 1986 and 1995, with higher reduction rates from 1995 to 2008. Therefore, the high reductions of Ni, V and Cr after 1995 could be due to various programs and incentives that aim to reduce combustion-related emissions from vehicles and industries, as well as the efforts to reduce ship emissions from harbor activity.

CPM-bound lead (Pb) also decreased considerably in the LA basin. Pb could originate from brake wear and wheel weights, gasoline exhaust and oil combustion as the extended upper tail of the fine PM mode, as well as metal processing industries (Harrison and Williams, 1983; Isakson et al., 2001; Pakbin et al., 2011). In downtown Los Angeles, Pb levels have decreased from an annual mean of 0.097 $\mu g/m^3$ to 0.030 $\mu g/m^3$ from 1986 to 1995, and further to 0.0023 $\mu g/m^3$ in 2008. As discussed previously, the early reduction of Pb could be resulted from Rule 1420, which was adopted in 1992 aiming to control lead emissions. The latter reduction (after 1995) could

partly be attributed to the complete elimination of the sales of leaded fuel for use in on-road vehicles in 1996. In Long Beach, ships (Isakson et al., 2001) and refineries emissions (Newhook et al., 2003) could also be potential sources of lead. The reduction in CPM lead concentrations in Long Beach was comparable to those observed in downtown LA (0.064 $\mu g/m^3$ in 1986 to 0.0015 $\mu g/m^3$ in 2007). Recent studies, including a study of CPM in Los Angeles and Long Beach conducted in 2008 (Pakbin et al., 2011; Root, 2000), indicated that Pb is now predominantly sourced from vehicular abrasion. Therefore, it is likely that the Pb reductions in the last two decades were largely driven by the phase-out of Pb in gasoline vehicles, as well as controlled emissions from various industries as discussed previously.

Vehicle abrasion. Particles originating from vehicular abrasion contribute to road dust PM, though the mass-fraction is typically small. Cu, which is present in brake linings as lubricants, is often used as tracers of brake wear in areas where industrial emission of Cu is not significant (Lin et al., 2005; Pakbin et al., 2011). Note that the high concentrations of Cu in 1986 likely resulted from emissions of metal processing industries, as discussed in the previous section, and therefore Cu might not be a reliable tracer of brake wear back in the 1980s. Nonetheless, a recent study in the LA basin suggested that majority of coarse particulate Cu was generated from the wear of brake linings based on CPM sampled from 2008 to 2009. Despite the considerable decrease of elements of combustion origins from 1995 to 2008 (Pakbin et al., 2011), the reduction of Cu was less significant in the same period. In Los Angeles, the higher annual average concentrations of Cu in 2008 compared to the 1995 levels could be due to the increased emissions from tire and brake wear from the greater number of both light-duty and heavy-duty vehicles on the road. The contribution of anthropogenic sources to elements, including Cu, is generally higher in Los

Angeles and Long Beach than Riverside (Cheung et al., 2011b). From 1995 to 2008, the lower reduction of Cu (46%) relative to other CPM species with anthropogenic origins (89, 88 and 93% for V, Cr and Ni respectively) in Riverside further confirms the lower reduction of non-tailpipe mobile source emissions. The reduction of Cu might also be a "side-benefit" as a result of the high reduction of mineral dust in Riverside.

Inorganic ions. In general, reductions of CPM inorganic ions were relatively lower than combustion related CPM due to their natural origins and, to a lesser extent, secondary formation. Nitrate is the most abundant inorganic species in the coarse fraction, accounting for an average of 17% of CPM mass in this basin (Cheung et al., 2011b). In the Los Angeles Basin, nitrate is primarily formed by sea salt depletion, a process involving the reaction of nitric acid with sodium chloride (Zhuang et al., 1999), and to a lesser extent the reactions with mineral dust and the condensation of alkaline salts on CPM surfaces when sea salt levels are low (Cheung et al., 2011c). In downtown Los Angeles and Riverside, the level of nitrate was reduced by 13% and 34% respectively from 1986 to 1995, while corresponding reductions were 38% and 42% from 1995 to 2008. Substantial efforts have been made to reduce emissions of nitrogen oxides, as demonstrated by the reduction of NO_x emissions from 1561 tons per day (TPD) in 1985 to 1332 TPD in 1995 and 742.2 TPD in 2010 in the South Coast Air Basin (Emission Inventory of CARB). In addition to the regulations to control mobile emissions as described previously, the SCAQMD has adopted a few rules to control NO_x emissions from stationary sources, including boilers and process heaters from refineries, cement kilns, gas melting furnaces and stationary gas turbines. Since 2001, the LA ports incorporated a voluntary vessel speed reduction program with the objective of reducing both NO_x and PM emissions by decreasing the vessel's speed to 12 knots

near the ports. The control of NO_x emissions may have an indirect effect on the reduction of coarse particulate nitrate by limiting the levels of its precursors, which could also decrease the CPM-bound nitrate associated with the hygroscopic growth of nitrate originally in the fine PM mode (Geller et al., 2004; Seinfeld and Pandis, 2006). In addition, the reduction of mineral dust, which could serve as a reaction site for nitrate (Usher et al., 2003), might have also indirectly reduced the levels of nitrate in CPM. Sulfate, on the other hand, has several potential sources, namely water-soluble gypsum and sea salt sulfate, as well as the upper tail of ammonium sulfate, and the reduction was insignificant. Chloride, primarily originating from sea salt in the coarse mode, is used as a tracer of fresh sea salt aerosols. Cl^- levels increased from 0.37μg/m^3 in 1995 to 0.55 μg/m^3 in 2008 in downtown Los Angeles. This could be due to yearly variations in sea salt level, as well as the reduction in nitrogen oxides emissions, which decreased the rate of sea salt depletion and increased the levels of unreacted chloride.

4.5. Summary and Conclusions

Overall, PM_{10} mass concentration has decreased by approximately half from 1988 to 2009 since the PM_{10} standard was put in place in 1987. PM_{10} daily concentrations from downtown Los Angeles and Long Beach show compliance with the federal EPA PM_{10} standard, while violating the more stringent California standard. These two sites also demonstrated equivalency for the current PM_{10} and proposed $PM_{10-2.5}$ standard. On the other hand, both PM_{10} and CPM levels were higher in Riverside as highlighted by some violations of the federal standards in late 80s and early 90s. This site also demonstrates that the proposed $PM_{10-2.5}$ standard is more stringent than the current PM_{10} standard. The reduction trends of combustion-related CPM namely EC, V, Cr and Ni were higher after 1995, consistent with the implementation of $PM_{2.5}$ standard in 1997. The

concentrations of Cu, a tracer of brake wear, has decreased at a lesser rate or remained comparable relative to other anthropogenic constituent after 1995, suggesting that the contribution of brake wear to CPM has become more significant despite the overall reduction in CPM mass since 1995. In general, the reduction of CPM mass was mostly driven by the reduction of mineral dust, while reduction of contributions from inorganic ions and non-tailpipe vehicular emission were less significant from 1995 to 2008.

4.6. Acknowledgments

The authors would like to acknowledge the support of the Science to Achieve Results program of the U.S. EPA (EPA-G2006-STAR-Q1). The authors would also like to thank Bong-Mann Kim at the South Coast Air Quality Management District for providing supplementary information regarding his project.

Chapter 5 Diurnal Trends in Coarse Particulate Matter Composition in the Los Angeles Basin

5.1. Abstract

To investigate the diurnal profile of the concentration and composition of ambient coarse particles, three sampling sites were set up in the Los Angeles Basin to collect coarse particulate matter (CPM) in four different time periods of the day (morning, midday, afternoon and overnight) in summer and winter. The samples were analyzed for total and water-soluble elements, inorganic ions and water-soluble organic carbon (WSOC). In summer, highest concentrations of CPM gravimetric mass, mineral and road dust, and WSOC were observed in midday and afternoon, when the prevailing onshore wind was stronger. In general, atmospheric dilution was lower in winter, contributing to the accumulation of air pollutants during stagnation conditions. Turbulences induced by traffic become a significant particle re-suspension mechanism, particularly during winter nighttime, when mixing height was lowest. This is evident by the high levels of CPM mass, mineral and road dust in winter overnight at the near-freeway sites located in urban Los Angeles, and to a lesser extent in Riverside. WSOC levels were higher in summer, with a similar diurnal profile with mineral and road dust, indicating that they either share common sources, or that WSOC may be adsorbed or absorbed onto the surfaces of these dust particles. In general, the contribution of inorganic ions to CPM mass was greater in the overnight sampling period at all sampling sites, suggesting that the prevailing meteorological conditions (lower temperature and higher relative humidity) favor the formation of these ions in the coarse mode. Nitrate, the most abundant CPM-bound inorganic species in this basin, is found to be predominantly formed by reactions with sea salt particles in summer. When the sea salt

concentrations were low, the reaction with mineral dust particles and the condensation of ammonium nitrate on CPM surfaces also contribute to the formation of nitrate in the coarse mode.

5.2. Introduction

Short term exposure of high concentrations of coarse particles was related to various adverse health endpoints (Lipsett et al., 2006). A study conducted in Chapel Hill, North Carolina also showed that small temporal increases in coarse particle concentrations could affect cardiopulmonary and lipid parameters in the adult asthmatics, and the investigators concluded that CPM-induced health effects may have been underappreciated in susceptible populations (Yeatts et al., 2007). To improve our understanding of the physical and chemical characteristics as well as the spatial and seasonal variation of CPM, a study was conducted earlier by our group using 24-hour time integrated samples collected in 10 sampling sites at the Los Angeles Basin, and the results were presented in our previous publications (Cheung et al., 2011a; Pakbin et al., 2010). It was found that both CPM mass concentrations and chemical composition varied considerably by season and displayed spatial heterogeneity. However, the long sampling periods (24-hour) suppressed the observation of the evolving CPM chemical characteristics due to the indisputable influence of many important atmospheric parameters, such as temperature, relative humidity, wind direction and speed, and mixing height, all of which vary in scales shorter than 24 hrs. The study presented here addresses this issue by focusing on the diurnal trends of coarse particles in the Los Angeles Basin, and provides information that will be vital in improving our understanding on how these atmospheric parameters influence the ambient coarse PM concentrations and composition.

5.3. Methodology

5.3.1. Sites description

Three sampling sites were selected to represent distinct geographical regions of the Los Angeles Basin. Figure 5.1 shows the locations of the three sampling sites: downtown Los Angeles (USC), Lancaster (LAN), and Riverside (RIV). The USC site is located in an urban area in downtown Los Angeles, and is approximately 150 m east of Freeway I-110 and 20 km east of the Pacific Ocean. The RIV site is located in Riverside, about 80 km inland of the USC site. Although Riverside is a semi-rural agricultural region, it is along the typical prevailing wind trajectory crossing the Los Angeles Basin from the coast to inland (Eiguren-Fernandez et al., 2008), and is thereby a receptor area of pollutants from urban Los Angeles. The site in Lancaster (LAN), located about 75 km north of the USC site and over 2 km west of highway CA-14, is characterized by a desert-like rural nature.

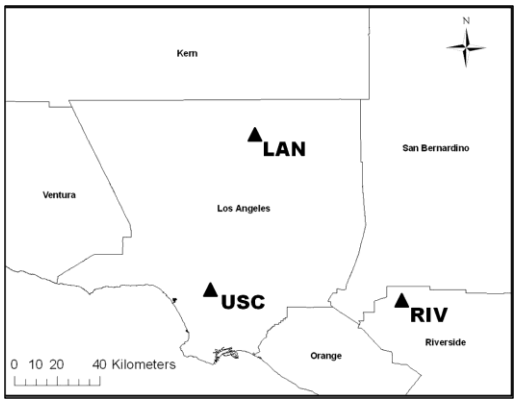

Figure 5-1: Map of the 3 sampling sites.

5.3.2. Sampling time and setup

The sampling campaign was conducted in both summer (July – August 2009) and winter (January – February 2010). Four distinct time periods — morning (7:00 a.m. to 11:00 a.m.),

midday (11:00 a.m. to 3:00 p.m.), afternoon (3:00 p.m. to 7:00 p.m.) and overnight (7:00 p.m. to 7:00 a.m.) — were selected to reflect the effect of different atmospheric parameters on CPM sources and formation mechanisms. Sampling continued for 4 to 6 weeks in each season depending on ambient concentrations.

Samples were collected using the USC Coarse Particle Concentrator (Misra et al., 2001) downstream of a PM_{10} inlet. The USC Coarse Particle Concentrator was composed of a virtual impactor placed upstream of a filter holder. Coarse particles were concentrated approximately 25-fold using the virtual impactor with an intake flow rate of 50 LPM and a minor flow of 2 LPM, and then collected on Teflon filters with a diameter 47 mm and a pore size of 2.0 μm. Four samplers were used at each site. Substrates from each time period were analyzed separately.

5.3.3. Chemical analyses

Teflon substrates were weighed before and after sampling to measure the collected PM mass. They were equilibrated for 24 hours under controlled relative humidity (30% ± 5%) and temperature ($21^{o}C \pm 2^{o}C$) before weighing by a microbalance (Model MT 5, Mettler-Toledo Inc., Highstown, NJ). Water extracts of the Teflon filters were analyzed for water soluble organic carbon (WSOC) using a Sievers Total Organic Carbon analyzer (General Electric, Inc.) (Zhang et al., 2008b) and inorganic ions by Ion Chromatography (Lough et al., 2005). The same aqueous extraction was used to measure the concentration of water soluble metals and elements using Inductively Coupled Plasma-Mass Spectroscopy (ICP-MS) (PQ Excell, Thermo Elemental). To determine the levels of total elements, the PM collected on Teflon filters was digested using a mixture of 1.0 mL of 16 N HNO_3, 0.1 mL of 28 N HF, and 0.25 mL of 12 N HCl in a microwave digestion unit and subsequently analyzed by magnetic-sector ICP-MS (SF-ICPMS) (Lough et al.,

2005). The samples were analyzed with field and laboratory blanks, filter spikes and external check standards. On average, replicates were analyzed once every ten samples and blank levels were less than 2% of the samples' levels. The uncertainties of some water soluble trace elements were high due to their low concentrations, and they were not included in the analysis. Spike recoveries were within the acceptance range of 85–115%.

5.4. Results and Discussion

5.4.1. Meteorology

Selected meteorological parameters in the two sampling periods are shown in Table 5.1, with vector-averaged wind direction and speed. This information was obtained from the online database of the California Air Resources Board. The meteorological station was located about 7 km northeast of the USC sampling site, while the meteorological stations were located at the same site as the sampling instruments at the RIV and LAN sites. In summer, highest temperature was observed in midday. Average temperature was higher inland in Lancaster and Riverside. The high temperature also extended from midday into the afternoon in the inland area. Relative humidity was highest overnight for all sampling sites. The "desert-like" characteristics of Lancaster are evident in Table 5.1 by the lower relative humidity and the higher temperature range. In summer, wind speed was highest in the midday and afternoon periods, with predominant wind direction from the west, which is typical in this region. Somewhat unexpectedly, the wind speed was high during the overnight period in Riverside. In winter, the Los Angeles Basin is characterized by lower mixing heights and frequent periods of air stagnation, resulting in the accumulation of air pollutants (Hildemann et al., 1994). In urban Los Angeles (USC), winds originated from the west during midday and afternoon, in accordance with the typical onshore

flow patterns of the basin. However, this pattern was not as persistent at the two inland sites, where the predominant wind direction was from the north. The low wind speed at the two inland sites during the sampling period indicates stagnant meteorological conditions, especially during the overnight period, when the temperature was lowest. In Lancaster, the average temperature in the morning and overnight periods dropped below 10^{o}C, highlighting its "desert-like" nature.

Table 5-1: Selected meteorological parameters at the 3 sampling sites in: (a) summer and (b) winter.

a) Summer

	Los Angeles (USC)				Riverside (RIV)				Lancaster (LAN)			
Summer	Morning	Midday	Afternoon	Overnight	Morning	Midday	Afternoon	Overnight	Morning	Midday	Afternoon	Overnight
Temperature (°C)	26.6	29.6	25.1	19.4	28.7	36	31.8	21.3	29.9	36.3	34.1	25.6
Relative Humidity (%)	53.9	46	46.4	73.3	52.5	33	43.1	74.1	21.4	15.9	20.2	25.6
Wind Speed (m/s)	1.3	3.6	3.8	1.2	0.63	3.2	3.1	3.2	0.63	2.4	4.1	0.98
Wind Direction	S	SW	W	W	W	W	W	W	W	W	SW	SW

b) Winter

	Los Angeles (USC)				Riverside (RIV)				Lancaster (LAN)			
Winter	Morning	Midday	Afternoon	Overnight	Morning	Midday	Afternoon	Overnight	Morning	Midday	Afternoon	Overnight
Temperature (°C)	16.1	22.3	18.3	12.5	14.1	21.9	18.9	10.9	8.2	13.6	14.2	8.2
Relative Humidity (%)	52.9	34.1	47.4	66.2	54.1	27.8	36.7	64.9	61.3	43.6	42.1	62.5
Wind Speed (m/s)	2.0	0.98	2.0	1.5	0.27	0.27	1.3	0.22	0.09	0.31	0.18	0.49
Wind Direction	NE	SW	W	NE	NE	N	NW	N	NW	NW	NW	SW

5.4.2. Coarse PM component model and data overview

Chemical components were classified into 5 groups according to their common sources: 1) crustal materials and trace elements (CM + TE); 2) vehicle abrasion (VA); 3) water soluble organic carbon (WSOC); 4) sea salt (SS) and 5) secondary ions (SI). Crustal material (CM) is calculated using the following equation (Chow et al., 1994; Hueglin et al., 2005):

$$CM = 1.89\ Al + 1.21\ K + 1.43\ Fe + 1.4\ Ca + 1.66\ Mg + 1.7\ Ti + 2.14\ Si \quad (1)$$

where Si is estimated from Al using a factor of 3.41 (Hueglin et al., 2005). The group of trace elements (TE) includes Rb, Sr and rare earth elements such as La and Ce, etc, and is grouped with CM because of their common crustal origins. Vehicle abrasion includes traffic related emissions such as Cu, Zn, and Ba (Harrison et al., 2001). Water-soluble organic carbon is obtained directly by the measured WSOC. The sea salt component is estimated using soluble Na^+ and the sea salt fraction of Cl^-, Mg^{2+}, K^+, Ca^{2+} and SO_4^{2-} from the typical sea water composition (Seinfeld and Pandis, 2006), represented by the equation below:

$$SS = Na^+ + ssCl^- + ssMg^{2+} + ssK^+ + ssCa^{2+} + ssSO_4^{2-} \qquad (2)$$

The use of Na ion as a sea salt tracer represents both fresh and aged sea salt aerosols. The group of secondary ions consists of ammonium, non-sea salt (nss) sulfate and nitrate.

Table 5.2 (a and b) shows the overview of the categorized chemical components concentrations during each time period and their 24-hour averages. Overall, crustal materials and trace elements is the most abundant category, with an average concentration of 4.54 $\mu g/m^3$ in summer and 3.85 $\mu g/m^3$ in winter across the three sampling sites. In particular, levels were higher at RIV (9.76 $\mu g/m^3$ and 5.71 $\mu g/m^3$ for summer and winter, respectively) due to its semi-rural nature and receptor location. In general, the CM + TE level in Lancaster was lower than Riverside due to its remote location and lack of anthropogenic sources and / or re-suspension of mineral and road dust. In particular, vehicles driving on dirt and / or unpaved roads in semi-rural Riverside could contribute substantially to the generation and re-entrainment of mineral and road dust. In summer afternoon, the level of crustal material at LAN was similar to RIV, due to the comparable high wind speed as the main re-suspension mechanism at both sites. CPM originating from vehicle abrasion, on the other hand, is less abundant (on average 0.061 $\mu g/m^3$, 0.14 $\mu g/m^3$ and

0.36 μg/m^3 for LAN, USC and RIV, respectively) compared with the crustal materials. The VA levels at RIV were relatively high. As discussed previously, unpaved roads or paved roads with unpaved shoulders in Riverside could contribute substantially to the fugitive dust components of CPM. Chow et al. (1992) showed that vehicle movement associated with agricultural planting and harvesting, as well as the transport of agricultural products along the unpaved roads, was the primary contributor of fugitive dust in the semi-rural agricultural area of San Joaquin Valley (Chow et al., 1992). Vehicle speed could be another factor in the re-suspension of VA (Nicholson et al., 1989). In the morning and afternoon period in downtown LA, vehicles travel at lower speeds due to high traffic volume. On the other hand, the levels of VA were higher in the midday at RIV and USC when traffic volume was lower. SS and SI contributed similarly at an average concentration of 0.41 μg/m^3 and 0.50 μg/m^3 respectively. SS concentrations experienced a seasonal variation with higher levels in summer (on average 0.53 μg/m^3) than winter (on average 0.28 μg/m^3). WSOC concentrations were low at LAN and USC (on average 0.070 μg/m^3 and 0.077 μg/m^3, respectively), with higher levels at RIV at 0.37 μg/m^3.

Table 5-2: Average diurnal concentration (μg/m^3) of chemical components at the three sampling sites in: (a) summer and (b) winter (± indicates uncertainties calculated based on the analytical uncertainties and uncertainties from blank corrections).

a) Summer

	Summer	CM + TE	VA	SS	SI	WSOC
LAN	Morning	1.18±0.07	0.042±0.002	0.31±0.03	0.24±0.02	0.1±0.01
	Midday	2.88±0.15	0.084±0.004	0.19±0.02	0.33±0.03	0.081±0.02
	Afternoon	7.99±0.41	0.18±0.008	0.82±0.08	0.76±0.06	0.31±0.02
	Overnight	0.62±0.04	0.038±0.002	0.042±0.005	0.067±0.01	0.018±0.01
	24-hr Avg.	2.32	0.070	0.24	0.26	0.091
USC	Morning	0.88±0.05	0.087±0.005	0.05±0.01	0.12±0.01	0.046±0.01
	Midday	3.49±0.19	0.19±0.009	0.66±0.06	0.73±0.06	0.1±0.02
	Afternoon	2.14±0.12	0.076±0.003	0.66±0.06	0.64±0.05	0.085±0.02
	Overnight	0.94±0.05	0.051±0.002	0.88±0.08	0.67±0.05	0.073±0.01
	24-hr Avg.	1.56	0.084	0.67	0.58	0.075
RIV	Morning	7.54±0.38	0.47±0.03	0.35±0.03	0.49±0.04	0.29±0.04
	Midday	4.91±0.25	0.15±0.03	0.29±0.03	0.59±0.05	0.17±0.02
	Afternoon	11.9±0.62	0.59±0.11	1.16±0.11	1.34±0.11	1.14±0.06
	Overnight	11.4±0.55	0.37±0.07	0.76±0.07	0.82±0.06	0.56±0.02
	24-hr Avg.	9.76	0.39	0.68	0.81	0.55

b) Winter

	Winter	CM+TE	VA	SS	SI	WSOC
LAN	Morning	1.76±0.08	0.085±0.003	0.049±0.005	0.055±0.02	0.06±0.01
	Midday	1.94±0.09	0.055±0.002	0.081±0.007	na	0.03±0
	Afternoon	1.18±0.06	0.047±0.002	0.11±0.01	0.03±0.02	0.03±0.01
	Overnight	1.56±0.08	0.039±0.001	0.072±0.007	0.11±0.01	0.06±0.01
	24-hr Avg.	1.59	0.051	0.076	0.083	0.050
USC	Morning	2.3±0.12	0.122±0.005	0.06±0.006	0.087±0.02	0.042±0.01
	Midday	2.85±0.15	0.097±0.003	0.26±0.024	0.23±0.03	0.056±0.01
	Afternoon	1.87±0.11	0.068±0.003	0.055±0.005	0.079±0.02	0.029±0.01
	Overnight	6.14±0.32	0.31±0.014	0.94±0.089	0.88±0.07	0.12±0.01
	24-hr Avg.	4.24	0.20	0.53	0.51	0.081
RIV	Morning	3.55±0.18	0.24±0.01	0.23±0.02	0.5±0.05	0.18±0.02
	Midday	3.03±0.16	0.1±0.005	0.18±0.02	0.26±0.03	0.12±0.01
	Afternoon	4.35±0.23	0.55±0.03	0.2±0.02	0.44±0.04	0.18±0.02
	Overnight	7.78±0.41	0.39±0.02	0.28±0.03	1.09±0.09	0.24±0.02
	24-hr Avg.	5.71	0.34	0.24	0.75	0.20

5.4.3. Diurnal profiles

Figures 5.2, 5.4 and 5.5 show the diurnal profile of CPM mass and the five chemical categories in summer and winter, with the group of secondary ions presented as ammonium, nitrate and nss-sulfate. Normalization to the corresponding 24-hr average (i.e. CPM mass / 24-hr average CPM mass concentrations, WSOC / 24-hr average WSOC concentrations, etc) are presented to highlight the diurnal trends of these species. A detailed discussion of each group is offered in the following sections.

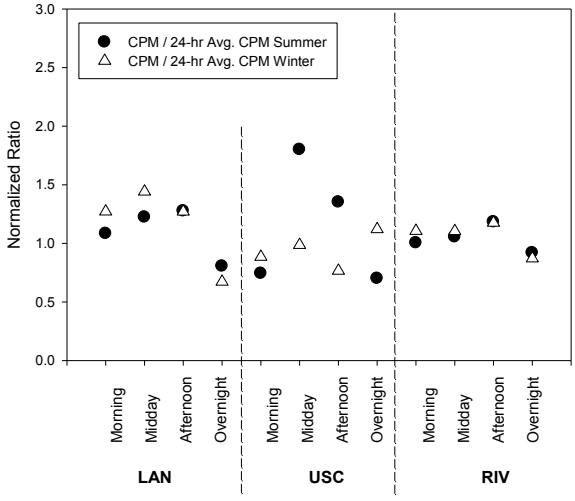

Figure 5-2: Diurnal profiles (normalization to the 24-hr average) of CPM mass.

CPM mass. In general, the diurnal profile of CPM gravimetric mass concentration closely followed the profile of wind speed in summer. The highest CPM normalized ratios were often observed in midday and / or afternoon, when the wind speed was stronger. This trend is not as persistent in winter when the wind speed was low. Despite the lower wind speed in winter, the overall CPM mass concentrations remained comparable to those of summer in this study, likely due to the stagnation atmospheric conditions as discussed earlier. In winter, the overnight CPM

mass concentration was high at USC (normalized ratio = 1.12), likely due to particle re-suspension by the northeasterly wind coupled with the lower mixing height at night. At Riverside, despite the low wind speed (ca. 0.22 m/s), the overnight CPM mass concentration remained high. Similar results have been observed in some previous studies showing higher levels of traffic-emitted pollutants, including EC and CO, in late night and early morning (compared with midday and afternoon) in Riverside (Polidori et al., 2007; Snyder and Schauer, 2007), as a result of lower atmospheric dilution in the nighttime period of winter. Furthermore, elevated turbulence induced by increased traffic activity might become a significant particle re-suspension mechanism in early morning when atmospheric dilution is low. Harrison et al. (2001) demonstrated that turbulence induced by vehicles provides a source strength that was approximately equal to that of exhaust emissions, and concluded that coarse particles predominantly come from vehicle-related re-suspension at the studied sampling sites in the United Kingdom. Additionally, heavy-duty vehicles are known to induce higher roadway CPM re-suspension than light duty vehicles (Charron and Harrison, 2005).

Carbon monoxide, sourced primarily from vehicles in urban atmospheres, has been used as a reliable tracer of primary emission (Ning et al., 2007). As traffic flow and pattern are consistent in both sampling periods, CO levels can be used to indicate the degree of atmospheric dilution in ambient conditions. Figure 5.3 (a-c) shows the diurnal CO levels at the three sampling sites acquired from the online database of the South Coast Air Quality Management District's monitoring stations located at or within 7 km of the sampling sites employed in this study. In summer, CO concentrations were higher during daytime, in contrast to the significant overnight peak experienced at all sampling sites in winter. Although the emission source strength was lower

during nighttime, the CO levels were approximately 2-4 times higher in winter overnight compared with daytime. In general, CO levels were also higher in winter than summer, particularly during the nighttime, highlighting the much lower atmospheric dilution experienced in the overnight sampling period in winter. Therefore, turbulence induced by vehicular traffic could become a significant mechanism of particle re-suspension that increases pollutant concentrations during the overnight period, especially considering the prevailing air stagnation conditions and the low atmospheric dilution at that time.

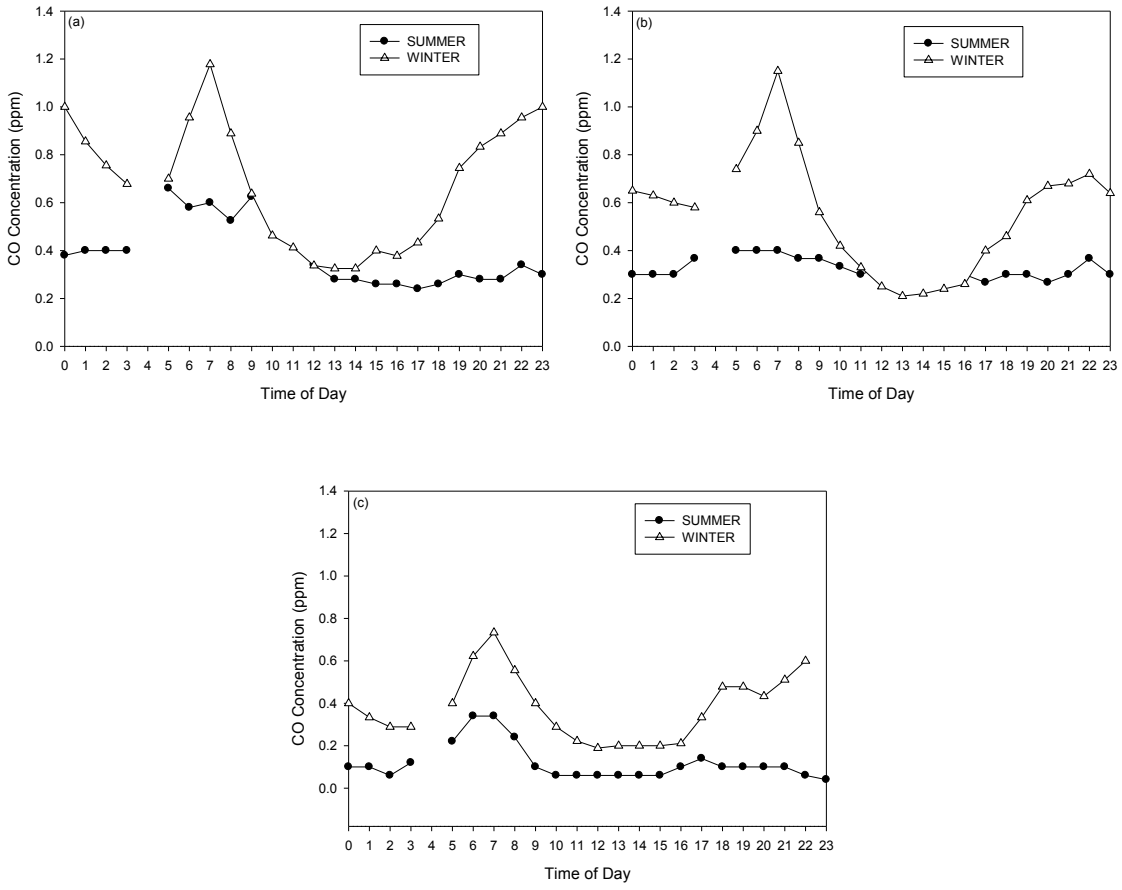

Figure 5-3: Carbon monoxide (CO) levels at: (a) Los Angeles-USC; (b) Lancaster-LAN; (c) Riverside-RIV.

Crustal materials and trace elements. Figure 5.4a shows the diurnal profile of CM + TE. In summer, the diurnal trend at Lancaster paralleled that of wind speed, peaking in the afternoon (normalized ratio = 3.44) when the average wind speed was strongest at 4.1 m/s. Crustal material and trace elements are the dominant sources of CPM at the Lancaster site which is located in a remote area away from freeways and urban pollutants. As previously discussed, RIV experienced higher CM + TE levels due to its downwind receptor location and semi-rural nature, with the highest normalized ratio in the afternoon. The average concentration was much lower in urban Los Angeles (USC), where the diurnal trend of CM + TE follows closely the CPM mass concentrations. In winter, overall CM + TE concentrations were lower in comparison to summer except for overnight. At USC, the relatively high wind speed, coupled with lower atmospheric dilution and traffic-induced turbulence in the overnight period may explain the high levels of CM + TE (normalized ratio = 1.45), consistent with the peak in the overall CPM mass concentration. On the other hand, CM + TE levels remained high (normalized ratio = 1.36) despite the relatively low CPM mass and low wind speed overnight at RIV. As mentioned previously, re-suspension induced by heavy-duty vehicles might be responsible for the re-entrainment of local mineral dust, which is a dominant source of CPM in Riverside (Cheung et al., 2011a).

Vehicle abrasion. Traditionally, both emission control strategies and regulations have specifically targeted tail-pipe exhaust sources from vehicles. Although non-tailpipe PM is currently unregulated, it has been shown to be a significant source of traffic-related emissions (Querol et al., 2004). Vehicle abrasion, such as tire and brake wear, is an important source of CPM in urban areas (Harrison et al., 2001; Lenschow et al., 2001). Unlike crustal materials, metals of anthropogenic origins have higher solubility (Birmili et al., 2006), and might have important

public health impacts. In general, the diurnal profile of VA follows a similar pattern with CM + TE, suggesting that they are re-suspended together as soil and road dust. The high VA levels in the winter overnight period at freeway-adjacent-USC (normalized ratio = 1.53), and to a lesser degree at RIV (normalized ratio = 1.13), further suggest the contribution of particle re-suspension induced by heavy-duty vehicles as a source of these species.

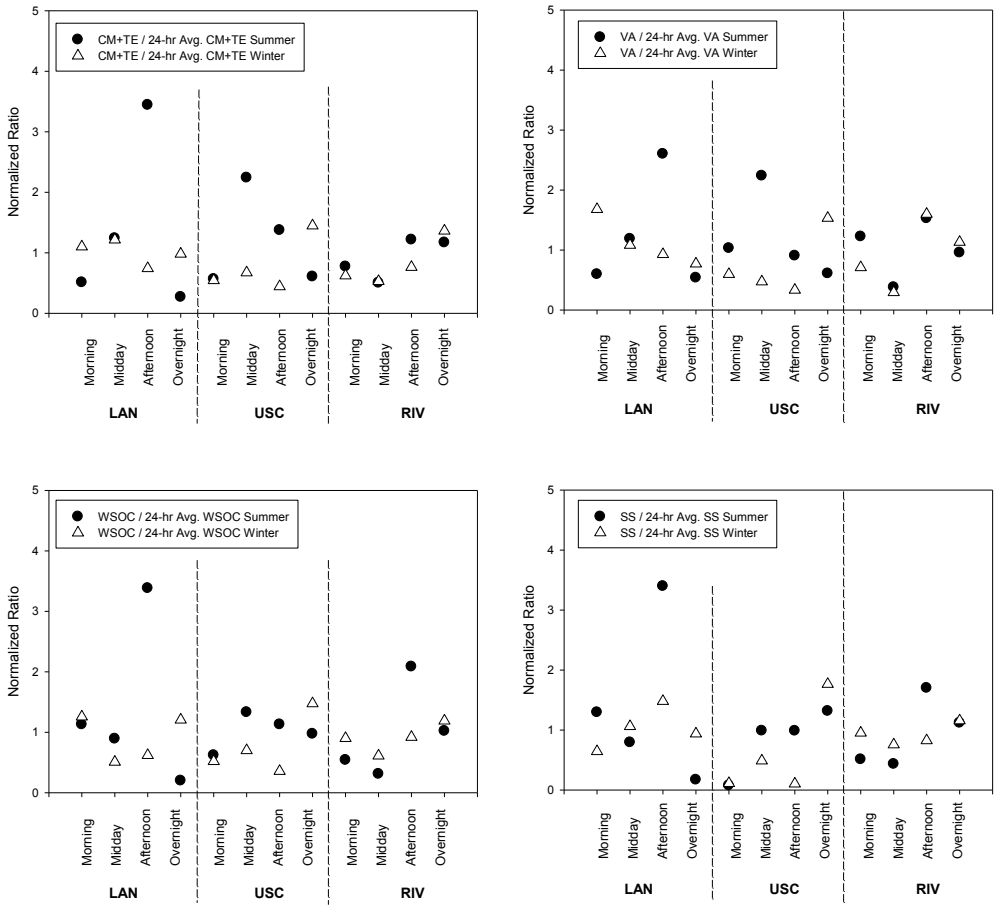

Figure 5-4: Diurnal profiles of: (a) crustal materials and trace elements; (b) vehicle abrasion; (c) water soluble organic carbon and (d) sea salt. Normalization to the 24-hr average is presented.

Water soluble organic carbon. WSOC has been shown to be associated with the production of reactive oxygen species in biological cells, which play a significant role in PM-induced health effects. Despite detailed investigation of WSOC in many studies, very limited literature exists

that addressed the sources of WSOC in the CPM mode. Some studies indicated that organic materials in this size range consist of biological materials, semi-volatile organic species, organic acids, as well as organic ions (Bauer et al., 2008; Falkovich et al., 2005). The diurnal trend of WSOC (Figure 5.4c) may give us some insights on the possible sources of the water-soluble fraction of organic carbon in this basin. In summer, WSOC follows a similar diurnal trend with CM + TE and VA, suggesting that WSOC either share common origins with mineral and road dust, or that WSOC may be adsorbed or absorbed onto these dust particles and re-suspended subsequently during PM sampling. RIV and LAN experienced the highest WSOC concentrations in the afternoon in summer (normalized ratio = 2.08 and 3.38 for RIV and LAN, respectively), which indicates that the sources of WSOC in these inland areas might be associated with upwind pollutants. This is further confirmed by the low levels of WSOC in the afternoon of the winter period, when the lower wind speed may limit the transport of upwind air pollutants, thereby eliminating the peak concentrations observed at RIV and LAN in summer.

Sea salt. The diurnal profile of sea salt aerosols in CPM is shown in Figure 5.4d. In summer, the strong prevailing onshore wind facilitated the transport of sea salt particles inland. The diurnal trend of sea salt concentration varied among the three locations depending on their relative distances from the ocean. The sea salt levels at USC, located around 20 km east of the Pacific Ocean, started to increase in midday (normalized ratio = 0.99) and remained high overnight (normalized ratio = 1.32), consistent with the high wind speed observed during daytime at that site. The Riverside site (RIV), which is around 70-100 km inland of the coast and is along the air mass trajectory of this basin, had the highest level of sea salt in the afternoon with a normalized ratio of 1.70. In the morning and midday, the regional transport of sea salt from coast to inland was

limited due to the low wind speed, resulting in lower sea salt concentrations. The high sea salt concentration observed overnight (normalized ratio = 1.11) might be resulting from the strong wind in the afternoon that transported particles from the coast to inland areas. We observed a similar diurnal pattern at the other inland site (Lancaster), with the highest level of sea salt in the afternoon (normalized ratio = 3.39). In winter, in addition to the lower mixing height in the overnight period, the high sea salt level at USC (normalized ratio = 1.77) could be due to the relatively strong wind in the afternoon. Furthermore, given the hygroscopic nature of marine aerosols, the higher relative humidity at night might have facilitated the growth of these particles from the upper range of fine PM to the lower range of the coarse fraction (Tursic et al., 2006), thereby contributing to the high levels of coarse particulate sea salt aerosol in the overnight period.

Secondary ions. Figure 5.5 (a-c) presents the diurnal profile of ammonium, nitrate and nss-sulfate ions, which composed the category of secondary ions. In general, secondary ions follow a similar pattern with sea salt, with higher concentrations in summer and less in winter except in the overnight period. In an urban atmosphere, the concentrations of both nitrate and sulfate depend on source strengths of their acid forms. HNO_3 and H_2SO_4, the precursors of nitrate and sulfate respectively, are formed secondarily from the emission of vehicular combustion in the Los Angeles Basin. The high correlation (R = 0.80) between sulfate and nitrate further confirms that they share a common origin. In cooler months, less photochemical oxidation of SO_2 and NO_2, decreases the source strengths of sulfate and nitrate particles. Therefore, levels of nitrate and sulfate were generally lower in winter than summer, with the exception of the overnight period. Ammonium, present in much lower concentrations, follows a similar trend with nitrate and

sulfate. The low ammonium level reported in this study is likely to be predominantly in the form of ammonium sulfate, which is a dominant species in fine PM, with an upper "tail" in its size distribution extending to the lower range of the coarse mode.

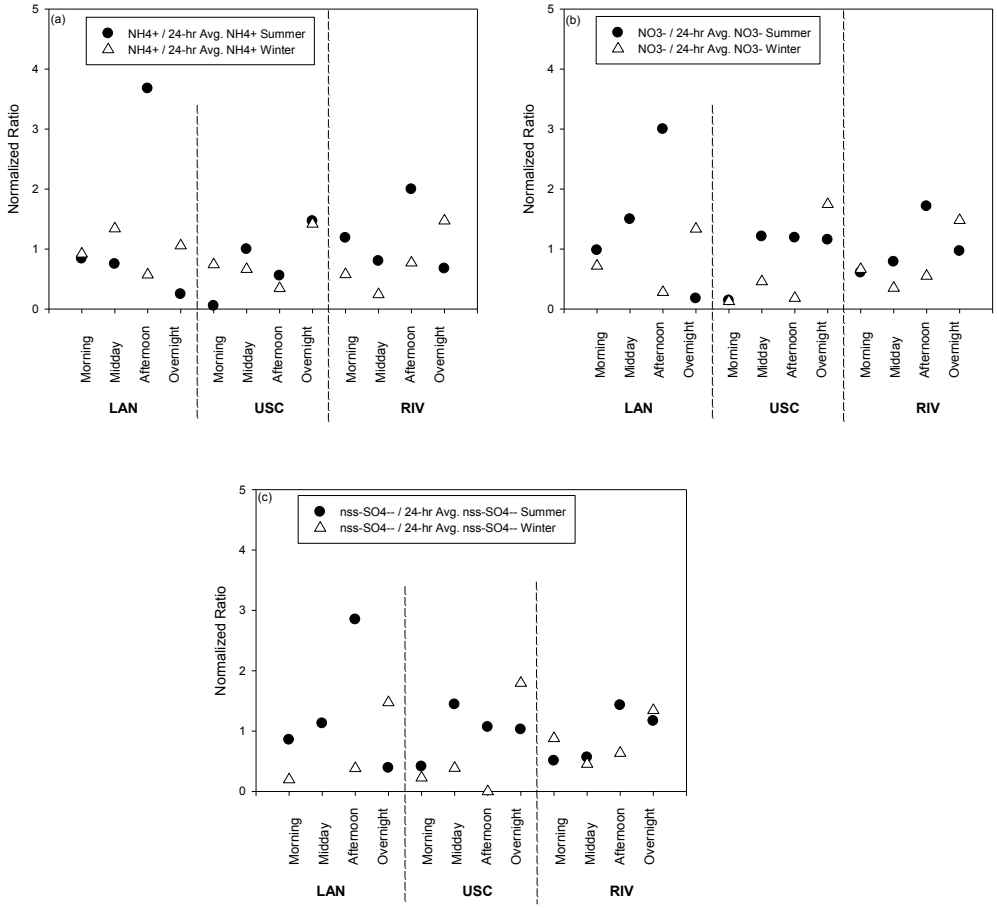

Figure 5-5: Diurnal profiles of: (a) ammonium; (b) nitrate and (c) non-sea salt sulfate. Normalization to the 24-hr average is presented.

In the winter overnight period at USC, the concentration of nitrate reached 705 ng/m^3. This high level likely results from the reaction of nitric acid with sea salt aerosols, which had a similar peak in the same time period. The reaction of nitric acid with sea salt to form sodium nitrate, a process known as chloride depletion, is observed previously in this basin (Hughes et al., 1999),

and will be discussed in more detail in the next section. Further inland at the Riverside site (RIV), the overnight peak of the inorganic ions was more significant than those for the sea salt aerosol and PM mass, suggesting that in addition to the reaction with sea salt, other formation mechanisms might be present at this site. With the abundant crustal materials detected overnight, it is possible that these secondary ions react on the surface of mineral dust particles (Usher et al., 2003). At LAN, the trends of secondary ions follow closely with sea salt and crustal materials in summer. As mentioned in the previous section, wind speed is the major mechanism re-suspending PM in Lancaster. In winter, the low wind speed prevents regional transport, coupled with the lack of local precursors of acidic gases, contributes to the lower concentrations of inorganic aerosols at Lancaster.

Overall, the overnight peaks for inorganic species are more significant compared with the corresponding PM mass, suggesting that in addition to the lower mixing height and/or stagnation conditions, the meteorological parameters during nighttime might facilitate the formation and / or re-entrainment of these inorganic ions. Furthermore, nitrate containing dust particles of > 1 μm were also found to be highly hydrophilic (Shi et al., 2008). The uptake of nitric acid on mineral dust particles tends to increase with increasing relative humidity (Vlasenko et al., 2006), which is consistent with the high levels of nitrate and mineral dust at the Riverside site overnight in this study. On the other hand, the gas/particle partitioning of ammonium salts is highly dependent on atmospheric conditions (Seinfeld and Pandis, 2006). The lower temperature at night favors the formation of ammonium salts in the particle phase, consistent with the higher levels of these inorganic ions observed in the overnight period.

5.4.4. Seasonal and spatial correlations

Table 5-3: Correlation coefficient between selected species in: (a) summer and (b) winter.

(a)	Ions						Soil Dust			Road Dust			Rare Earth Element				Soil/sea salt			Meteorology		
	Cl-	NO3-	SO4--	Na+	NH4+	K+	Al	Ti	Fe	Cu	Zn	Ba	Rb	Cs	Dy	Yb	WS Mg	WS Ca	WIS Na	RH	Temp	Vec WS
WSOC	0.51	0.68	0.63	0.52	0.38	0.96	0.88	0.70	0.68	0.85	0.55	0.62	0.71	0.77	0.73	0.80	0.84	0.79	0.27	0.12	0.13	0.13
Cl-		0.65	0.65	0.82	0.39	0.60	0.45	0.44	0.44	0.35	0.20	0.52	0.38	0.35	0.34	0.34	0.77	0.68	0.26	0.37	-0.21	0.23
NO3-			0.90	0.90	0.76	0.70	0.57	0.49	0.48	0.52	0.32	0.50	0.46	0.48	0.47	0.48	0.91	0.77	0.19	0.43	-0.11	0.45
SO4--				0.91	0.77	0.68	0.61	0.62	0.62	0.41	0.36	0.65	0.58	0.55	0.56	0.52	0.90	0.86	0.29	0.31	-0.07	0.50
Na+					0.77	0.59	0.43	0.44	0.44	0.31	0.18	0.50	0.38	0.35	0.36	0.34	0.88	0.74	0.25	0.46	-0.27	0.39
NH4+						0.36	0.25	0.24	0.25	0.24	0.16	0.27	0.21	0.20	0.17	0.17	0.66	0.49	0.37	0.44	-0.26	0.26
K+							0.88	0.73	0.71	0.84	0.48	0.67	0.75	0.79	0.79	0.82	0.89	0.86	0.28	0.22	0.02	0.05
Al								0.93	0.92	0.86	0.72	0.88	0.94	0.97	0.95	0.97	0.78	0.86	0.61	0.04	0.28	0.25
Ti									1.00	0.70	0.75	0.97	0.98	0.96	0.93	0.90	0.69	0.87	0.75	-0.10	0.39	0.35
Fe										0.67	0.73	0.97	0.98	0.95	0.93	0.89	0.68	0.86	0.76	-0.09	0.38	0.36
Cu											0.63	0.66	0.71	0.78	0.73	0.79	0.67	0.69	0.44	0.22	0.12	0.00
Zn												0.71	0.68	0.74	0.64	0.65	0.41	0.56	0.61	-0.25	0.55	0.44
Ba													0.93	0.89	0.87	0.83	0.69	0.88	0.78	-0.01	0.31	0.42
Rb														0.98	0.98	0.95	0.68	0.84	0.75	-0.04	0.32	0.23
Cs															0.99	0.98	0.69	0.81	0.73	-0.02	0.33	0.22
Dy																0.98	0.69	0.81	0.69	0.04	0.25	0.18
Yb																	0.70	0.77	0.65	0.07	0.22	0.15
WS Mg																		0.91	0.36	0.41	-0.13	0.28
WS Ca																			0.47	0.16	0.12	0.37
WIS Na																				0.04	0.26	0.12
RH																					-0.82	-0.23
Temp																						0.44

(b)	Ions						Soil Dust			Road Dust			Rare Earth Element				Soil/sea salt			Meteorology		
	Cl-	NO3-	SO4--	Na+	NH4+	K+	Al	Ti	Fe	Cu	Zn	Ba	Rb	Cs	Dy	Yb	WS Mg	WS Ca	nssNa	RH	Temp	mph
WSOC	0.29	0.81	0.64	0.36	0.91	0.50	0.82	0.90	0.84	0.84	0.69	0.63	0.90	0.94	0.84	0.55	0.59	0.75	0.00	0.26	-0.03	-0.26
Cl-		0.76	0.92	0.97	0.24	0.89	0.69	0.55	0.69	0.33	0.59	0.90	0.57	0.41	0.64	0.38	0.96	0.86	0.95	0.45	-0.24	0.19
NO3-			0.92	0.72	0.81	0.86	0.98	0.89	0.98	0.68	0.71	0.92	0.93	0.86	0.97	0.68	0.89	0.94	0.77	0.40	-0.15	-0.09
SO4--				0.92	0.55	0.90	0.86	0.78	0.86	0.59	0.71	0.92	0.78	0.70	0.83	0.52	0.99	0.98	0.98	0.37	-0.14	0.04
Na+					0.23	0.82	0.66	0.57	0.65	0.40	0.59	0.84	0.53	0.43	0.61	0.28	0.96	0.86	0.95	0.27	-0.01	0.20
NH4+						0.49	0.85	0.88	0.87	0.79	0.64	0.63	0.92	0.92	0.89	0.74	0.48	0.64	0.08	0.34	-0.14	-0.22
K+							0.87	0.69	0.84	0.48	0.61	0.92	0.72	0.58	0.82	0.55	0.91	0.91	0.00	0.52	-0.19	0.32
Al								0.91	0.97	0.74	0.74	0.88	0.93	0.89	0.99	0.72	0.83	0.90	0.42	0.35	-0.01	0.03
Ti									0.94	0.93	0.91	0.82	0.96	0.90	0.91	0.69	0.75	0.84	0.41	0.29	-0.02	-0.05
Fe										0.76	0.78	0.93	0.97	0.88	0.97	0.74	0.83	0.90	0.50	0.49	-0.19	-0.04
Cu											0.90	0.63	0.82	0.80	0.74	0.53	0.56	0.65	0.33	0.19	0.06	-0.02
Zn												0.78	0.80	0.68	0.71	0.61	0.70	0.74	0.41	0.25	0.01	0.16
Ba													0.84	0.68	0.86	0.64	0.93	0.92	0.49	0.56	-0.23	0.12
Rb														0.94	0.95	0.71	0.73	0.85	0.47	0.44	-0.23	-0.18
Cs															0.92	0.55	0.65	0.78	0.38	0.24	-0.09	-0.33
Dy																0.70	0.80	0.88	0.00	0.37	-0.08	-0.07
Yb																	0.45	0.56	0.00	0.33	-0.10	0.28
WS Mg																		0.96	0.99	0.37	-0.05	0.12
WS Ca																			0.95	0.39	-0.11	0.04
WIS Na																				0.03	0.20	-0.05
RH																					-0.78	0.09
Temp																						0.30

Table 5.3 presents the correlation coefficient (R) of selected individual species in summer and winter using the pooled data from the three sampling sites. In both seasons, tracers of vehicle abrasion (Cu, Zn and Ba) are highly correlated with soil dust tracers of Al, Ti and Fe (R values range from 0.67 to 0.97) and also the earth elements of Rb and Cs (R values range from 0.53 to 0.93), highlighting their common origins of re-suspended dust. Sodium ion, on the other hand, is highly correlated with chloride ion, (R= 0.82 and 0.98 for summer and winter, respectively), confirming that sodium ion is a reliable tracer of sea salt aerosols. Table 5.4 presents the correlation analysis, structured by location, using pooled summer and winter data points. Non-sea-salt sodium (nss-Na), calculated as the difference between WS Na and sea-salt fraction of Na estimated using Cl ion, represents aged aerosols with sea salt origins. Nss-Na exhibited

high correlations with inorganic ions and low correlations with soil dust tracers at USC, and to a lesser extent RIV, suggesting that the non-sea-salt fraction of sodium is mainly derived from the reaction with these ions. In the site of Lancaster, CPM is primarily re-suspended by wind, as evidenced by the high correlations between individual species and wind speed (R values range from 0.64 to 0.89). The effect of relative humidity and temperature on these CPM species are also more significant in Lancaster compared with the other two sites, highlighting that meteorology plays a significant role in ambient coarse particle levels in that area.

Table 5-4: Correlation coefficient between selected species in: (a) Lancaster (LAN); (b) Los Angeles (USC) and (c) Riverside (RIV).

(a)	Cl-	NO3-	SO4--	Na+	NH4+	Al	Ti	Fe	Cu	Zn	Ba	Rb	Cs	nssMg	nssCa	nss Na	RH	Temp	WS
WSOC	0.72	0.79	0.89	0.81	0.95	0.96	0.95	0.96	0.83	0.63	0.85	0.96	0.91	0.96	0.86	0.82	-0.39	0.52	0.84
Cl-		0.92	0.93	0.98	0.83	0.64	0.79	0.78	0.30	0.28	0.78	0.76	0.59	0.44	0.95	0.97	-0.28	0.34	0.65
NO3-			0.96	0.94	0.84	0.77	0.86	0.84	0.47	0.54	0.71	0.84	0.72	0.61	0.95	0.94	-0.47	0.58	0.83
SO4--				0.96	0.91	0.84	0.91	0.89	0.56	0.51	0.74	0.89	0.76	0.72	0.94	0.96	-0.54	0.63	0.87
Na+					0.86	0.72	0.83	0.82	0.41	0.32	0.72	0.80	0.64	0.59	0.95	1.00	-0.42	0.48	0.72
NH4+						0.93	0.97	0.97	0.72	0.56	0.91	0.96	0.90	0.89	0.93	0.88	-0.26	0.36	0.77
Al							0.97	0.97	0.89	0.79	0.86	0.98	0.98	0.98	0.83	0.73	-0.37	0.51	0.89
Ti								1.00	0.79	0.72	0.92	1.00	0.95	0.91	0.93	0.84	-0.32	0.45	0.87
Fe									0.80	0.70	0.94	1.00	0.96	0.92	0.92	0.82	-0.27	0.41	0.85
Cu										0.86	0.71	0.83	0.89	0.92	0.55	0.42	-0.31	0.45	0.78
Zn											0.60	0.74	0.83	0.73	0.52	0.33	-0.30	0.47	0.79
Ba												0.91	0.90	0.83	0.87	0.72	0.05	0.10	0.64
Rb													0.96	0.93	0.91	0.81	-0.33	0.47	0.88
Cs														0.97	0.80	0.66	-0.21	0.37	0.82
nssMg															0.69	0.62	-0.36	0.52	0.82
nssCa																0.95	-0.27	0.38	0.77
nssNa																	-0.41	0.48	0.72
RH																		-0.97	-0.65
Temp																			0.78

(b)	Cl-	NO3-	SO4--	Na+	NH4+	Al	Ti	Fe	Cu	Zn	Ba	Rb	Cs	nssMg	nssCa	nssNa	RH	Temp	WS
WSOC	0.18	0.64	0.76	0.47	0.77	0.66	0.43	0.48	0.60	0.34	0.40	0.51	0.46	0.94	0.75	0.52	0.02	0.03	0.36
Cl-		0.60	0.30	0.65	0.12	0.48	0.48	0.57	0.49	0.44	0.63	0.54	0.53	0.74	0.65	0.45	0.36	-0.25	-0.16
NO3-			0.86	0.94	0.77	0.70	0.66	0.67	0.62	0.55	0.59	0.73	0.70	0.95	0.79	0.95	0.13	0.04	0.49
SO4--				0.87	0.81	0.12	0.03	0.07	0.18	0.00	0.01	0.17	0.12	0.92	0.53	0.93	0.18	0.22	0.46
Na+					0.74	0.16	0.14	0.20	0.17	0.09	0.21	0.26	0.24	0.95	0.55	0.97	0.37	-0.01	0.25
NH4+						-0.18	-0.22	-0.18	-0.14	-0.21	-0.16	-0.12	-0.13	0.90	0.26	0.83	0.42	-0.07	0.12
Al							0.96	0.97	0.91	0.92	0.92	0.96	0.95	0.90	0.86	0.03	-0.04	-0.19	0.16
Ti								0.98	0.87	0.97	0.92	0.99	0.98	0.79	0.79	0.01	-0.11	-0.15	0.17
Fe									0.88	0.94	0.98	0.98	0.99	0.78	0.85	0.06	0.04	-0.28	0.06
Cu										0.88	0.83	0.92	0.87	0.91	0.84	0.05	-0.02	-0.04	0.13
Zn											0.89	0.95	0.94	0.76	0.74	-0.03	-0.04	-0.17	0.13
Ba												0.92	0.95	0.69	0.82	0.05	0.20	-0.44	-0.11
Rb													0.99	0.86	0.87	0.13	-0.06	-0.12	0.20
Cs														0.78	0.84	0.12	-0.02	-0.19	0.11
nssMg															0.95	0.98	0.21	-0.03	0.38
nssCa																0.45	0.12	-0.15	0.18
nssNa																	0.32	0.06	0.34
RH																		-0.81	-0.48
Temp																			0.54

(c)	Cl-	NO3-	SO4--	Na+	NH4+	Al	Ti	Fe	Cu	Zn	Ba	Rb	Cs	nssMg	nssCa	nss Na	RH	Temp	WS
WSOC	0.94	0.73	0.94	0.98	0.07	0.88	0.67	0.52	0.60	0.57	0.17	0.61	0.61	0.93	0.87	0.97	-0.19	0.44	0.55
Cl-		0.90	0.93	0.94	0.30	0.93	0.73	0.71	0.54	0.50	0.42	0.70	0.75	0.93	0.94	0.89	0.03	0.29	0.47
NO3-			0.73	0.70	0.62	0.78	0.63	0.75	0.48	0.47	0.62	0.56	0.66	0.72	0.81	0.63	0.12	0.14	0.42
SO4--				0.98	-0.03	0.95	0.73	0.61	0.48	0.38	0.19	0.78	0.69	0.99	0.88	0.97	-0.13	0.51	0.58
Na+					-0.03	0.92	0.69	0.54	0.53	0.46	0.14	0.70	0.65	0.97	0.88	0.99	-0.17	0.48	0.56
NH4+						0.16	0.32	0.56	0.42	0.50	0.84	0.08	0.34	0.00	0.29	-0.13	0.48	-0.47	-0.19
Al							0.86	0.80	0.58	0.46	0.42	0.89	0.86	0.98	0.93	0.89	0.07	0.37	0.38
Ti								0.91	0.81	0.67	0.66	0.91	0.89	0.79	0.82	0.66	0.35	0.12	0.06
Fe									0.62	0.51	0.86	0.87	0.91	0.68	0.81	0.48	0.53	-0.06	-0.05
Cu										0.96	0.52	0.53	0.56	0.52	0.56	0.51	0.13	0.09	0.09
Zn											0.50	0.33	0.41	0.41	0.51	0.43	0.10	0.00	0.05
Ba												0.52	0.68	0.54	0.54	0.05	0.75	-0.47	-0.35
Rb													0.89	0.80	0.80	0.68	0.31	0.25	0.12
Cs														0.86	0.86	0.61	0.52	-0.08	-0.08
nssMg															0.91	0.96	-0.04	0.46	0.48
nssCa																	0.29	0.10	0.19
nssNa																	-0.22	0.53	0.58
RH																		-0.84	-0.78
Temp																			0.84

5.4.5. Chloride depletion

Chloride depletion plays an important role in atmospheric processes as it changes the deliquescence points and optical properties of coarse particles (Finlayson-Pitts, 2003). Many studies have reported the depletion of chloride along coastal areas. Yet, the factors affecting the degree of depletion are not completely understood. Zhuang et al. (1999) attributed the depletion of sea salt to both HNO_3 and H_2SO_4 in Hong Kong, and observed that the rate of depletion was dependent on relative humidity, particle size and the relative abundance of Ca^{2+} and Na^{+}. Another study in Newark, New Jersey concluded that nitrate, and to a lesser extent sulfate and organic acids, were responsible for chloride depletion in that area, and less depletion was observed when the air masses were directly originated from the Atlantic Ocean (Zhao and Gao, 2008a). In this study, the degree of chloride depletion was examined at the three sampling sites in different periods of the day, enabling us to understand the factors that influence this depletion process.

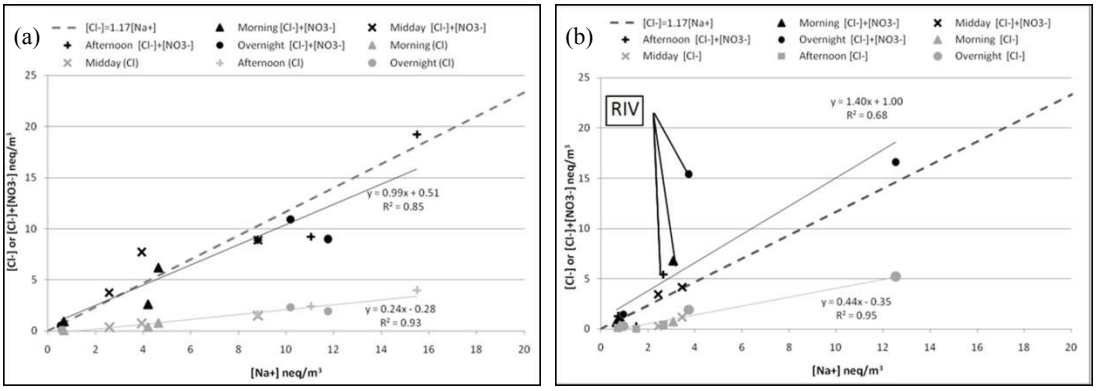

Figure 5-6: Chloride depletion and nitrate replacement scatter-plots in a) summer and b) winter. Dark legends refer to the sum of [Cl-] + [NO3-], and gray legends refer to [Cl-].

Figure 5.6 (a and b) shows scatter plots of $[Cl^-]$ against $[Na^+]$, in the unit of molar equivalent concentrations. The average observed $[Cl^-]/[Na^+]$ equivalent ratio is lower in summer (slope =

0.24) compared with winter (slope = 0.44), indicating that more depletion is observed in summer due to enhanced photochemistry and higher concentrations of acidic gas-phase species under higher temperature. Less depletion, as shown by the higher $[Cl^-]/[Na^+]$ equivalent ratio, as presented in Figure 5.6 and 5.7, was observed in the overnight sampling period in both seasons due to lower levels of acidic gases at night (Wall et al., 1988), which further confirms that the concentration of acidic gas is an important parameter influencing the degree of depletion in this basin.

As depletion primarily results from nitric acid reacting with sodium chloride to form sodium nitrate and hydrochloric acid, the ratios of the sum of $[Cl^-]$ and $[NO_3^-]$ / $[Na^+]$ is also plotted as the dark legend in Figure 5.6. The regression slope in summer (slope = 0.99) falls close to the theoretical seawater ratio of $[Cl^-]/[Na^+]$ (slope = 1.17), with a R^2 of 0.85, confirming the role of nitrate in chloride depletion, and that nitrate in CPM is predominantly formed by the depletion reaction in summer. The slightly lower slope indicates that a minor fraction of the depletion might be caused by other species such as nss-SO_4^{2-} and organic acids, as shown in other studies (Zhuang et al., 1999). In winter, both the sea salt concentration and the rate of depletion were lower. The regression slope of sum of $[Cl^-]$ and $[NO_3^-]$ / $[Na^+]$ is 1.40, indicating that excess nitrate, generated by means other than sea salt depletion, is present.

In addition to chloride depletion, the two other major formation mechanisms of coarse mode nitrate particles are: 1) reactions of nitric acid on soil dust PM, and 2) condensation of ammonium nitrate on CPM surfaces, which would be expected in cooler winter months. Noble and Prather (1996) demonstrated the association of both marine and soil particles to super-micron nitrate particles in Riverside, CA. Many studies have also observed the presence of sulfate and nitrate on

soil particles (Wu and Okada, 1994; Zhang et al., 2000; Zhuang et al., 1999). A study conducted in Italy suggested that NO_3^- shifts to the super-micron range in episodes of high coarse dust concentrations by adsorption of HNO_3 onto dust particles (Putaud et al., 2004). The abundance of both soil and sea salt particles would therefore explain the high nitrate concentrations in this study.

Figure 5.7 shows the diurnal concentrations of excess ammonium, as well as equivalent ratios of $[Cl^-] / [Na^+]$ and sum of $[Cl^-]$ and $[NO_3^-] / [Na^+]$. When sea salt concentration was high, the $[Cl^-] + [NO_3^-] / [Na^+]$ ratio was within 20% of the theoretical value of 1.17. In some periods when sea salt concentration was low in summer (LAN midday, PIU morning, RIV morning and midday), a small fraction of excess nitrate was observed, probably due to the analytical uncertainty associated with low concentrations. In summer, ammonium concentrations were not high enough to fully neutralize sulfate in CPM with the exception of the USC overnight period. In winter, $NH_4^+ / nssSO_4^{2-} > 2$ for most of the time periods, indicating the presence of excess ammonium, as illustrated in Figure 5.7b. At RIV, high levels of excess nitrate were observed (equivalent ratio of the sum of $[Cl^-] + [NO_3^-] / [Na^+] > 2$) when levels of excess ammonium were also high, suggesting the presence of ammonium nitrate at that site. As previously mentioned, many studies observed the uptake of nitric acid on mineral dust particles, particularly in the form of $Ca(NO_3)_2$ and $Mg(NO_3)_2$ (Usher et al., 2003). In this study, levels of nss-Ca (on average 97.6 ng/m^3 and 78.9 ng/m^3 in summer and winter respectively) were much higher than nss-Mg (on average 8.70 ng/m^3 and 4.22 ng/m^3 in summer and winter respectively). Correlation coefficient (R) between nitrate and nss-Ca and nss-Na is 0.81 and 0.63 at RIV respectively, suggesting that both chloride depletion and the reaction with soil particles are important formation mechanisms

of coarse particulate nitrate at this site. These results imply that the excess nitrate present in winter at Riverside can be in the form of soil-associated calcium nitrate, as well as ammonium nitrate, in addition to $NaNO_3$ generated by sea salt depletion.

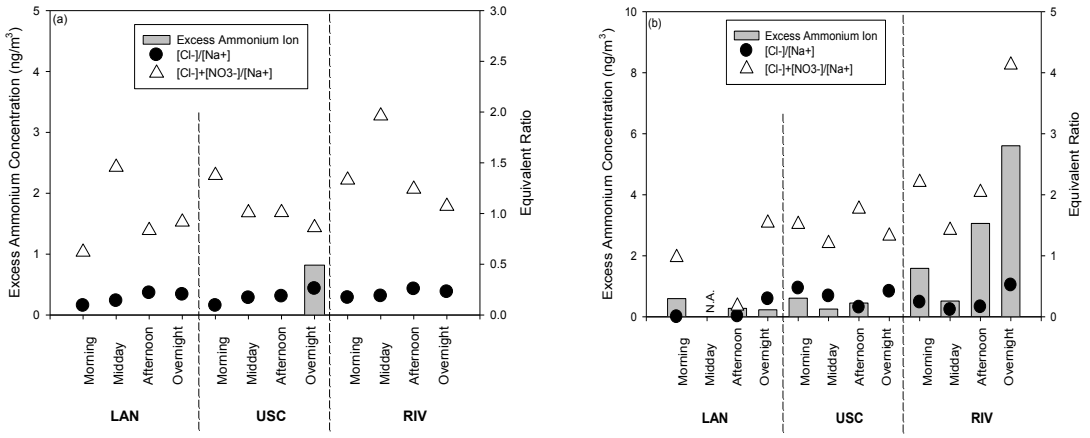

Figure 5-7: Diurnal profile of excess ammonium ion concentration (ng/m3) and molar equivalent ratios of [Cl-] / [Na+] and sum of [Cl-] and [NO3-] / [Na+] in: (a) summer and (b) winter.

5.5. Summary and Conclusions

The diurnal profile of chemical groups and constituents of CPM differs significantly in summer and winter. Highest concentrations of CPM gravimetric mass, crustal materials and trace elements, vehicle abrasion, and water soluble organic carbon were observed in summer midday and / or afternoon when the wind speed was higher for all the three sampling sites. On the other hand, high levels of sea salt particles and secondary ions were experienced in the summer overnight period at USC. In winter, the Los Angeles Basin is characterized by frequent stagnation conditions, and vehicle-induced turbulence becomes a significant mechanism of particle re-suspension when mixing height was low, as highlighted by the high concentrations of CPM mass, as well as soil and road dust in the winter overnight period at the near freeway sampling sites. Nitrate, which has been shown to be the most abundant species in the CPM, is

predominantly formed by chloride depletion in summer. A significant nitrate peak is observed in the afternoon at the inland sites (LAN and RIV), consistent with the diurnal profile of sea salt concentrations. In winter, high levels of nitrate were found during overnight. Due to the overall lower sea salt levels in winter, the reactions with sea salt and mineral dust particles, as well as the condensation of ammonium nitrate on PM surfaces are the dominant formation mechanisms of nitrate in the coarse particles.

5.6. Acknowledgements

This study was funded by the Science to Achieve Results program of the United States Environmental Protection Agency (EPA-G2006-STAR-Q1). The authors would also like to thank the staff at the Wisconsin State Laboratory of Hygiene for the assistance with chemical analyses.

Chapter 6 Diurnal Trends in Oxidative Potential of Coarse Particulate Matter in the Los Angeles Basin and Their Relation to Sources and Chemical Composition

6.1. Abstract

To investigate the relationship between sources, chemical composition and redox activity of coarse particulate matter (CPM), three sampling sites were setup up in the Los Angeles Basin to collect ambient coarse particles at four time periods (morning, midday, afternoon and overnight) in summer 2009 and winter 2010. The generation of reactive oxygen species (ROS) was used to assess the redox activity of these particles. Our results present distinct diurnal profiles of CPM-induced ROS formation in the two seasons, with much higher levels in summer than winter. Higher ROS activity was observed in the midday / afternoon during summertime, while the peak activity occurred in the overnight period in winter. Crustal materials, the major component of CPM, demonstrated very low water-solubility, in contrast with the modestly water-soluble anthropogenic metals, including Ba and Cu. The water-soluble fraction of four elements (V, Pd, Cu and Rh) with primary anthropogenic origins displayed the highest associations with ROS activity (R^2>0.60). Our results show that coarse particles generated by anthropogenic activities, despite their low contribution to CPM mass, are important to the biological activity of CPM, and that a more targeted control strategy may be needed to protect the public health from these toxic CPM sources.

6.2. Introduction

A review article of over 30 epidemiological studies on the effect of fine and coarse particles on mortality and morbidity revealed evidence that CPM had similar, or stronger short-term effects as fine PM on asthma and respiratory hospital admissions, as well as chronic obstructive

pulmonary disease (Brunekreef and Forsberg, 2005). In particular, the investigators called for consideration in studying and regulating CPM separately from fine particles. Whereas the temporal, spatial and toxicological characteristics associated with $PM_{2.5}$ and PM_{10} is more thoroughly investigated, there is a dearth of equivalent information on coarse particles. To develop cost-effective air quality regulations for protecting the public health from CPM exposure, it is essential to establish the linkage between their sources and chemical composition to toxicity. Although a number of studies investigated the relationship between sources and toxicity in ultrafine PM, $PM_{2.5}$ and PM_{10} (Hu et al., 2008; Shafer et al., 2010; Verma et al., 2009a), very limited literature has examined the effects of CPM independently. Unlike the dominance of organic materials and secondary ions in fine particles (Arhami et al., 2009; Ning et al., 2007), metals and elements are the core components of CPM in both rural and urban environments (Cheung et al., 2011b; Hueglin et al., 2005; Sillanpaa et al., 2006). Furthermore, metals in the coarse fraction primarily arise from mineral and road dust, in contrast to the combustion origins of the ultrafine and accumulation particles. Since chemical characteristics directly affects the generation of PM-associated toxicity (Cho et al., 2005; Schwarze et al., 2007; Shafer et al., 2010), the different chemical composition of CPM might induce toxicity differently than other fractions of PM.

The generation of ROS and the subsequent induction of oxidative stress plays a significant role in adverse health outcomes related to particle exposure (Nel, 2005; Tao et al., 2003). A number of studies have shown that PM components can induce pro-inflammatory responses in human airways through their ability to form ROS (Barnes, 1990; Nel et al., 2001). The presence of transition metals could enhance the formation of hydroxyl radical- a strong oxidizing species,

via Fenton or Fenton-like reactions. In particular, water-soluble species, especially metals, have been shown to be the key drivers of ROS generation (Goldsmith et al., 1998; Prophete et al., 2006). On the other hand, key atmospheric parameters such as mixing height, wind speed and direction, as well as emission sources and their strengths all vary in scales shorter than 24 hours, which could result in the diurnal variation of chemical composition and thus redox activity. The temporal variability of CPM-induced toxicity has important implications in terms of exposure and risk assessment of CPM exposure, and will help determine the actual impact of CPM toxicity on public health. In this study, CPM was collected at four daily time periods (morning, midday, afternoon and overnight) at three distinct sampling sites to study the diurnal characteristics of chemical composition and oxidative potential of ambient coarse particles. The CPM-induced generation of ROS was measured by an in-vitro bioassay and used to evaluate the toxic activity of these particles. The goals of this study are to determine the diurnal variability of CPM-induced oxidative potential and to identify specific CPM species / source classes (if any) that drive the ROS activity. This information will ultimately help the regulatory communities to design more targeted and effective control strategies to protect the public health from CPM exposure.

6.3. Methodology

Details of the sampling location, equipment and methods are described in the previous chapter (Chapter 5).

6.3.1. Chemical analyses

To determine the concentration of total metals and elements, the substrates were digested in an acid mixture (1.0 mL of 16 N HNO_3, 0.1 mL of 28 N HF, and 0.25 mL of 12 N HCl) in a Teflon digestion bomb using a microwave-assisted digestion unit. The digestates were

subsequently analyzed by high resolution inductively coupled plasma-mass spectroscopy techniques (HR-ICPMS) (Shafer et al., 2010). The levels of water-soluble metals and elements were quantified using the same HR-ICPMS technique, with the extraction conducted using 10 mL of Milli-Q water (Millipore, Bedford, MA, USA) followed by filtration using 0.45 μm filters. The water extracts were also analyzed by a Sievers total organic carbon analyzer (General Electric, Inc.) (Zhang et al., 2008b) and ion chromatography (Lough et al., 2005) to determine the levels of water-soluble organic carbon (WSOC) and water-soluble ions, respectively.

The generation of ROS was quantified using an in-vitro assay described in greater detail elsewhere (Landreman et al., 2008; Zhang et al., 2008b). Briefly, substrates were extracted with 1.0 mL of Milli-Q water for 16 hours, in the dark, on a shaker table. After removing the filters, samples were centrifuged at 6600 RPM for 1 minute and the supernatant were filtered through 0.22 μm polypropylene syringe filters. The aqueous solutions were then buffered using 10× concentrated Salts Glucose Medium. The buffered PM extract solutions were subsequently split to prepare aliquots of diluted and non-diluted samples in triplicates. The aliquots were mixed with 2'7'- dichlorofluorescin diacetate and then added to rat alveolar macrophage cells (cell line NR8383) that were previously plated into 96-well plates, and incubated at 37^{o}C for 2 hours. The plates were read 5 times (at 0, 30, 60, 90, 120 minutes) using a Cytoflour II automated fluorescence plate reader at a wavelength of 485/530nm. The samples were analyzed along with positive (Zymosan, urban dust extracts) and negative (method blanks) controls. ROS activity was reported as the increase in the fluorescence intensity of the PM samples relative to that observed in the controls. The results were reported in units of Zymosan equivalents. Samples were analyzed with laboratory and field blanks, and all reported values have been method and field

blank corrected. On average, field blank levels contributed to less than 2% of the samples' levels, with the exception of four water-soluble trace elements (Th, Lu, Cs and Sn), which experienced high field blanks concentrations, and were excluded in the analysis. Total uncertainties were determined based on the analytical uncertainties and uncertainties of field blanks.

6.4. Results and Discussion

6.4.1. Overview

Chemical species were categorized into: (1) crustal materials and trace elements (CM + TE); (2) abrasive vehicular emissions (AVE); (3) water-soluble organic carbon (WSOC); (4) sea salt (SS) and (5) secondary ions (SI). Their diurnal profiles have been presented in the Chapter 5, and only a brief summary is described here. It should be noted that although coarse particulate Fe is a major soil constituent, it could be enriched by anthropogenic sources in urban areas (Gietl et al., 2010). The inclusion of Fe in the crustal material group might have overestimated the contribution of soil from Fe.

Overall, the group of CM + TE, primarily composed of crustal elements of Al, Fe and Si, was the most abundant category of CPM at all three sampling sites (avg.=4.20 $\mu g/m^3$). Levels of these crustal materials were higher at RIV (avg.=7.7 $\mu g/m^3$) than LAN (avg.=2.0 $\mu g/m^3$) / USC (avg.=3.4 $\mu g/m^3$), due to the semi-rural receptor nature of the area. Abrasive vehicular emissions refer to the emissions from the abrasion processes of tire wear, brake linings, catalyst deterioration, etc. Metals and elements that originated predominantly from vehicular abrasion (Cu, Ba and Zn) were much less abundant (avg.=0.19 $\mu g/m^3$). Sea salt levels were higher in summer (avg.=0.53 $\mu g/m^3$) than winter (avg.=0.28 $\mu g/m^3$). Secondary ions, primarily composed of nitrate, and to a lesser extent sulfate and ammonium, had an overall average of 0.50 $\mu g/m^3$, with lower

concentrations at LAN. WSOC concentrations were low at LAN (avg.=0.071 μg/m^3) and USC (avg.=0.078 μg/m^3), with higher levels at RIV (avg.=0.65 μg/m^3). The diurnal profiles of CPM differ substantially in summer and winter (Figure 6.1), due to the combined effects of different source strengths, meteorology and primary re-suspension mechanisms. Levels of CPM mass, mineral and road dust, as well as WSOC were highest in summer midday / afternoon, concurrent with the higher wind speed during those periods. In winter, atmospheric dilution was lower due to stagnation conditions during the sampling period, resulting in the accumulation of air pollutants. In particular, turbulence induced by vehicular movement (especially heavy-duty vehicles) became a major re-suspension mechanism of CPM in the calm and stagnant atmosphere during winter nighttime (Cheung et al., 2011c). As a result, levels of mineral and road dust were elevated at the near-freeway USC site, and to a lesser extent the RIV site during winter overnight. This finding is consistent with many other studies that showed vehicular movement could contribute substantially to the re-entrainment of coarse mode aerosols (Charron and Harrison, 2005; Harrison et al., 2001; Pakbin et al., 2010).

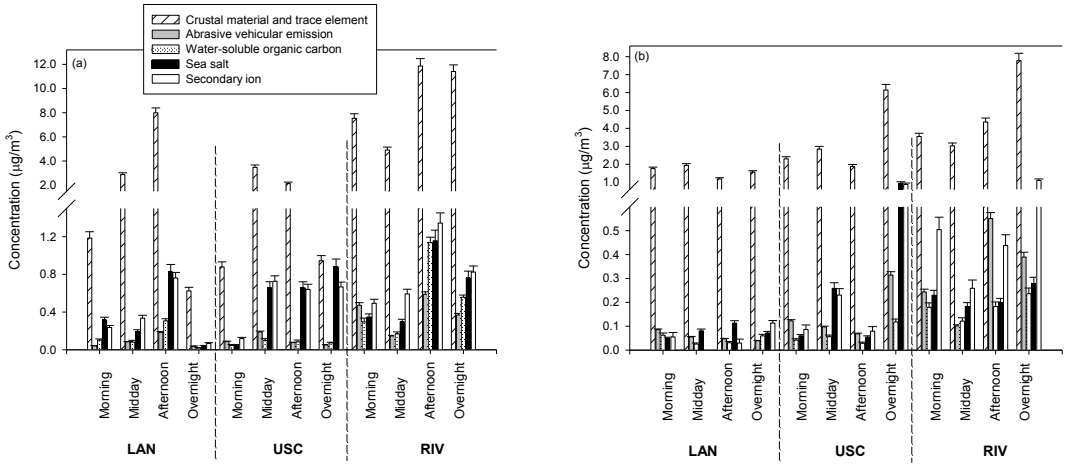

Figure 6-1: Diurnal profile of chemical composition in: (a) summer and (b) winter. Error bars represent analytical uncertainties.

6.4.2. Water solubility of elements

Particle solubility is an important physico-chemical property that affects its bioavailability to human cells (Costa and Dreher, 1997). The water-soluble components of particles are more easily bioavailable, and they have been shown to be the key drivers of PM-induced toxicity in both in-vivo (Roberts et al., 2007) and in-vitro studies (Goldsmith et al., 1998). Figure 6.2 shows the overall water solubility of selected metals and elements of the CPM sampled in this study, calculated as the ratio of the water-soluble to the total elemental concentration for each species. In general, the trend of water solubility was similar seasonally and spatially, and the first, second and third quartiles of solubility are presented. Species with more than 25% of data (i.e. $\geq$ 7 out of 24 data points) under detection limit (2 x total uncertainties) were not included in this analysis. Using such criteria, 12 out of 45 elements, mostly rare earth elements, were excluded due to the trace levels of the water-soluble fraction of these species. As seen in Figure 6.2, elements with sea salt origins, such as sodium (Na), magnesium (Mg) and calcium (Ca), are quite soluble. Although not shown, the fraction of water-soluble Na was highest in the afternoon and overnight periods in summer, parallel to the high sea salt levels observed. The median water-soluble fraction of Na was also highest at USC due to its proximity to the coast compared to RIV and LAN, leading to higher fractions of sea salt particles at that site. While metals and elements are the dominant components of ambient coarse particles (Cheung et al., 2011b; Sillanpaa et al., 2006), most of these crustal materials are insoluble in water. This is evident from the very low solubility of these crustal materials including Al (overall median=0.48%) and Ce (overall median=0.60%). One particular exception would be Ca, since gypsum ($CaSO_4 \cdot 2H_2O$) is moderately water-soluble. Calcium nitrate, resulting from the reaction of mineral dust (or sea salt) and nitric acid, is highly

water-soluble as well (Cheung et al., 2011c; Usher et al., 2003). On the other hand, elements of anthropogenic origins experienced moderate solubility, consistent with previous published work (Birmili et al., 2006). Metals primarily originated from brake wear, such as Ba and Cu, have a median solubility of 15% and 12%, respectively. Zn, with several potential anthropogenic sources including industrial emissions as well as tire and brake wear (Pakbin et al., 2011), also exhibited moderate solubility with a median of 21%.

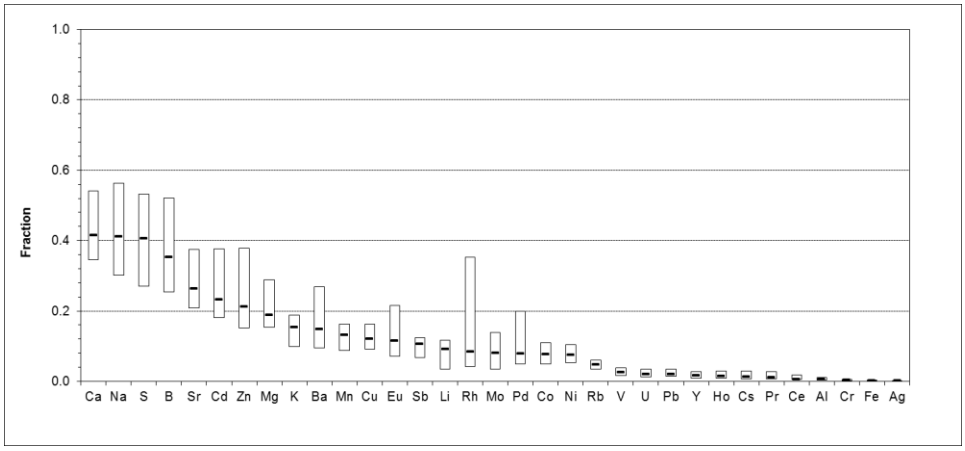

Figure 6-2: Water solubility of selected metals and elements, calculated across three sites, four periods and two seasons. 1st quartile, median and 3rd quartile is shown. Species with > 25% of data points under detection limit (2 x total uncertainties) were excluded.

6.4.3. ROS activity

ROS is a collective term to describe species that contains oxygen and is highly reactive, such as oxygen and hydroxyl radicals. ROS activity, assessed by an in-vitro method in this study, represents the oxidative potential of ambient coarse particles. This cellular method provides a comprehensive evaluation of PM-induced ROS activity as it takes account into both the direct (by the PM aqueous extracts) and indirect (resulting from cellular stimulation) formation of ROS, and provides an assessment of total ROS activity resulting from hydroxyl radical, peroxide,

superoxide radical, and peroxynitrite (Shafer et al., 2010). Note that ROS is naturally produced in cells as a "byproduct" of normal metabolic activity – and is held in check by cytoplasm antioxidants (e.g. glutathione).This baseline activity is accounted for in the assay by a series of negative controls / blanks. The ROS activity of the PM measured / reported is that in excess of baseline and thereby allows for effective comparison of PM oxidative potential. We perform the assay under conditions where the ROS produced is not overtly toxic to the macrophage cells to ensure that cell viability issues do not impact our assessment of the relative and absolute oxidative potential of the PM.

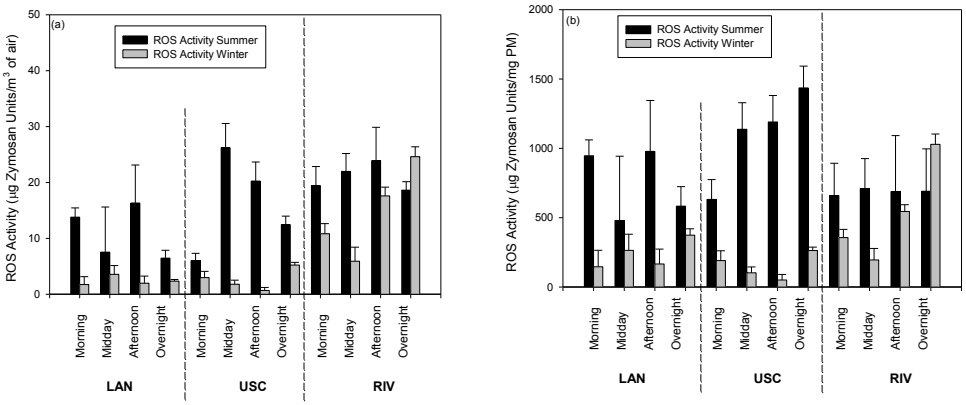

Figure 6-3: Diurnal profile of ROS activity on a: (a) air volume basis and (b) PM mass basis.

Figure 6.3 (a-b) shows the diurnal profile of ROS activity (expressed per air volume and per PM mass basis) of the three sampling sites in summer and winter. ROS activity expressed per volume of air represents the toxicological activity imparted on the environment by these particles, which, in some respect, makes it more relevant in the context of population exposure, compared to the more traditional representation of toxicity on a per PM mass basis. On a per air volume basis, ROS activity was generally higher in summer than winter. In summer, ROS activity peaked

in midday / afternoon. At USC, ROS activity was highest in midday at 26.2 μg Zymosan units/m^3, while the peak occurred in the afternoon at RIV (23.9 μg Zymosan units/m^3) and LAN (16.3 μg Zymosan units/m^3). In winter, higher ROS activity was observed overnight at USC (5.2 μg Zymosan units/m^3) and RIV (24.6 μg Zymosan units/m^3). This finding indicates significant diurnal and seasonal variations in the toxicity of ambient coarse particles, which should be considered in the air-quality related regulation and policy. In general, the diurnal trend of ROS activity is similar on both per mass and per volume basis, with the exception of USC in summer. The mass-based ROS activity of summer overnight (1440 μg Zymosan units/mg of CPM) was at a similar level with the midday (1140 μg Zymosan units/mg of CPM) and afternoon (1190 μg Zymosan units/mg of CPM) activity, in contrast to the lower overnight activity, compared to midday / afternoon, on a per volume basis. This suggests that the mass fraction of CPM emitted by sources that drive ROS generation was higher overnight, either due to an increase in their emission strengths, or to a reduction in the fraction of non-ROS active components.

6.4.4. Association between ROS activity and water-soluble elements

To elucidate the relationship between ROS activity and individual elements (and possibly classes of CPM sources), a linear regression analysis was performed. Table 6.1 shows the coefficient of determination (R-squared) between ROS (Zymosan units/m^3) and the water-soluble (WS) fraction of selected elements (ng/m^3). High correlations (R^2>0.60) were observed for WS vanadium (V), palladium (Pd), copper (Cu) and rhodium (Rh), which are indicative of anthropogenic sources (Pakbin et al., 2011). These high associations were consistent in summer and winter, as illustrated in Figure 6.4 using WS Cu as an example. On the other hand, lower associations were found for WS Fe and Al, the tracers of crustal materials (Cheung et al., 2011b),

probably because of the very low water solubility of these elements, and / or the low intrinsic redox properties of crustal elements in the coarse fraction. The regression analysis was repeated using concentrations of total elements as independent variables. Although not shown, the coefficients of determination between ROS activity and total metals all fall below 0.56. The overall lower associations are consistent with the fact that the bioassay was conducted using filtered aqueous extracts, and only the water-soluble elements were exposed to the macrophage cells.

Table 6-1: Coefficient of determination (R^2) between ROS activity and selected water-soluble (WS) elements.

	WS-V	WS-Pd	WS-Cu	WS-Rh	WS-Ba	WS-Ni	WS-Pb	WS-Fe	WS-Ti	WS-Al
ROS	0.74	0.78	0.73	0.64	0.16	0.23	0.03	0.42	0.14	0.16
WS-V		0.86	0.67	0.64	0.36	0.26	0.04	0.39	0.15	0.27
WS-Pd			0.85	0.86	0.27	0.26	0.06	0.35	0.11	0.34
WS-Cu				0.71	0.33	0.29	0.08	0.29	0.12	0.28
WS-Rh					0.14	0.34	0.11	0.25	0.07	0.53
WS-Ba						0.08	0.01	0.07	0.04	0.25
WS-Ni							0.05	0.04	0.00	0.19
WS-Pb								0.29	0.26	0.28
WS-Fe									0.85	0.17
WS-Ti										0.06

Platinum group elements (PGEs) of Pd and Rh are commonly used in automobile catalytic converters. They are believed to be emitted to the atmosphere from mechanical and thermal stresses in operation (Zereini et al., 2001), and their presence have been observed in both the fine and coarse fractions of ambient PM in many other areas (Kanitsar et al., 2003; Rauch et al., 2001). Rauch et al. (2005) observed the presence of super-micron-PGEs (as a major or minor component on Al/Si oxide) in automobile exhaust and urban air in Sweden using scanning electron microscopy. In this study, the overall average concentration of total Pd and Rh was 0.0438 ± 0.041 ng/m^3 and 0.0138 ± 0.015 ng/m^3, respectively, with higher concentrations observed during USC winter overnight and in the afternoon and overnight period at RIV in winter. Traffic-induced turbulence might be a major re-suspension mechanism of CPM during winter nighttime when

atmospheric dilution was lowest, leading to the high levels of the traffic-related emissions in these periods, as discussed in a greater detail in Chapter 5.

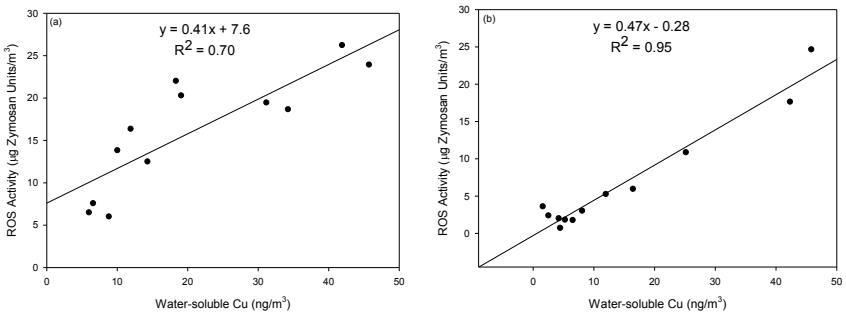

Figure 6-4: Correlations between measured ROS activity and water-soluble Cu in: (a) summer and (b) winter.

CPM-bound copper is typically produced by the wear of brake pads and linings (Garg et al., 2000; Hjortenkrans et al., 2007; Lin et al., 2005). Cu is used as high-temperature lubricant in brake linings, and is emitted primarily from mechanical wear (Sanders et al., 2003). The overall average concentration of total Cu was 154 (±150) ng/m^3, and it could be considered as the most significant element with anthropogenic origins in CPM. Higher levels were observed at USC and RIV, where the sites are more heavily influenced by vehicular emissions and re-suspension. In particular, agricultural activities and vehicle movement on dirt, unpaved roads, or paved roads with unpaved shoulders, could generate and re-entrain a significant amount of road dust in semi-rural regions (Chow et al., 1992), and might contribute to the high levels of Cu at the RIV site.

The sources of vanadium are more diverse. A recent study conducted in the Los Angeles Basin suggested that even in CPM, V could be generated from ship emissions (Pakbin et al., 2011). A study in the Los Angeles-Long Beach Harbor area also revealed significant levels (ca.

1-2 ng/m^3) of V in the accumulation and coarse PM mode, and suggested that V could be originated from emissions of bunker-fuel and oil combustion (Krudysz et al., 2008). Additionally, Schauer et al. (2006) demonstrated the presence of vanadium in brake wear and road dust. Overall, CPM-bound vanadium, with an overall average concentration of 0.93 ng/m^3, could be generated from a variety of sources. The high correlations between the water-soluble fraction of V and Pd (R^2=0.86), to a lesser extent Cu (R^2=0.67), suggest that water-soluble V could be largely originated from vehicular abrasive emissions in the coarse fraction of PM in this study.

Certain organic compounds, such as quinones and nitro-PAHs, are capable of generating superoxide radicals (Cho et al., 2005), which are responsible for the recycling of the precursors of Fenton (or Fenton-like) reactions, and play a critical role in subsequent formation of the highly reactive hydroxyl radicals. In particular, previous studies have demonstrated high correlations between WSOC / OC content of PM and the consumption of dithiothreitol (DTT), an assay that measures the generation of superoxide radicals (Verma et al., 2009a; Verma et al., 2011). Nonetheless, these studies were conducted based on fine or quasi-ultrafine particles, and the role of organics on the toxicity of CPM is not well studied. While fine-particulate WSOC consists of polar organic compounds and could originate from vehicular emissions (Kawamura and Kaplan, 1987) and secondary formation (Verma et al., 2009a), its source could be different in the coarse mode. In addition to the condensation of semi-volatile species on coarse particles, WSOC could be distinctly originated from biological materials, which is the major component of CPM-bound OC in this basin (Cheung et al., 2011b). The WSOC level of this study was reported previously, and it was highest at RIV among the three sampling sites (Cheung et al., 2011c). Correlation between ROS and WSOC is moderate (R^2=0.31) in this study. The site-specific correlation at RIV,

which experienced the highest WSOC concentrations, was moderately low as well (R^2=0.22), suggesting that the high WSOC content at RIV was driven by non-ROS active soluble organics. Note that the term WSOC refers to a mixture of the water-soluble fraction of organic compounds, which is likely to be originated from different sources with different physical and chemical properties. Therefore, it is possible that some of the compounds within the WSOC, although in low concentrations, could comprise redox-active materials that initiate the formation of ROS. Overall, the role of organics in CPM-induced toxicity is rather unclear due to the dominance of biological material in OC / WSOC fraction. The organic content in CPM and its relationships with oxidative potential is a subject that may require further investigation.

In summary, the higher associations between ROS and the water-soluble fractions of V, Pd, Cu and Rh suggest that, although in smaller mass fractions compared with crustal materials, these species could be primarily responsible for the oxidative potential of ambient CPM. In particular, vehicular abrasive emission-the common origin of V, Pd, Cu and Rh in the coarse mode- could be a potential source driving CPM toxicity. The high internal correlations among these four species do not allow further investigation of their independent contribution. The use of more sophisticated statistical analysis methods, such as Principal Component Analysis (PCA) or Positive Matrix Factorization (PMF), which could potentially provide more insightful results linking ROS and CPM species / sources was precluded by the limited number of data points generated in this study.

6.4.5. Comparisons with other studies

A number of studies have been conducted to evaluate the oxidative potential of aerosols of different size fractions and distinctive origins. Table 6.2 shows a summary of the studies that

quantify ROS generation using the same method (in-vitro bioassay) as described in section 6.3. In an earlier study conducted in the downtown Los Angeles area, water-soluble V, Ni and Cd were the significant predictors-which have intrinsic redox properties- of ROS activity in quasi-ultrafine particles (Verma et al., 2009a). Hu et al. (2008) investigated the chemical and toxicological characteristics of PM in the coarse, accumulation and quasi-ultrafine mode in the Los Angeles-Long Beach Harbor area, and revealed that organic carbon, water-soluble V and Ni were linked to the generation of ROS. In 2007, fine particles were collected before and after a wildfire event to characterize the impact of wildfire on PM in Los Angeles, and high associations between ROS activity and a group of water-soluble metals including Cr, Ba, Pb, Fe, Ni, and V were reported (Verma et al., 2009b). Based on the three studies conducted in the Los Angeles Basin, ROS generation was linked to emission of combustion origins, particularly heavy oil combustion (V and Ni). The results from our work, focusing solely on CPM, revealed that species of abrasive origins could be responsible for generation of ROS activity in the coarse mode.

Table 6-2: Summary of studies that employed the same in-vitro bioassay as our study to examine oxidative potential in ambient particulate matter.

Author and Published Year	Location	Time/Period	Size Fractions	Association: High R^2 (>0.6) and p<0.05
Current study	Los Angeles Basin, CA	Diurnal samples in summer 2009 and winter 2010	Coarse particles	Water-soluble V, Pd, Rh and Cu
[25] Zhang et al., 2008	Denver, CO	Daily samples for one year in 2003	$PM_{2.5}$	Iron source and soil dust source apportioned using water-soluble elements, and water soluble carbon factor
[9] Hu et al., 2008	Long Beach and Los Angeles, CA	Weekly composites on daily samples from Mar-May 2007	Coarse, accumulation and quasi-ultrafine particles	OC, Water-soluble V, Ni
[51] Verma et al., 2009	Los Angeles, CA	Integrated samples in Oct-Nov of 2007, during and after wildfire	$PM_{2.5}$	Water-soluble Cr, Ba, Pb, Fe, Ni, V
[8] Verma et al., 2009	Los Angeles, CA	Morning and afternoon samples in June and August 2008	Quasi-ultrafine (< 180 nm) particles	Water-soluble Ca, S, V, Cd, Ni
[7] Shafer et al., 2010	Lahore, Pakistan	Samples collected every sixth day for a full year from January 2007 to January 2008	PM_{10} and $PM_{2.5}$	For PM_{10}: water-soluble Mn, Co; For $PM_{2.5}$: water-soluble Mn, Cd, Ce

A few studies evaluating PM-toxicity using other methods yielded results similar to our study. To investigate the toxicity of PM originating from contrasting traffic profiles in Europe, Gerlofs-Nijland et al. (2007) sampled coarse and fine PM, and reported associations between toxicological responses and brake wear (Cu, Ba) in coarse particles. In 2007-2008, Godri et al. (2011) collected size-fractionated particles at roadside and urban background school sites in London, and evaluated the oxidative potential using the depletion of ascorbate and glutathione. The highest activity (per volume) was found for PM ranging from 1.9 to 10.2 μm. Oxidative potential, assessed using glutathione depletion, also increased with increasing particle size, consistent with the increased levels of Fe, Ba and Cu, which were likely emitted by brake wear (Godri et al., 2011). Wang et al. (2010) conducted a study on coarse mode aerosols collected in Los Angeles and Riverside, California, and suggested that the majority of hydrogen peroxide is mediated by soluble Fe, Cu and Zn. A recent study also found that water-soluble Cu collected in San Joaquin Valley, California is a potent source of generating hydrogen peroxide and hydroxyl radical in fine and coarse particles (Shen and Anastasio, 2011). Furthermore, Fe but particularly Cu were linked to hydroxyl radical generating properties, measured by electron paramagnetic resonance, in fine particles collected in Paris (Baulig et al., 2004). Water-soluble Cu was also shown to be a major contributor to the generation of hydroxyl radical, characterized by the consumption of ascorbic acid and the formation of dihydroxybenzoate, based on results from diesel exhaust particles and ambient particles (PM < 180 nm) (DiStefano et al., 2009). The abovementioned studies suggested that Cu was an important indicator of toxicity. In particular, mechanical wear of automobiles, a major source of soluble Cu in CPM, might represent a source that induces the generation of ROS in this size fraction.

6.5. Summary and Conclusions

Overall, the ROS activity of coarse particle experienced distinct diurnal variation. In summer, ROS activity peaked in midday / afternoon when wind speed was higher. Higher ROS activity was observed overnight in winter as CPM was re-suspended primarily by traffic-induced turbulence. It should be noted that the CPM-related oxidative potential described here represents the toxicity of coarse particles in an outdoor environment. Particle intrusion from outdoor to indoor is lower in coarse than fine PM (Abt et al., 2000). Polidori et al. (2009) showed that the indoor-to-outdoor ratio was lowest for elemental coarse particles in comparison to those of quasi-ultrafine and accumulation particles. The diurnal trend of oxidative potential presented here needs to be combined with personal exposure models in various microenvironments to estimate the actual toxicity imparted by coarse particles on public health. Based on our results, regulating coarse particles using $PM_{10-2.5}$ or PM_{10} mass standards might not be effective in controlling the toxic sources of CPM. The elements that drive ROS activity in the coarse fraction are mainly anthropogenic, and contribute to a relatively low mass fraction in that size range. More targeted regulation may therefore be needed to protect public health from toxic sources of coarse particles.

6.6. Acknowledgements

The study was supported by United States Environmental Protection Agency under the Science to Achieve Results program (EPA-G2006-STAR-Q1) to University of Southern California. The authors would also like to thank the staff at the Wisconsin State Lab of Hygiene (WSLH) for chemical and toxicological analysis of the PM samples.

Chapter 7 Conclusions

7.1. Characteristics of Coarse Particles

7.1.1. Mass concentration

The annual average of CPM mass concentrations ranged from 9.37 to 13.4 μg / m^3 at the 10 sampling sites based on data from the USC comprehensive CPM study (details described in Chapters 2 and 3). Concentrations were 2 to 4 times higher in summer than winter. In particular, higher CPM levels were observed at the two Riverside sites in warmer months, when high wind speed facilitated regional transport and enhanced local re-suspension of coarse mode aerosols. In winter, the CPM mass concentrations were generally lower due to the lower wind speed, with the exception of the Long Beach site, where port-related activities contributed to both the emissions and re-suspension of coarse particles throughout the year. The overall correlation coefficients (R) between $PM_{10-2.5}$ and PM_{10} vary between 0.71-0.91 among the 10 sampling sites, indicating that PM_{10} is a good surrogate of coarse particles. In general, higher correlations are observed in spring and fall (R ranging from 0.80-0.98). In summer, the association between $PM_{10-2.5}$ and PM_{10} was lower (R ranging from 0.40-0.74) due to the high contribution of secondary aerosol formation to fine PM as facilitated by photo-chemical reactions in warmer months in this basin (Pakbin et al., 2010). Additionally, the strong onshore wind facilitated the transport of marine aerosols inland in summer, resulting in significant contribution of sea salt aerosols to the CPM mass. In winter, the lower correlation (R ranging from 0.40-0.85) was driven by lower levels of CPM due to lower wind speed which decreased its contribution to PM_{10}. In general, the overall associations between $PM_{10-2.5}$ and PM_{10} were good, with seasonal variations due to the diverse sources of fine and coarse particles.

7.1.2. Chemical composition

As presented in Chapter 2, Chapter 4 and Chapter 5, the chemical composition of coarse particles – which mostly comprise of mineral and road dust, and to a lesser extent inorganic ions and organic matter – is different from those of fine PM. The major origins of fine particles are fossil fuel combustion and photochemical reactions in urban atmospheres, leading to the high levels of carbonaceous compounds and secondary ions in the fine PM mode as previously reported in the Los Angeles Basin. In contrast to anthropogenic origins of fine particles, CPM arises primarily from natural sources such as mineral dust, as well as fresh and aged sea salt aerosols. Although the concentrations of crustal materials and organic matter varied among seasons, their relative contributions to CPM were consistent throughout the year, suggesting the source strength of soil dust and the associated biota is not significantly affected by the seasonal variation of meteorological conditions. On the other hand, both the concentrations and the fractions of sea salt (both fresh and aged) experienced seasonal variations. Their levels were higher in spring and summer, when the prevailing onshore wind was strong and regional transport facilitated the transport of marine aerosols from coast to inland. In addition to the seasonal variation, the diurnal variation of the chemical composition is significant. In summer, the concentrations of CPM mass, mineral and road dust, and WSOC were highest in the midday / afternoon, in parallel with the high wind speeds during those periods. In winter, the levels of mineral and road dust, sea salt and inorganic ions peaked overnight, when atmospheric dilution was low and traffic-induced turbulences became a dominant re-suspension mechanism. This is particularly evident at the near-freeway sites in Los Angeles and Riverside. Overall, the different sources and formation mechanism, as well as the strength of the primary re-suspension

mechanism of coarse and fine PM are the key drivers of their differential mass concentrations observed.

7.1.3. Health effects

The generation of reactive oxygen species is used to characterize the oxidative potential of coarse particles. The CPM-induced ROS activity displayed distinct diurnal profiles in summer and winter, with higher levels in the warmer months. Higher ROS activity was observed in the midday / afternoon sampling periods (11 a.m. to 3 p.m. and 3 p.m. to 7 p.m. respectively) during summertime, while the peak activity occurred in the overnight period (7 p.m. to 7 a.m.) in winter. Crustal materials, the most dominant component of CPM, displayed very low water solubility. On the other hand, metals generated from anthropogenic activities such as tire and brake wear experienced modest water solubility, which could increase their bioavailability to human cells. Correlation analysis suggests that water-soluble fraction of V, Pd, Cu and Rh are the key drivers of ROS activity. These constituents primarily originate from anthropogenic activities of coarse particles. Despite their low contributions to the mass concentrations, they are important to the biological activity of CPM.

7.2. Discussions and Recommendations

7.2.1. Limitations of current investigation

This investigation aimed to identify the linkage between source, chemical composition and toxicity of coarse particles, and to help the regulatory community to establish cost-effective PM regulations. Through the current investigation, the chemical mass composition, as well as their spatial and temporal characteristics is well characterized in the Los Angeles Basin, thereby providing valuable scientific information for environmental policy decision making. Nonetheless,

due to the higher settling velocity and heterogeneity of coarse particles, the results generated from this study might only be applicable in the Los Angeles Basin. Since the sources and formation mechanism of coarse particles could vary considerably spatially, extrapolation of the findings developed based on this investigation to other areas needs to be proceeded with cautions.

On the other hand, the toxicity of coarse particles is evaluated using the in-vitro ROS assay method, as described in a greater detail in Chapter 6. This bioassay is selected due to its sensitivity to elements, which are abundant in CPM. More importantly, this assay has been shown to be associated with airway and systematic biomarkers (using exhaled NO and plasma IL-6 respectively) in 60 human subjects (Delfino et al., 2010), whereas other commonly used molecular assays, such as the dithiothreitol (DTT) assay and the ascorbate assay, did not correlate with the observed health outcomes of that study. Therefore, the use of the cellular ROS assay is very relevant in terms of health effects of airborne PM pollutants and thus is particularly appropriate for the scope of this study. Nonetheless, although this bioassay is designed to be responsive to ROS generated by a wide range of mechanisms and active species (peroxide, hydroxyl radical, super-oxide radial, organic-peroxides), and thereby providing a comprehensive evaluation of the oxidative potential induced by PM, the high levels of biological constituents present in coarse particles, which might be partly responsible for CPM-induced adverse health effects, might not be characterized in this bioassay. Therefore, it is important to note that the toxicity data generated from this investigation represent only one of the many ways of evaluating PM-induced toxicity.

7.2.2. Implications on epidemiological studies

In epidemiological studies, the mass concentrations of coarse particles are estimated either

using direct (based on cascade sampling or impactors) or indirect (based on the difference between the measured PM_{10} and $PM_{2.5}$ levels) measurements. The latter of which is affected by two measurement errors. The higher spatial heterogeneity of CPM, compared to PM_{10} and $PM_{2.5}$, might also introduce uncertainty in the exposure characterization of coarse particles (Moore et al., 2010; Pakbin et al., 2010). In addition, the infiltration of ambient coarse particles in an indoor environment is moderate to low, resulting in lower levels of CPM indoor (Polidori et al., 2009). Therefore, the actual exposure dose of coarse particles might be much lower than the ones estimated based on the measured ambient levels in subjects that spent a consideration amount of time indoor. All of the abovementioned conditions need to be carefully considered in the design phase, as well as the exposure assessment of CPM in epidemiological studies.

7.2.3. Recommendations for future research

Exposure to bioaerosols, which are predominantly comprised of plant pollen, spores and microorganisms, can result in allergic, toxic and infectious responses in a large fraction of the population (Levetin and Perry, 1995; Ross et al., 2002; Targonski et al., 1995). The results of current investigation suggest that the biological material is a major component of the organic fraction of CPM. Therefore, further characterization of bioaerosols including the quantification of fungi, bacteria, plant pollen, and spore materials might provide important knowledge on the toxicity induced by the biological fraction of CPM.

As discussed in Chapter 6, the results from this study, focusing solely on CPM, as well as a few other studies evaluating PM toxicity using other methods (Gerlofs-Nijland et al., 2007; Godri et al., 2011), revealed that species of abrasive origins could be responsible for generation of ROS activity in the coarse mode. Therefore, road dust – comprising of crustal materials enriched by

both tailpipe and non-tailpipe vehicular emissions – could be an important source of coarse particle that generates redox-active constituents. In addition to the in-vitro evaluations of toxicity, in-vivo studies will be useful to evaluate the toxicity of road dust and / abrasive materials generated from dynamometer studies. Further characterization on the physico-chemical and toxicological properties of road dust is also recommended.

7.2.4. Recommendations on coarse particle regulation

In contrast to the anthropogenic origins of fine particles, CPM predominantly arises from natural sources including crustal and biological materials. Due to the distinct sources and formation mechanism of fine and coarse PM, regulating coarse particles under the mass-based PM_{10} standard might not be appropriate. The past and current PM standards are effective in controlling particles of combustion origins, resulting in significant reductions of fine PM in the last decade in this basin. In contrast, the levels of CPM remained similar in the last few years. In the PM NAAQS review in 2006, the U.S. EPA has proposed to use a new $PM_{10-2.5}$ standard in replacement of the PM_{10} standard to regulate coarse particles. The proposed $PM_{10-2.5}$ standard, which is designed to be comparable to the current PM_{10} standard, displayed equivalency in the urban areas of the Los Angeles Basin. On the other hand, in sub-urban or rural areas, where both the wind speed and source strength of crustal materials are higher, the proposed standards are more stringent. Therefore, the proposed $PM_{10-2.5}$ standard is likely to impose a greater impact in rural areas, where CPM concentrations are mostly driven by windblown dust. Although it is more appropriate to control coarse particles using a $PM_{10-2.5}$ standard, PM_{10} is generally a good surrogate of coarse particles based on data collected in the Los Angeles Basin, where the levels of coarse and fine PM are comparable. Using oxidative potential as a metric to evaluate toxicity,

constituents that drive ROS activity of CPM are mainly anthropogenic in origin, and their contributions to CPM mass are low. Therefore, using a mass-based standard, regardless of its form, may not be effective in reducing the CPM sources that drive ROS activity. Based on the results of this investigation, it is recommended to regulate coarse particles using target controls. Prioritizing the critical PM sources that are responsible for inducing adverse health effects may be the most effective approach to protect the public health from CPM exposure.

Bibliography

Abbey, D.E., Lebowitz, M.D., Mills, P.K., Petersen, F.F., Beeson, W.L., Burchette, R.J., 1995. Long-Term Ambient Concentrations of Particulates and Oxidants and Development of Chronic Disease in a Cohort of Nonsmoking California Residents. Inhal Toxicol 7, 19-34.

Abt, E., Suh, H.H., Catalano, P., Koutrakis, P., 2000. Relative contribution of outdoor and indoor particle sources to indoor concentrations. Environ Sci Technol 34, 3579-3587.

Andrews, E., Saxena, P., Musarra, S., Hildemann, L.M., Koutrakis, P., McMurry, P.H., Olmez, I., White, W.H., 2000. Concentration and composition of atmospheric aerosols from the 1995 SEAVS experiment and a review of the closure between chemical and gravimetric measurements. J Air Waste Manage 50, 648-664.

Arhami, M., Minguillon, M.C., Polidori, A., Schauer, J.J., Delfino, R.J., Sioutas, C., 2010. Organic compound characterization and source apportionment of indoor and outdoor quasi-ultrafine particulate matter in retirement homes of the Los Angeles Basin. Indoor Air 20, 17-30.

Arhami, M., Sillanpaa, M., Hu, S.H., Olson, M.R., Schauer, J.J., Sioutas, C., 2009. Size-Segregated Inorganic and Organic Components of PM in the Communities of the Los Angeles Harbor. Aerosol Sci Tech 43, 145-160.

American Lung Association. State of the air: 2011, Available at: http://www.stateoftheair.org. Accessed November 30, 2011.

Barnes, P.J., 1990. Reactive Oxygen Species and Airway Inflammation. Free Radical Biology and Medicine 9, 235-243.

Bauer, H., Schueller, E., Weinke, G., Berger, A., Hitzenberger, R., Marr, I.L., Puxbaum, H., 2008. Significant contributions of fungal spores to the organic carbon and to the aerosol mass balance of the urban atmospheric aerosol. Atmospheric Environment 42, 5542-5549.

Baulig, A., Poirault, J.J., Ausset, P., Schins, R., Shi, T.M., Baralle, D., Dorlhene, P., Meyer, M., Lefevre, R., Baeza-Squiban, A., Marano, F., 2004. Physicochemical characteristics and biological activities of seasonal atmospheric particulate matter sampling in two locations of Paris. Environ Sci Technol 38, 5985-5992.

Birch, M.E., Cary, R.A., 1996. Elemental carbon-based method for monitoring occupational exposures to particulate diesel exhaust. Aerosol Sci Tech 25, 221-241.

Birmili, W., Allen, A.G., Bary, F., Harrison, R.M., 2006. Trace metal concentrations and water solubility in size-fractionated atmospheric particles and influence of road traffic. Environ Sci Technol 40, 1144-1153.

Biswas, S., Verma, V., Schauer, J.J., Sioutas, C., 2009. Chemical speciation of PM emissions from heavy-duty diesel vehicles equipped with diesel particulate filter (DPF) and selective catalytic reduction (SCR) retrofits. Atmospheric Environment 43, 1917-1925.

Brunekreef, B., Forsberg, B., 2005. Epidemiological evidence of effects of coarse airborne particles on health. European Respiratory Journal 26, 309-318.

Cahill, T.M., 2010. Size-Resolved Organic Speciation of Wintertime Aerosols in California's Central Valley. Environmental Science & Technology 44, 2315-2321.

Campa, A.M.S.d.l., Moreno, T., Rosa, J.d.l., Alastuey, A., Querol, X., 2011. Size distribution and chemical composition of metalliferous stack emissions in the San Roque petroleum refinery complex, southern Spain. Journal of Hazardous Materials, 713-722.

Castillejos, M., Borja-Aburto, V.H., Dockery, D.W., Gold, D.R., Loomis, D., 2000. Airborne coarse particles and mortality. Inhal Toxicol 12, 61-72.

Castranova, V., Ma, J.Y.C., Yang, H.M., Antonini, J.M., Butterworth, L., Barger, M.W., Roberts, J., Ma, J.K.H., 2001. Effect of exposure to diesel exhaust particles on the susceptibility of the lung to infection. Environ Health Persp 109, 609-612.

Castro, L., Freeman, B., 2001. Reactive oxygen species in human health and disease. Nutrition 17, 161-165.

Chan, W.H., Vet, R.J., Lusis, M.A., Skelton, G.B., 1983. Airborne Particulate Size Distribution Measurements in Nickel Smelter Plumes. Atmospheric Environment 17, 1173-1181.

Charron, A., Harrison, R.M., 2005. Fine (PM2.5) and coarse (PM2.5-10) particulate matter on a heavily trafficked London highway: Sources and processes. Environ Sci Technol 39, 7768-7776.

Chen, L., Yang, W., Jennison, B.L., Omaye, S.T., 2000. Air particulate pollution and hospital admissions for chronic obstructive pulmonary disease in Reno, Nevada. Inhal Toxicol 12, 281-298.

Chen, Y., Yang, Q.Y., Krewski, D., Burnett, R.T., Shi, Y.L., McGrail, K.M., 2005. The effect of coarse ambient particulate matter on first, second, and overall hospital admissions for respiratory disease among the elderly. Inhal Toxicol 17, 649-655.

Cheng, Y., Brook, J.R., Li, S.M., Leithead, A., 2011. Seasonal variation in the biogenic secondary organic aerosol tracer cis-pinonic acid: Enhancement due to emissions from regional and local biomass burning. Atmospheric Environment 45, 7105-7112.

Cheung, K., Daher, N., Kam, W., Shafer, M.M., Ning, Z., Schauer, J.J., Sioutas, C., 2011a. Spatial and Temporal Variation of Chemical Composition and Mass Closure of Ambient Coarse Particulate Matter (PM10-2.5) in the Los Angeles Area. Atmospheric Environment, doi:10.1016/j.atmosenv.2011.1002.1066.

Cheung, K., Daher, N., Kam, W., Shafer, M.M., Ning, Z., Schauer, J.J., Sioutas, C., 2011b. Spatial and temporal variation of chemical composition and mass closure of ambient coarse particulate matter (PM10-2.5) in the Los Angeles area. Atmospheric Environment 45, 2651-2662.

Cheung, K., Shafer, M.M., Schauer, J.J., Sioutas, C., 2011c. Diurnal trends in coarse particulate matter composition in the Los Angeles Basin. Journal of Environmental Monitoring DOI: 10.1039/c1em10296f.

Cheung, K., Shafer, M.M., Schauer, J.J., Sioutas, C., 2012. Historical trends in the mass and chemical species concentrations of coarse particulate matter in the Los Angeles Basin and relation to sources and air quality regulations. J Air Waste Manage 62, 541-556.

Cheung, K.L., Ntziachristos, L., Tzamkiozis, T., Schauer, J.J., Samaras, Z., Moore, K.F., Sioutas, C., 2010. Emissions of Particulate Trace Elements, Metals and Organic Species from Gasoline, Diesel, and Biodiesel Passenger Vehicles and Their Relation to Oxidative Potential. Aerosol Sci Tech 44, 500-513.

Cho, A.K., Sioutas, C., Miguel, A.H., Kumagai, Y., Schmitz, D.A., Singh, M., Eiguren-Fernandez, A., Froines, J.R., 2005. Redox activity of airborne particulate matter at different sites in the Los Angeles Basin. Environ Res 99, 40-47.

Chow, J.C., Watson, J.G., Fujita, E.M., Lu, Z.Q., Lawson, D.R., Ashbaugh, L.L., 1994. Temporal and Spatial Variations of Pm(2.5) and Pm(10) Aerosol in the Southern California Air-Quality Study. Atmospheric Environment 28, 2061-2080.

Chow, J.C., Watson, J.G., Lowenthal, D.H., Chen, L.W.A., Zielinska, B., Mazzoleni, L.R., Magliano, K.L., 2007. Evaluation of organic markers for chemical mass balance source apportionment at the Fresno Supersite. Atmos Chem Phys 7, 1741-1754.

Chow, J.C., Watson, J.G., Lowenthal, D.H., Solomon, P.A., Magliano, K.L., Ziman, S.D., Richards, L.W., 1992. Pm10 Source Apportionment in California San-Joaquin Valley. Atmospheric Environment Part a-General Topics 26, 3335-3354.

Costa, D.L., Dreher, K.L., 1997. Bioavailable transition metals in particulate matter mediate cardiopulmonary injury in healthy and compromised animal models. Environ Health Persp 105, 1053-1060.

Daher, N., Ruprecht, A., Invernizzi, G., De Marco, C., Miller-Schulze, J., Heo, J.B., Shafer, M.M., Schauer, J.J., Sioutas, C., 2011. Chemical Characterization and Source Apportionment of Fine and Coarse Particulate Matter Inside the Refectory of Santa Maria Delle Grazie Church, Home of Leonardo Da Vinci's "Last Supper". Environ Sci Technol 45, 10344-10353.

Delfino, R.J., Sioutas, C., Malik, S., 2005. Potential role of ultrafine particles in associations between airborne particle mass and cardiovascular health. Environ Health Persp 113, 934-946.

Delfino, R.J., Staimer, N., Tjoa, T., Arhami, M., Polidori, A., Gillen, D.L., George, S.C., Shafer, M.M., Schauer, J.J., Sioutas, C., 2010. Associations of Primary and Secondary Organic Aerosols With Airway and Systemic Inflammation in an Elderly Panel Cohort. Epidemiology 21, 892-902.

Dentener, F.J., Carmichael, G.R., Zhang, Y., Lelieveld, J., Crutzen, P.J., 1996. Role of mineral aerosol as a reactive surface in the global troposphere. J Geophys Res-Atmos 101, 22869-22889.

DiStefano, E., Eiguren-Fernandez, A., Delfino, R.J., Sioutas, C., Froines, J.R., Cho, A.K., 2009. Determination of metal-based hydroxyl radical generating capacity of ambient and diesel exhaust particles. Inhal Toxicol 21, 731-738.

Docherty, K.S., Stone, E.A., Ulbrich, I.M., DeCarlo, P.F., Snyder, D.C., Schauer, J.J., Peltier, R.E., Weber, R.J., Murphy, S.M., Seinfeld, J.H., Grover, B.D., Eatough, D.J., Jimenez, J.L., 2008. Apportionment of Primary and Secondary Organic Aerosols in Southern California during the 2005 Study of Organic Aerosols in Riverside (SOAR-1). Environ Sci Technol 42, 7655-7662.

Dockery, D.W., Pope, C.A., 1994. Acute Respiratory Effects of Particulate Air-Pollution. Annual Review of Public Health 15, 107-132.

Dockery, D.W., Pope, C.A., Xu, X.P., Spengler, J.D., Ware, J.H., Fay, M.E., Ferris, B.G., Speizer, F.E., 1993. An Association between Air-Pollution and Mortality in 6 United-States Cities. New England Journal of Medicine 329, 1753-1759.

Dutton, S.J., Rajagopalan, B., Vedal, S., Hannigan, M.P., 2010. Temporal patterns in daily measurements of inorganic and organic speciated PM2.5 in Denver. Atmospheric Environment 44, 987-998.

Eiguren-Fernandez, A., Miguel, A.H., Lu, R., Purvis, K., Grant, B., Mayo, P., Di Stefano, E., Cho, A.K., Froines, J., 2008. Atmospheric formation of 9,10-phenanthraquinone in the Los Angeles air basin. Atmospheric Environment 42, 2312-2319.

Eldering, A., Solomon, P.A., Salmon, L.G., Fall, T., Cass, G.R., 1991. Hydrochloric-Acid - a Regional Perspective on Concentrations and Formation in the Atmosphere of Southern California. Atmospheric Environment Part a-General Topics 25, 2091-2102.

Falkovich, A.H., Graber, E.R., Schkolnik, G., Rudich, Y., Maenhaut, W., Artaxo, P., 2005. Low molecular weight organic acids in aerosol particles from Rondonia, Brazil, during the biomass-burning, transition and wet periods. Atmos Chem Phys 5, 781-797.

Falkovich, A.H., Schkolnik, G., Ganor, E., Rudich, Y., 2004. Adsorption of organic compounds pertinent to urban environments onto mineral dust particles. J Geophys Res-Atmos 109, -.

Fine, P.M., Chakrabarti, B., Krudysz, M., Schauer, J.J., Sioutas, C., 2004a. Diurnal variations of individual organic compound constituents of ultrafine and accumulation mode particulate matter in the Los Angeles basin. Environ Sci Technol 38, 1296-1304.

Fine, P.M., Shen, S., Sioutas, C., 2004b. Inferring the sources of fine and ultrafine particulate matter at downwind receptor sites in the Los Angeles basin using multiple continuous measurements. Aerosol Sci Tech 38, 182-195.

Finlayson-Pitts, B.J., 2003. The tropospheric chemistry of sea salt: A molecular-level view of the chemistry of NaCl and NaBr. Chemical Reviews 103, 4801-4822.

Folkmann, J.K., Risom, L., Hansen, C.S., Loft, S., Moller, P., 2007. Oxidatively damaged DNA and inflammation in the liver of dyslipidemic ApoE(-/-) mice exposed to diesel exhaust particles. Toxicology 237, 134-144.

Garg, B.D., Cadle, S.H., Mulawa, P.A., Groblicki, P.J., Laroo, C., Parr, G.A., 2000. Brake wear particulate matter emissions. Environ Sci Technol 34, 4463-4469.

Gauderman, W.J., McConnell, R., Gilliland, F., London, S., Thomas, D., Avol, E., Vora, H., Berhane, K., Rappaport, E.B., Lurmann, F., Margolis, H.G., Peters, J., 2000. Association between air pollution and lung function growth in southern California children. American Journal of Respiratory and Critical Care Medicine 162, 1383-1390.

Gauderman, W.J., Vora, H., McConnell, R., Berhane, K., Gilliland, F., Thomas, D., Lurmann, F., Avoli, E., Kunzli, N., Jerrett, M., Peters, J., 2007. Effect of exposure to traffic on lung development from 10 to 18 years of age: a cohort study. Lancet 369, 571-577.

Geller, M.D., Fine, P.M., Sioutas, C., 2004. The relationship between real-time and time-integrated coarse (2.5-10 mu m), intermodal (1-2.5 mu m), and fine (< 2.5 mu m) particulate matter in the Los Angeles Basin. J Air Waste Manage 54, 1029-1039.

Geller, M.D., Kim, S., Misra, C., Sioutas, C., Olson, B.A., Marple, V.A., 2002. A methodology for measuring size-dependent chemical composition of ultrafine particles. Aerosol Sci Tech 36, 748-762.

Gerlofs-Nijland, M.E., Dormans, J.A.M.A., Bloemen, H.J.T., Leseman, D.L.A.C., Boere, A.J.F., Kelly, F.J., Mudway, I.S., Jimenez, A.A., Donaldson, K., Guastadisegni, C., Janssen, N.A.H., Brunekreef, B., Sandstrom, T., Cassee, F.R., 2007. Toxicity of coarse and fine particulate matter from sites with contrasting traffic profiles. Inhal Toxicol 19, 1055-1069.

Gertler, A.W., Gillies, J.A., Pierson, W.R., 2000. An assessment of the mobile source contribution to PM10 and PM2.5 in the United States. Water Air and Soil Pollution 123, 203-214.

Gietl, J.K., Lawrence, R., Thorpe, A.J., Harrison, R.M., 2010. Identification of brake wear particles and derivation of a quantitative tracer for brake dust at a major road. Atmospheric Environment 44, 141-146.

Godri, K.J., Harrison, R.M., Evans, T., Baker, T., Dunster, C., Mudway, I.S., Kelly, F.J., 2011. Increased Oxidative Burden Associated with Traffic Component of Ambient Particulate Matter at Roadside and Urban Background Schools Sites in London. Plos One 6.

Goldsmith, C.A.W., Imrich, A., Danaee, H., Ning, Y., Kobzik, L., 1998. Analysis of air pollution particulate-mediated oxidant stress in alveolar macrophages. Journal of Toxicology and Environmental Health-Part A 54, 529-545.

Goodman, A.L., Underwood, G.M., Grassian, V.H., 2000. A laboratory study of the heterogeneous reaction of nitric acid on calcium carbonate particles. J Geophys Res-Atmos 105, 29053-29064.

Harrison, R.M., Williams, C.R., 1983. Physicochemical Characterization of Atmospheric Trace-Metal Emissions from a Primary Zinc-Lead Smelter. Sci Total Environ 31, 129-140.

Harrison, R.M., Yin, J.X., Mark, D., Stedman, J., Appleby, R.S., Booker, J., Moorcroft, S., 2001. Studies of the coarse particle (2.5-10 mu m) component in UK urban atmospheres. Atmospheric Environment 35, 3667-3679.

Hays, M.D., Gullett, B., King, C., Robinson, J., Preston, W., Touati, A., 2011. Characterization of Carbonaceous Aerosols Emitted from Outdoor Wood Boilers. Energy & Fuels 25, 5632-5638.

Herckes, P., Engling, G., Kreidenweis, S.M., Collett, J.L., 2006. Particle size distributions of organic aerosol constituents during the 2002 Yosemite Aerosol Characterization Study. Environ Sci Technol 40, 4554-4562.

Hildemann, L.M., Mazurek, M.A., Cass, G.R., Simoneit, B.R.T., 1994. Seasonal Trends in Los-Angeles Ambient Organic Aerosol Observed by High-Resolution Gas-Chromatography. Aerosol Sci Tech 20, 303-317.

Hinds, W.C., 1999. Aerosol Technology: Properties, Behavior, and Measurement of Airborne Particles, 2nd ed. Wiley-Interscience, New York.

Hjortenkrans, D.S.T., Bergback, B.G., Haggerud, A.V., 2007. Metal emissions from brake linings and tires: Case studies of Stockholm, Sweden 1995/1998 and 2005. Environ Sci Technol 41, 5224-5230.

Ho, K.F., Lee, S.C., Cao, J.J., Chow, J.C., Watson, J.G., Chan, C.K., 2005. Seasonal variations and mass closure analysis of particulate matter in Hong Kong. Sci Total Environ 355, 276-287.

Hoek, G., Brunekreef, B., Goldbohm, S., Fischer, P., van den Brandt, P.A., 2002. Association between mortality and indicators of traffic-related air pollution in the Netherlands: a cohort study. Lancet 360, 1203-1209.

Hu, S., Polidori, A., Arhami, M., Shafer, M.M., Schauer, J.J., Cho, A., Sioutas, C., 2008. Redox activity and chemical speciation of size fractioned PM in the communities of the Los Angeles-Long Beach harbor. Atmos Chem Phys 8, 6439-6451.

Huang, X.F., Yu, J.Z., 2008. Size distributions of elemental carbon in the atmosphere of a coastal urban area in South China: characteristics, evolution processes, and implications for the mixing state. Atmos Chem Phys 8, 5843-5853.

Hueglin, C., Gehrig, R., Baltensperger, U., Gysel, M., Monn, C., Vonmont, H., 2005. Chemical characterisation of PM2.5, PM10 and coarse particles at urban, near-city and rural sites in Switzerland. Atmospheric Environment 39, 637-651.

Hughes, L.S., Allen, J.O., Kleeman, M.J., Johnson, R.J., Cass, G.R., Gross, D.S., Gard, E.E., Galli, M.E., Morrical, B.D., Fergenson, D.P., Dienes, T., Noble, C.A., Silva, P.J., Prather, K.A., 1999. Size and composition distribution of atmospheric particles in southern California. Environ Sci Technol 33, 3506-3515.

Hwang, I., Hopke, P.K., Pinto, J.P., 2008. Source apportionment and spatial distributions of coarse particles during the regional air pollution study. Environ Sci Technol 42, 3524-3530.

Isakson, J., Persson, T.A., Lindgren, E.S., 2001. Identification and assessment of ship emissions and their effects in the harbour of G(o)over-circleteborg, Sweden. Atmospheric Environment 35, 3659-3666.

Jia, Y.L., Clements, A.L., Fraser, M.P., 2010. Saccharide composition in atmospheric particulate matter in the southwest US and estimates of source contributions. J Aerosol Sci 41, 62-73.

Kanitsar, K., Koellensperger, G., Hann, S., Limbeck, A., Puxbaum, H., Stingeder, G., 2003. Determination of Pt, Pd and Rh by inductively coupled plasma sector field mass spectrometry (ICP-SFMS) in size-classified urban aerosol samples. Journal of Analytical Atomic Spectrometry 18, 239-246.

Karageorgos, E.T., Rapsomanikis, S., 2007. Chemical characterization of the inorganic fraction of aerosols and mechanisms of the neutralization of atmospheric acidity in Athens, Greece. Atmos Chem Phys 7, 3015-3033.

Kawamura, K., Kaplan, I.R., 1987. Motor Exhaust Emissions as a Primary Source for Dicarboxylic-Acids in Los-Angeles Ambient Air. Environ Sci Technol 21, 105-110.

Khalili, N.R., Scheff, P.A., Holsen, T.M., 1995. Pah Source Fingerprints for Coke Ovens, Diesel and Gasoline-Engines, Highway Tunnels, and Wood Combustion Emissions. Atmospheric Environment 29, 533-542.

Kim, B.M., Teffera, S., Zeldin, M.D., 2000a. Characterization of PM2.5 and PM10 in the South Coast Air Basin of southern California: Part 1 - Spatial variations. J Air Waste Manage 50, 2034-2044.

Kim, B.M., Teffera, S., Zeldin, M.D., 2000b. Characterization of PM2.5 and PM10 in the South Coast Air Basin of southern California: Part 2 - Temporal variations. J Air Waste Manage 50, 2045-2059.

Kleeman, M.J., Hughes, L.S., Allen, J.O., Cass, G.R., 1999. Source contributions to the size and composition distribution of atmospheric particles: Southern California in September 1996. Environ Sci Technol 33, 4331-4341.

Kleeman, M.J., Robert, M.A., Riddle, S.G., Fine, P.M., Hays, M.D., Schauer, J.J., Hannigan, M.P., 2008. Size distribution of trace organic species emitted from biomass combustion and meat charbroiling. Atmospheric Environment 42, 3059-3075.

Kleinman, M.T., Sioutas, C., Froines, J.R., Fanning, E., Hamade, A., Mendez, L., Meacher, D., Oldham, M., 2007. Inhalation of concentrated ambient particulate matter near a heavily trafficked road stimulates antigen-induced airway responses in mice. Inhal Toxicol 19, 117-126.

Koulouri, E., Saarikoski, S., Theodosi, C., Markaki, Z., Gerasopoulos, E., Kouvarakis, G., Makela, T., Hillamo, R., Mihalopoulos, N., 2008. Chemical composition and sources of fine and coarse aerosol particles in the Eastern Mediterranean. Atmospheric Environment 42, 6542-6550.

Krudysz, M.A., Froines, J.R., Fine, P.M., Sioutas, C., 2008. Intra-community spatial variation of size-fractionated PM mass, OC, EC, and trace elements in the Long Beach, CA area. Atmospheric Environment 42, 5374-5389.

Kulmala, M., Vehkamaki, H., Petaja, T., Dal Maso, M., Lauri, A., Kerminen, V.M., Birmili, W., McMurry, P.H., 2004. Formation and growth rates of ultrafine atmospheric particles: a review of observations. J Aerosol Sci 35, 143-176.

Landreman, A.P., Shafer, M.M., Hemming, J.C., Hannigan, M.P., Schauer, J.J., 2008. A macrophage-based method for the assessment of the reactive oxygen species (ROS) activity of atmospheric particulate matter (PM) and application to routine (daily-24 h) aerosol monitoring studies. Aerosol Sci Tech 42, 946-957.

Lenschow, P., Abraham, H.J., Kutzner, K., Lutz, M., Preuss, J.D., Reichenbacher, W., 2001. Some ideas about the sources of PM10. Atmospheric Environment 35, S23-S33.

Levetin, E., Perry, C., 1995. Evaluation of Airborne Fungi with a Dichloran-Glycerol Agar. Journal of Allergy and Clinical Immunology 95, 168-168.

Li, N., Sioutas, C., Cho, A., Schmitz, D., Misra, C., Sempf, J., Wang, M.Y., Oberley, T., Froines, J., Nel, A., 2003. Ultrafine particulate pollutants induce oxidative stress and mitochondrial damage. Environ Health Persp 111, 455-460.

Lin, C.C., Chen, S.J., Huang, K.L., Hwang, W.I., Chang-Chien, G.P., Lin, W.Y., 2005. Characteristics of metals in nano/ultrafine/fine/coarse particles collected beside a heavily trafficked road. Environ Sci Technol 39, 8113-8122.

Lipsett, M.J., Tsai, F.C., Roger, L., Woo, M., Ostro, B.D., 2006. Coarse particles and heart rate variability among older adults with coronary artery disease in the Coachella Valley, California. Environ Health Persp 114, 1215-1220.

Lough, G.C., Schauer, J.J., Park, J.S., Shafer, M.M., Deminter, J.T., Weinstein, J.P., 2005. Emissions of metals associated with motor vehicle roadways. Environ Sci Technol 39, 826-836.

Lun, X.X., Zhang, X.S., Mu, Y.J., Nang, A., Jiang, G.B., 2003. Size fractionated speciation of sulfate and nitrate in airborne particulates in Beijing, China. Atmospheric Environment 37, 2581-2588.

Mader, B.T., Schauer, J.J., Seinfeld, J.H., Flagan, R.C., Yu, J.Z., Yang, H., Lim, H.J., Turpin, B.J., Deminter, J.T., Heidemann, G., Bae, M.S., Quinn, P., Bates, T., Eatough, D.J., Huebert, B.J., Bertram, T., Howell, S., 2003. Sampling methods used for the collection of particle-phase organic and elemental carbon during ACE-Asia. Atmospheric Environment 37, 1435-1449.

Marcazzan, G.M., Vaccaro, S., Valli, G., Vecchi, R., 2001. Characterisation of PM10 and PM2.5 particulate matter in the ambient air of Milan (Italy). Atmospheric Environment 35, 4639-4650.

McConnell, R., Berhane, K., Gilliland, F., London, S.J., Vora, H., Avol, E., Gauderman, W.J., Margolis, H.G., Lurmann, F., Thomas, D.C., Peters, J.M., 1999. Air pollution and bronchitic symptoms in Southern California children with asthma. Environ Health Persp 107, 757-760.

Miguel, A.H., Eiguren-Fernandez, A., Jaques, P.A., Froines, J.R., Grant, B.L., Mayo, P.R., Sioutas, C., 2004. Seasonal variation of the particle size distribution of polycyclic aromatic hydrocarbons and of major aerosol species in Claremont, California. Atmospheric Environment 38, 3241-3251.

Minguillon, M.C., Arhami, M., Schauer, J.J., Sioutas, C., 2008. Seasonal and spatial variations of sources of fine and quasi-ultrafine particulate matter in neighborhoods near the Los Angeles-Long Beach harbor. Atmospheric Environment 42, 7317-7328.

Misra, C., Geller, M.D., Shah, P., Sioutas, C., Solomon, P.A., 2001. Development and evaluation of a continuous coarse (PM10-PM2.5) particle monitor. J Air Waste Manage 51, 1309-1317.

Moore, K.F., Verma, V., Minguillon, M.C., Sioutas, C., 2010. Inter- and Intra-Community Variability in Continuous Coarse Particulate Matter (PM10-2.5) Concentrations in the Los Angeles Area. Aerosol Sci Tech 44, 526-540.

Neiburger, M., Wurtele, M.G., 1949. On the Nature and Size of Particles in Haze, Fog, and Stratus of the Los-Angeles Region. Chemical Reviews 44, 321-335.

Nel, A., 2005. Air pollution-related illness: Effects of particles. Science 308, 804-806.

Nel, A.E., Diaz-Sanchez, D., Li, N., 2001. The role of particulate pollutants in pulmonary inflammation and asthma: evidence for the involvement of organic chemicals and oxidative stress. Current opinion in pulmonary medicine 7, 20-26.

Newhook, R., Hirtle, H., Byrne, K., Meek, M.E., 2003. Releases from copper smelters and refineries and zinc plants in Canada: human health exposure and risk characterization. Sci Total Environ 301, 23-41.

Nicholson, K.W., Branson, J.R., Giess, P., Cannell, R.J., 1989. The Effects of Vehicle Activity on Particle Resuspension. J Aerosol Sci 20, 1425-1428.

Ning, Z., Geller, M.D., Moore, K.F., Sheesley, R., Schauer, J.J., Sioutas, C., 2007. Daily variation in chemical characteristics of urban ultrafine aerosols and inference of their sources. Environ Sci Technol 41, 6000-6006.

Noble, C.A., Prather, K.A., 1996. Real-time measurement of correlated size and composition profiles of individual atmospheric aerosol particles. Environ Sci Technol 30, 2667-2680.

Oberdorster, G., Sharp, Z., Atudorei, V., Elder, A., Gelein, R., Kreyling, W., Cox, C., 2004. Translocation of inhaled ultrafine particles to the brain. Inhal Toxicol 16, 437-445.

Pakbin, P., Hudda, N., Cheung, K.L., Moore, K.F., Sioutas, C., 2010. Spatial and Temporal Variability of Coarse (PM10-2.5) Particulate Matter Concentrations in the Los Angeles Area. Aerosol Sci Tech 44, 514-525.

Pakbin, P., Ning, Z., Shafer, M.M., Schauer, J.J., Sioutas, C., 2011. Seasonal and Spatial Coarse Particle Elemental Concentrations in the Los Angeles Area. Aerosol Sci Tech 45, 949-U156.

Paode, R.D., Shahin, U.M., Sivadechathep, J., Holsen, T.M., Franek, W.J., 1999. Source apportionment of dry deposited and airborne coarse particles collected in the Chicago area. Aerosol Sci Tech 31, 473-486.

Pelicano, H., Carney, D., Huang, P., 2004. ROS stress in cancer cells and therapeutic implications. Drug Resistance Updates 7, 97-110.

Peters, A., Veronesi, B., Calderón-Garcidueñas, L., Gehr, P., Chen, L.C., Geiser, M., Reed, W., Rothen-Rutishauser, B., Schürch, S., Schulz, H., 2006. Translocation and potential neurological effects of fine and ultrafine particles a critical update. Particle and Fibre Toxicology 3:13.

Polidori, A., Arhami, M., Sioutas, C., Delfino, R.J., Allen, R., 2007. Indoor/outdoor relationships, trends, and carbonaceous content of fine particulate matter in retirement homes of the Los Angeles basin. J Air Waste Manage 57, 366-379.

Polidori, A., Cheung, K.L., Arhami, M., Delfino, R.J., Schauer, J.J., Sioutas, C., 2009. Relationships between size-fractionated indoor and outdoor trace elements at four retirement communities in southern California. Atmos Chem Phys 9, 4521-4536.

Pope, C.A., Dockery, D.W., 2006. Health effects of fine particulate air pollution: Lines that connect. J Air Waste Manage 56, 709-742.

Prophete, C., Maciejczyk, P., Salnikow, K., Gould, T., Larson, T., Koenig, J., Jaques, P., Sioutas, C., Lippmann, M., Cohen, M., 2006. Effects of select PM-associated metals on alveolar macrophage phosphorylated ERK1 and-2 and iNOS expression during ongoing alteration in iron homeostasis. Journal of Toxicology and Environmental Health-Part a-Current Issues 69, 935-951.

Putaud, J.P., Van Dingenen, R., Dell'Acqua, A., Raes, F., Matta, E., Decesari, S., Facchini, M.C., Fuzzi, S., 2004. Size-segregated aerosol mass closure and chemical composition in Monte Cimone (I) during MINATROC. Atmospheric Chemistry and Physics 4, 889-902.

Qiu, H., Yu, I.T., Tian, L., Wang, X., Tse, L.A., Tam, W., Wong, T.W., 2012. Effects of Coarse Particulate Matter on Emergency Hospital Admissions for Respiratory Diseases: A Time Series Analysis in Hong Kong. Environ Health Perspect.

Querol, X., Alastuey, A., Ruiz, C.R., Artinano, B., Hansson, H.C., Harrison, R.M., Buringh, E., ten Brink, H.M., Lutz, M., Bruckmann, P., Straehl, P., Schneider, J., 2004. Speciation and origin of PM10 and PM2.5 in selected European cities. Atmospheric Environment 38, 6547-6555.

Rauch, S., Hemond, H.F., Barbante, C., Owari, M., Morrison, G.M., Peucker-Ehrenbrink, B., Wass, U., 2005. Importance of automobile exhaust catalyst emissions for the depostion of platinum, palladium, and rhodium in the Northern Hemisphere. Environ Sci Technol 39, 8156-8162.

Rauch, S., Lu, M., Morrison, G.M., 2001. Heterogeneity of platinum group metals in airborne particles. Environ Sci Technol 35, 595-599.

Roberts, J.R., Young, S.H., Castranova, V., Antonini, J.M., 2007. Soluble metals in residual oil fly ash alter innate and adaptive pulmonary immune responses to bacterial infection in rats. Toxicology and Applied Pharmacology 221, 306-319.

Rogge, W.F., Hildemann, L.M., Mazurek, M.A., Cass, G.R., Simoneit, B.R.T., 1993a. Sources of Fine Organic Aerosol .3. Road Dust, Tire Debris, and Organometallic Brake Lining Dust - Roads as Sources and Sinks. Environ Sci Technol 27, 1892-1904.

Rogge, W.F., Hildemann, L.M., Mazurek, M.A., Cass, G.R., Simoneit, B.R.T., 1993b. Sources of Fine Organic Aerosol .4. Particulate Abrasion Products from Leaf Surfaces of Urban Plants. Environmental Science & Technology 27, 2700-2711.

Rogge, W.F., Hildemann, L.M., Mazurek, M.A., Cass, G.R., Simoneit, B.R.T., 1998. Sources of fine organic aerosol. 9. Pine, oak and synthetic log combustion in residential fireplaces. Environ Sci Technol 32, 13-22.

Rogge, W.F., Hildemann, L.M., Mazurek, M.A., Cass, G.R., Simonelt, B.R.T., 1991. Sources of Fine Organic Aerosol .1. Charbroilers and Meat Cooking Operations. Environ Sci Technol 25, 1112-1125.

Rogge, W.F., Mazurek, M.A., Hildemann, L.M., Cass, G.R., Simoneit, B.R.T., 1993c. Quantification of Urban Organic Aerosols at a Molecular-Level - Identification, Abundance and Seasonal-Variation. Atmospheric Environment Part a-General Topics 27, 1309-1330.

Root, R.A., 2000. Lead loading of urban streets by motor vehicle wheel weights. Environ Health Persp 108, 937-940.

Ross, M.A., Persky, V.W., Chung, J., Curtis, L., Ramakrishnan, V., Wadden, R.A., Hryhorczuk, D.O., 2002. Effect of ozone and aeroallergens on the respiratory health of asthmatics. Archives of Environmental Health 57, 568-578.

Ruzer, L.S., Harley, N.H., 2004. Aerosols Handbook: Measurement, Dosimetry, and Health Effects, 1st ed. CRC Press.

Samy, S., Robinson, J., Hays, M.D., 2011. An advanced LC-MS (Q-TOF) technique for the detection of amino acids in atmospheric aerosols. Analytical and Bioanalytical Chemistry 401, 3103-3113.

Sanders, P.G., Xu, N., Dalka, T.M., Maricq, M.M., 2003. Airborne brake wear debris: Size distributions, composition, and a comparison of dynamometer and vehicle tests. Environ Sci Technol 37, 4060-4069.

Sardar, S.B., Fine, P.M., Sioutas, C., 2005. Seasonal and spatial variability of the size-resolved chemical composition of particulate matter (PM10) in the Los Angeles Basin. J Geophys Res-Atmos 110, -.

Schauer, J.J., Kleeman, M.J., Cass, G.R., Simoneit, B.R.T., 2002. Measurement of emissions from air pollution sources. 4. C-1-C-27 organic compounds from cooking with seed oils. Environ Sci Technol 36, 567-575.

Schauer, J.J., Lough, G.C., Shafer, M.M., Christensen, W.F., Arndt, M.F., DeMinter, J., Park, J.-S., 2006. Characterization of Metals Emitted from Motor Vehicles. Health Effects Institute 133, 1-88.

Schnelle-Kreis, E., Sklorz, M., Peters, A., Cyrys, J., Zimmermann, R., 2005. Analysis of particle-associated semi-volatile aromatic and aliphatic hydrocarbons in urban particulate matter on a daily basis. Atmospheric Environment 39, 7702-7714.

Schwartz, J., Dockery, D.W., Neas, L.M., Wypij, D., Ware, J.H., Spengler, J.D., Koutrakis, P., Speizer, F.E., Ferris, B.G., 1994. Acute Effects of Summer Air-Pollution on Respiratory Symptom Reporting in Children. American Journal of Respiratory and Critical Care Medicine 150, 1234-1242.

Schwarze, P.E., Ovrevik, J., Hetland, R.B., Becher, R., Cassee, F.R., Lag, M., Lovik, M., Dybing, E., Refsnes, M., 2007. Importance of size and composition of particles for effects on cells in vitro. Inhal Toxicol 19, 17-22.

Seinfeld, J.H., Pandis, S.N., 2006. Atmospheric Chemistry and Physics - From Air Pollution to Climate Change, Second edition ed. John Wiley & Sons, Inc, New York.

Shafer, M.M., Perkins, D.A., Antkiewicz, D.S., Stone, E.A., Quraishi, T.A., Schauer, J.J., 2010. Reactive oxygen species activity and chemical speciation of size-fractionated atmospheric particulate matter from Lahore, Pakistan: an important role for transition metals. Journal of Environmental Monitoring 12, 704-715.

Sheesley, R.J., Schauer, J.J., Bean, E., Kenski, D., 2004. Trends in secondary organic aerosol at a remote site in Michigan's upper peninsula. Environ Sci Technol 38, 6491-6500.

Shen, H., Anastasio, C., 2011. A Comparison of Hydroxyl Radical and Hydrogen Peroxide Generation in Ambient Particle Extracts and Laboratory Metal Solutions. Atmospheric Environment doi: 10.1016/j.atmosenv.2011.10.006.

Shi, Z., Zhang, D., Hayashi, M., Ogata, H., Ji, H., Fujiie, W., 2008. Influences of sulfate and nitrate on the hygroscopic behaviour of coarse dust particles. Atmospheric Environment 42, 822-827.

Sillanpaa, M., Hillamo, R., Saarikoski, S., Frey, A., Pennanen, A., Makkonen, U., Spolnik, Z., Van Grieken, R., Branis, M., Brunekreef, B., Chalbot, M.C., Kuhlbusch, T., Sunyer, J., Kerminen, V.M., Kulmala, M., Salonen, R.O., 2006. Chemical composition and mass closure of particulate matter at six urban sites in Europe. Atmospheric Environment 40, S212-S223.

Simoneit, B.R.T., 1986. Characterization of Organic-Constituents in Aerosols in Relation to Their Origin and Transport - a Review. International Journal of Environmental Analytical Chemistry 23, 207-237.

Simoneit, B.R.T., 1999. A review of biomarker compounds as source indicators and tracers for air pollution. Environmental Science and Pollution Research 6, 159-169.

Simoneit, B.R.T., Kobayashi, M., Mochida, M., Kawamura, K., Lee, M., Lim, H.J., Turpin, B.J., Komazaki, Y., 2004. Composition and major sources of organic compounds of aerosol particulate matter sampled during the ACE-Asia campaign. J Geophys Res-Atmos 109.

Singh, M., Jaques, P.A., Sioutas, C., 2002. Size distribution and diurnal characteristics of particle-bound metals in source and receptor sites of the Los Angeles Basin. Atmospheric Environment 36, 1675-1689.

Smith, R.L., Spitzner, D., Kim, Y., Fuentes, M., 2000. Threshold dependence of mortality effects for fine and coarse particles in Phoenix, Arizona. J Air Waste Manage 50, 1367-1379.

Snyder, D.C., Schauer, J.J., 2007. An inter-comparison of two black carbon aerosol instruments and a semi-continuous elemental carbon instrument in the urban environment. Aerosol Sci Tech 41, 463-474.

Solomon, P.A., Fall, T., Salmon, L., Cass, G.R., 1989. Chemical Characteristics of Pm10 Aerosols Collected in the Los-Angeles Area. Japca-the Journal of the Air & Waste Management Association 39, 154-163.

Solomon, P.A., Fall, T., Salmon, L., Lin, P., Vasquez, F., Cass, G.R., 1988. Acquisition of acid vapor and aerosol concentration data for use in dry deposition studies in the South Coast Air Basin, in: 25, E.Q.L.R.N. (Ed.). California Air Resources Board.

Solomon, P.A., Salmon, L.G., Fall, T., Cass, G.R., 1992. Spatial and Temporal Distribution of Atmospheric Nitric-Acid and Particulate Nitrate Concentrations in the Los-Angeles Area. Environ Sci Technol 26, 1594-1601.

Sram, R.J., Binkova, B., Rossner, P., Rubes, J., Topinka, J., Dejmek, J., 1999. Adverse reproductive outcomes from exposure to environmental mutagens. Mutation Research-Fundamental and Molecular Mechanisms of Mutagenesis 428, 203-215.

Stayner, L., Dankovic, D., Smith, R., Steenland, K., 1998. Predicted lung cancer risk among miners exposed to diesel exhaust particles. Am J Ind Med 34, 207-219.

Tao, F., Gonzalez-Flecha, B., Kobzik, L., 2003. Reactive oxygen species in pulmonary inflammation by ambient particulates. Free Radical Biology and Medicine 35, 327-340.

Targonski, P.V., Persky, V.W., Ramekrishnan, V., 1995. Effect of Environmental Molds on Risk of Death from Asthma during the Pollen Season. Journal of Allergy and Clinical Immunology 95, 955-961.

Taylor, S.R., McLennan, S.M., 1985. The Continental crust: Its Composition and Evolution. Blackwell, Oxford.

Terzi, E., Argyropoulos, G., Bougatioti, A., Mihalopoulos, N., Nikolaou, K., Samara, C., 2010. Chemical composition and mass closure of ambient PM10 at urban sites. Atmospheric Environment 44, 2231-2239.

Turpin, B.J., Lim, H.J., 2001. Species contributions to PM2.5 mass concentrations: Revisiting common assumptions for estimating organic mass. Aerosol Sci Tech 35, 602-610.

Tursic, J., Podkrajsek, B., Grgic, I., Ctyroky, P., Berner, A., Dusek, U., Hitzenberger, R., 2006. Chemical composition and hygroscopic properties of size-segregated aerosol particles collected at the Adriatic coast of Slovenia. Chemosphere 63, 1193-1202.

U.S.EPA, 2004. Air Quality Criteria for Particulate Matter. Office of Research and Development, National Center for Environmental Assessment, U.S. Environmental Protection Agency, Research Triangle Park, NC.

U.S.EPA, 2006. National Ambient Air Quality Standards for Particulate Matter; Proposed Rule, 40 CFR Part 50. US Office of the Federal Register, National Archives and Records Administration, Washington, DC.

Usher, C.R., Michel, A.E., Grassian, V.H., 2003. Reactions on mineral dust. Chemical Reviews 103, 4883-4939.

Verma, V., Ning, Z., Cho, A.K., Schauer, J.J., Shafer, M.M., Sioutas, C., 2009a. Redox activity of urban quasi-ultrafine particles from primary and secondary sources. Atmospheric Environment 43, 6360-6368.

Verma, V., Pakbin, P., Cheung, K.L., Cho, A.K., Schauer, J.J., Shafer, M.M., Kleinman, M.T., Sioutas, C., 2011. Physicochemical and oxidative characteristics of semi-volatile components of quasi-ultrafine particles in an urban atmosphere. Atmospheric Environment 45, 1025-1033.

Verma, V., Polidori, A., Schauer, J.J., Shafer, M.M., Cassee, F.R., Sioutas, C., 2009b. Physicochemical and Toxicological Profiles of Particulate Matter in Los Angeles during the October 2007 Southern California Wildfires. Environ Sci Technol 43, 954-960.

Vlasenko, A., Sjogren, S., Weingartner, E., Stemmler, K., Gaggeler, H.W., Ammann, M., 2006. Effect of humidity on nitric acid uptake to mineral dust aerosol particles. Atmos Chem Phys 6, 2147-2160.

Wall, S.M., John, W., Ondo, J.L., 1988. Measurement of Aerosol Size Distributions for Nitrate and Major Ionic Species. Atmospheric Environment 22, 1649-1656.

Wang, G., Kawamura, K., Xie, M., Hu, S., Gao, S., Cao, J., An, Z., Wang, Z., 2009. Size-distributions of n-alkanes, PAHs and hopanes and their sources in the urban, mountain and marine atmospheres over East Asia. Atmos Chem Phys 9, 8869-8882.

Wang, Y., Arellanes, C., Curtis, D.B., Paulson, S.E., 2010. Probing the Source of Hydrogen Peroxide Associated with Coarse Mode Aerosol Particles in Southern California. Environ Sci Technol 44, 4070-4075.

Winiwarter, W., Bauer, H., Caseiro, A., Puxbaum, H., 2009. Quantifying emissions of primary biological aerosol particle mass in Europe. Atmospheric Environment 43, 1403-1409.

Wu, P.M., Okada, K., 1994. Nature of Coarse Nitrate Particles in the Atmosphere - a Single, Particle Approach. Atmospheric Environment 28, 2053-2060.

Yeatts, K., Svendsen, E., Creason, J., Alexis, N., Herbst, M., Scott, J., Kupper, L., Williams, R., Neas, L., Cascio, W., Devlin, R.B., Peden, D.B., 2007. Coarse particulate matter (PM2.5-10) affects heart rate variability, blood lipids, and circulating eosinophils in adults with asthma. Environ Health Persp 115, 709-714.

Yoshizumi, K., Hoshi, A., 1985. Size Distributions of Ammonium-Nitrate and Sodium-Nitrate in Atmospheric Aerosols. Environ Sci Technol 19, 258-261.

Yue, Z.W., Fraser, M.P., 2004. Polar organic compounds measured in fine particulate matter during TexAQS 2000. Atmospheric Environment 38, 3253-3261.

Zereini, F., Wiseman, C., Alt, F., Messerschmidt, J., Muller, J., Urban, H., 2001. Platinum and rhodium concentrations in airborne particulate matter in Germany from 1988 to 1998. Environ Sci Technol 35, 1996-2000.

Zhang, D.Z., Shi, G.Y., Iwasaka, Y., Hu, M., 2000. Mixture of sulfate and nitrate in coastal atmospheric aerosols: individual particle studies in Qingdao (36 degrees 04 ' N, 120 degrees 21 ' E), China. Atmospheric Environment 34, 2669-2679.

Zhang, T., Claeys, M., Cachier, H., Dong, S.P., Wang, W., Maenhaut, W., Liu, X.D., 2008a. Identification and estimation of the biomass burning contribution to Beijing aerosol using levoglucosan as a molecular marker. Atmospheric Environment 42, 7013-7021.

Zhang, Y.X., Schauer, J.J., Shafer, M.M., Hannigan, M.P., Dutton, S.J., 2008b. Source apportionment of in vitro reactive oxygen species bioassay activity from atmospheric particulate matter. Environ Sci Technol 42, 7502-7509.

Zhang, Y.Y., Muller, L., Winterhalter, R., Moortgat, G.K., Hoffmann, T., Poschl, U., 2010. Seasonal cycle and temperature dependence of pinene oxidation products, dicarboxylic acids and nitrophenols in fine and coarse air particulate matter. Atmos Chem Phys 10, 7859-7873.

Zhao, Y.L., Gao, Y., 2008a. Acidic species and chloride depletion in coarse aerosol particles in the US east coast. Sci Total Environ 407, 541-547.

Zhao, Y.L., Gao, Y., 2008b. Mass size distributions of water-soluble inorganic and organic ions in size-segregated aerosols over metropolitan Newark in the US east coast. Atmospheric Environment 42, 4063-4078.

Zhuang, H., Chan, C.K., Fang, M., Wexler, A.S., 1999. Formation of nitrate and non-sea-salt sulfate on coarse particles. Atmospheric Environment 33, 4223-4233.

Zygadlo, J.A., Maestri, D.M., Grosso, N.R., 1994. Alkane Distribution in Epicuticular Wax of Some Solanaceae Species. Biochemical Systematics and Ecology 22, 203-209.